DYNAMIC BALANCING OF INDUSTRIAL MANIPULATORS USING POINT MASS MODELS AND TLBO

Ph.D. Thesis

DEVI SINGH KUMANI

(ID. No. 2009RME103)

DEPARTMENT OF MECHANICAL ENGINEERING

MALAVIYA NATIONAL INSTITUTE OF TECHOLOGY, JAIPUR

FEBRUARY, 2018

Dynamic Balancing of Industrial Manipulators Using Point Mass Models and TLBO

Submitted in

Fulfillment of the requirements for the degree of

Doctor of Philosophy

by

DEVI SINGH KUMANI

(ID: 2009RME103)

Under the Supervision of

Dr. Himanshu Chaudhary

Department of Mechanical Engineering

Malaviya National Institute of Technology Jaipur, India

February, 2018

Certificate

This is to certify that the thesis entitled **Dynamic Balancing of Industrial Manipulators using Point Mass Models and TLBO** being submitted by **Devi Singh Kumani** to the Malaviya National Institute of Technology Jaipur for the award of the degree of **Doctor of Philosophy** is a bonafide record of original research work carried out by him under my supervision in conformity with rules and regulations of the institute.

The work incorporated in this thesis have not been submitted, in part or in full, to any other University or Institute for the award of any Degree or Diploma.

Dr. Himanshu Chaudhary

Associate Professor

Mechanical Engineering Department

Malaviya National Institute of Technology Jaipur

Jaipur – 302017, India

DECLARATION

I, Devi Singh Kumani, declare that the thesis titled, **"Dynamic Balancing of Industrial Manipulators Using Point Mass Models and TLBO"**, and the work presented in it, are my own, I confirm that:

- This work was done wholly or mainly while in candidature for a research degree at this university.

- The work incorporated in this thesis has not been submitted elsewhere for the award of any degree or any other qualification at this university or any other institution.

- Where I have consulted the published work of others, this is always clearly attributed (reference is given).

- Where I have quoted from the work of others, the source (reference) is always given. With the exception of such quotation, this thesis is entirely my own work.

- I have acknowledged all main sources of help.

Date:

(Devi Singh Kumani)

(2009RME103)

Abstract

Industrial robots are extensively used worldwide in the automobile industry and variety of other applications. Present day manipulators operate at high speed. The inertia induced force and moment if not balanced, shake the manipulator, create vibrations and noise, fatigue etc. These unbalanced inertia force and moment are known as the shaking force and the shaking moment. Hence, to improve the dynamic performance these are to be minimized. The balancing of inertia induced force and moment in an industrial manipulator is referred to as dynamic balancing. The aim of this dissertation is to provide an optimization methodology for the dynamic balancing of industrial manipulators.

The octahedron seven point-mass model, hexahedron six and five point mass models and four point mass model configurations for dynamically representing the rigid links of an industrial manipulator are developed to ensure positive value for the equivalent point masses. For the same the concept of equimomental system of point masses, a convenient way to represent the inertia properties of a rigid link of Industrial Manipulator, is used. The expressions for computing the location of point masses and their value in terms of rigid link parameters are derived for the different proposed models. The proposed point-mass models to dynamically represent links of the manipulator are used to formulate optimization problem to minimize the shaking force and shaking moment simultaneously.

The population based evolutionary algorithms, Genetic Algorithm (GA) and recently developed Teaching Learning Based Optimization (TLBO) algorithm, are used to solve the constrained optimization problem developed. The effectiveness of methodology is demonstrated by applying it to a six-dofs PUMA robot. The evolutionary techniques offer multiple solutions close to the optimal solution. The

TLBO Algorithm is used for the first time for spatial linkages balancing as optimization solver.

Significant reductions of about 71% and 81% using GA and TLBO, respectively, in the shaking moment are obtained by proposed methodology. It is observed that TLBO gives better results with less computational efforts.

CONTENTS

List of Figures

x

List of Tables

List of Symbols and Abbreviations

$\mathbf{a}_{i,i+1}$ Position vector of the origin O_{i+1} of $(i+1)^{\text{th}}$ link, from origin O_i of ith link

$\mathrm{a}_{i,i+1}$ Magnitude of $\mathbf{a}_{i,i+1}$, link length

C_i The mass center of ith link

$\mathbf{d}_i$ Position vector of the mass center C_i of ith link, from origin O_i

$\mathbf{d}_{ij}$ Position vector of the jth point-mass of ith link, from origin O_i

$\tilde{\mathbf{d}}_i$ The 3×3 skew symmetric matrix associated with vector $\mathbf{d}_i$

$\mathbf{f}_i^{\mathbf{c}}$ Resultant force acting on i^{th} link at center of mass C_i

$\mathbf{f}_{sh}$ Shaking force in a manipulator having n moving links

$\mathbf{f}_{i-1,i}$ Constraint force at the origin O_i on i^{th} link due to $(i-1)^{\text{st}}$ link

$\mathbf{f}_i^e$ External force on i^{th} link at the origin O_i

$\mathbf{f}_i^*$ The inertia force of ith link at the origin O_i

$\tilde{f}_{sh}$ Root Mean Square (RMS) value of shaking force

$\mathbf{I}_i$ Inertia tensor of ith link about the origin O_i

$\mathbf{I}_i^{\mathbf{c}}$ Inertia tensor of ith link about mass center C_i

$I_{ixx}, I_{iyy}, I_{izz}$ Moments of inertia of ith link

$I_{ixy}, I_{iyz}, I_{ixz}$ Products of inertia of ith link

m_i Mass of ith link

m_{ij} Mass of jth point-mass of ith link

$\mathbf{n}_i$ Resultant of the pure moment and moment of forces of ith link about O_i

$\mathbf{n}_i^{\mathbf{c}}$ Resultant of the pure moment and moment of forces of ith link about C_i

$\mathbf{n}_{sh}$ Shaking moment

$\mathbf{n}_{i-1,i}$ Constraint moment at the origin O_i on i^{th} link due to $(i-1)^{\text{st}}$ link

$\mathbf{n}_i^e$	External moment on i^{th} link at and about the origin O_i
O_i	Origin of ith link
O_{i+1}	Origin of $(i+1)^{\text{st}}$ link
$\mathbf{P}$	Set of design vectors $\mathbf{X}_k$ of the population
r_i	Position vector of the mass center of m_i from the origin O_{i+1}
r_{ij}	Position vector of point mass m_{ij} from the origin O_{i+1}
$\mathbf{v}_i$	Linear velocity of origin O_i of ith link
$\mathbf{v}_i^c$	Linear velocity of the mass center C_i of ith link
$\dot{\mathbf{v}}_i$	Linear acceleration of origin O_i of ith link
$\dot{\mathbf{v}}_i^c$	Linear acceleration of the mass center C_i of ith link
w_1, w_2	Weighing factors of multiple objective functions
$\mathbf{X}_i$	Design vector for i^{th} link
$\mathbf{X}$	Design vector
$\mathbf{X}^*$	Design vector of design variables m_{ij}^* for which function value (FV) is minimum and it acts as teacher in TLBO
$\bar{\mathbf{X}}$	Design vector of mean of design variables in TLBO
$\mathbf{X}_q, \mathbf{X}_r$	Design vectors of two randomly selected learners for learning in TLBO
$\mathbf{X}_{new}$	New values of design variables after teachers phase in TLBO
$\mathbf{X}_{kq}, \mathbf{X}_{kr}$	New values of design variables of kth population after learning from k^{th} and r^{th} learner in TLBO
$x_{i,} y_{i,} z_i$	Body fixed frame fixed to the ith link
$x_{ij,} y_{ij,} z_{ij}$	Coordinates of jth point mass of ith link
$\bar{x}_i, \bar{y}_i, \bar{z}_i$	Coordinates of the mass center of mass m_i of ith link
θ_i	Angular position of ith link at any time t
$\boldsymbol{\omega}_i$	Angular velocity of ith link

$\dot{\boldsymbol{\omega}}_i$	Angular acceleration of ith link
ρ	Random number for each design variable m_{ij} to be generated in the range of 0 to1 during teacher phase in TLBO
ρ_{lp}	Random number for each design variable m_{ij} to be generated in the range of 0 to1 during learner phase in TLBO
GA	Genetic Algorithm
TLBO	Teaching-Learning-based-Based-Optimization
FV	Function value

Vectors are shown by bold Fonts

Introduction

The industrial robot is a manipulator to move materials, parts, tools, and perform a variety of programmable tasks in manufacturing. Industrial robots are extensively used worldwide in the automobile industry. Robot applications are growing fast. These applications can be found in manufacturing industries, medical applications, entertainment, work at dangerous places like nuclear power plants, space applications, etc. Few examples are shown in Fig.1.1. The inertia induced force and moment if not balanced, shakes the manipulator, create vibrations and noise, fatigue, etc. at high speeds of operation. These unbalanced inertia force and moment are known as the shaking force and the shaking moment. Hence, to improve the dynamic performance, these are to be minimized. The balancing of inertia induced force and moment in an industrial manipulator is referred to as dynamic balancing. The prime objective of this dissertation is to develop a methodology for the dynamic balancing of industrial manipulators. The dynamic balancing requires trade-off between these competing shaking force and shaking moment. Thus, an industrial manipulator balancing problem can be formulated as an optimization problem to simultaneously minimize the shaking force and shaking moment. At the same time, constraints are imposed properly to assure the feasible mechanism for industrial manipulators. Mass of each moving link and its distribution plays a significant role in the balancing, it contributes to the shaking force and shaking moment.

Thus the determination of inertial properties of the links of an industrial manipulator to optimally minimize the shaking force and shaking moment constitutes the main problem. These inertia properties can be represented more conveniently using the

dynamically equivalent system of point masses. The dynamically equivalent system is termed as the equimomental system.

IRB 2400 Industrial Robot from ABB
[http://www02.abb.com]

Automated Pipe Welding
[http://www.robots.com/automated-pipe-welding-with-robots]

Strongarm 375 / 500 Series Industrial Manipulator [http://www.strongmanindustries.com]

Fig. 1.1 Examples of industrial manipulator applications

The equimomental concept is used to represent the moving links into point-mass models. The optimization problem for dynamic balancing of the industrial manipulator is thus formulated in this study using different point mass models which will ensure positive values for point masses. There are several algorithms available to

solve any optimization problem. Among the evolutionary algorithms, Genetic Algorithm (GA) and Teaching-Learning-Based-Optimization algorithm (TLBO) are explored for the dynamic balancing problem. TLBO is an optimization algorithm of recent origin, which has been successfully used in recent times for optimization applications in many areas. Use of TLBO for optimization of industrial manipulator has not been reported so far as evident from Literature review (Chapter 2). The evolutionary optimization algorithms find multiple solutions near to the global optimum solution and the solution which is more suitable for link shape formulation can be used.

The algorithms are compared in terms of convergence to reach to the global optimum solution. To demonstrate the effectiveness of the proposed methodology, it is applied to balance a six degree of freedom PUMA robot.

1.1 Balancing of industrial manipulator mechanism

The interaction between a mechanism and its surrounding is an important aspect to be considered by the industrial manipulator designers. Some of the industrial manipulators are operated at high speed. The resultant inertial forces and moments of the moving links of the industrial manipulator are termed as shaking force and shaking moment is crucial in design of such manipulator. These inertial force and moment have no opposite reaction forces to cancel out internally in the manipulators mechanism. Hence, they transmit to the base/frame on which the manipulator is mounted. As a consequence, resulting vibrations, wear, noise and fatigue adversely affect the dynamic performance of the industrial manipulator. All the applied and constraint forces have equal and opposite reaction forces, and that vanish within the system including frame. However, there will be no reaction force for the inertia forces

and moments, and hence these need to be balanced. The mechanism balancing also helps in reducing the fluctuations in the input torque required to maintain a constant drive speed of the manipulator.

The shaking force and shaking moment depends on the masses, their distribution, and accelerations of the moving links of the manipulator. The shaking force can be balanced either by redistributing the link masses or by adding the counterweights which result in the overall increase in mass of the balanced mechanism. The balancing of the shaking moment along with the shaking force can be achieved by using the additional links having opposite motion that makes the balanced mechanism very complex.

Thus the complete balance of shaking force and shaking moment is not recommended in most of the studies. To overcome this difficulty, some method suggests to reduce the shaking force and shaking moment simultaneously using the optimization methods. The researchers all over the world are continuously trying to explore the new ideas and techniques to balance the shaking force and shaking moment in the planar and spatial mechanisms. Though, a good amount of research in this area has been carried out in the past for planar mechanisms, relatively less work is reported for spatial mechanisms due to dynamic complexities involved in it.

In most of the methods available in the literature, the analytical method is derived for complete force balance of simple mechanisms and very few are extended for the complex planar mechanisms and spatial mechanisms. Few methods use the dynamically equivalent systems to balance the planar and spatial mechanisms through optimization. The convex optimization method is also used to design optimally the counterweights to balance the planar and spatial mechanisms. Some other methods are

based on the mixed mass redistribution approach in which the principles of mass distribution and counterweight addition are combined to achieve dynamic balancing in the planar and spatial mechanisms.

After pondering over the issue, it is decided to use optimization approach for minimization of shaking force and shaking moment using equimomental point masses for moving link of a manipulator that offers simple dynamic equations to be handled in the program. Simultaneously, investigate new point mass models in various configurations to ensure positive value for equivalent point masses. It is further decided to use Evolutionary techniques like Genetic Algorithms and recently introduced teaching-learning-based optimization algorithm to solve the optimization problem formulated.

1.2 Contributions of the Research

The contributions of this research work are summarized as follows:

1. Seven point-mass octahedron, Six and five point-mass hexahedron and Four point-mass models are proposed in this study to ensure positive value for equivalent point masses to facilitate link shape formulation.

2. The problem of dynamic balancing for the industrial manipulators is proposed as an optimization problem.

3. Industrial manipulators are balanced by finding the optimum mass distribution for their links instead of using the counterweights and/or additional members.

4. Evolutionary optimization techniques are explored to find the optimum solution for the proposed optimization problem. The techniques like Genetic Algorithm and Teaching-learning-based optimization algorithm (TLBO) are applied for the industrial manipulators balancing. TLBO's use is demonstrated

on the specific problem of robot, to reduce shaking moments through optimization. Coding of TLBO to solve the optimization problem is developed. It is established that TLBO is computationally more efficient than the popular optimization algorithm, genetic algorithm (GA).

1.3 Thesis Organization

This thesis contains nine chapters arranged as follows:

Chapter 1: Introduction

The objective and motivation of the research work to develop a method for the dynamic balancing of industrial manipulators is presented in this chapter. It introduces the planar and spatial mechanisms balancing approaches. It also highlights the major contributions of the research work and outlines the organization of the thesis.

Chapter 2: Literature Review

The various methods developed for complete force balance, complete force and moment balance, partial force and moment balance including the optimization methods are discussed in this chapter. The drawbacks and limitations of these methods are mentioned to identify the research gap.

Chapter 3: Point-mass Models

The various equimomental point mass models for dynamic representation of the moving links of the manipulator are discussed. The seven point-mass octahedron, six and five point-mass hexahedron and four point mass configurations are developed. Such configurations ensure positive values for equimomental point masses.

Chapter 4: Dynamic Analysis

This chapter gives the equations of motion applicable to an open-loop system (industrial manipulator) to compute reaction forces and moments at the joints. The

dynamic formulation applicable to point-masses system and the expressions used to compute shaking forces and shaking moments are also given.

Chapter 5: Optimization Problem Formulation

The optimization problem is formulated to balance the open-loop system (industrial manipulators) dynamically in this Chapter. A numerical example of six degrees of freedom PUMA robot is solved to minimize the shaking force and shaking moment. The RMS values of shaking force and shaking moment over one cycle of operation for the known trajectory of manipulators operation are optimized.

Since, the optimization results are trajectory dependent, we need to make computations for all possible trajectory combinations and select the solutions best suited for all possible trajectories for which the robot is likely to be used.

Chapter 6: Evolutionary Optimization Techniques

This chapter explores the evolutionary optimization algorithms. It differentiates the various parameters required to search the solution in the entire design space for these optimization algorithms. The two evolutionary optimization algorithms, (1) Genetic Algorithm (GA) and (2) Teaching-Learning-Based Optimization (TLBO) algorithm, are explained, and their applications are discussed in this chapter.

Chapter 7: Optimization Using Genetic Algorithm

The optimization problem formulated in Chapter 5 is solved using Genetic Algorithm. The results are presented in the tabular and graphical form and discussed in this chapter.

Chapter 8: Optimization Using TLBO

The results obtained using Teaching-Learning-Based-Optimization Algorithm (TLBO) are presented and discussed here.

Chapter 9: Comparative Results

The results obtained using different point-masses models and two optimization technique i.e. GA and TLBO are discussed and compared in this chapter. It also explains the matching of curves for balanced and original PUMA at Joint 5 & 6 and reverse phenomenon observed in cases at Joint 5 & 6 for TLBO cases.

Chapter 10: Conclusions

In this chapter, the thesis work is summarized and the recommendations / suggestions based on the findings in the thesis are also made. Further, the recommendations for future work are also presented.

1.4 Summary

The dynamic balancing for the industrial manipulators is introduced in chapter 1. This chapter describes the motivation and objective of the research work and also outlines the thesis contributions. It also contains brief information about the nine chapters of the thesis.

Literature Review

This chapter reviews various methods developed and reported for balancing of the planar and spatial mechanisms. The methods used for complete force balance, complete force and moment balance, partial force and moment balance are reviewed. The review also includes the optimization methods as well as the methods used for the optimal design and balancing of Industrial Manipulators/Robots. Review papers such as Kamenskii (1968), Lowen and Berkof (1968), Lowen et al. (1983), Kochev (2000), Arakelian and Smith (2005), Wijk et al. (2009), and Arakelian and Briot (2015) throw light on the quantum of work carried out on the dynamic balancing of the planar, spatial mechanisms and industrial manipulators.

2.1 Shaking force balancing of mechanisms

Lowen and Berkof (1968) reported the survey on "Balancing the Linkages" emphasizing on the need of balancing of linkages running at high speed or massive links where considerable shaking force and shaking moments are transmitted to surroundings. These disturbances cause vibration, noise, wear and fatigue problems reducing the full potential of many machines. Contemporary, enough literature was published related to the balancing of slider-crank mechanism and little publication existed on the balancing of other types of planar or spatial linkages. Static balancing is achieved, if the center of mass of the system of moving links is kept stationary. Shaking force reduces to zero in the statically balanced system. It can be achieved by the method of principal vectors, use of cams or use of duplicate mechanisms as reported by different researchers.

Kamenski (1968 a) review report "On the Question of balancing the Linkages" stated that the use of counterweights had been made for static balancing of linkages. The position of the center of mass of the system of moving links is determined by the resultant of principal vector (The vectors directed along the links of the mechanism are termed as principal vectors) system which is equal to the sum of principal vectors of all moving links. He emphasized that the static balancing may affect the dynamic unbalance of a mechanism (it may even increase it). Any mechanism even if theoretically balanced shows unbalance because of inaccuracies of manufacture i.e. clearances at joints. Therefore dynamic balancing may be carried out together with static balancing or after it. Kamenskii (1968 b) used the cam mechanism, to completely balance the shaking force in the planar mechanisms. The reduction of the inertia forces is achieved by using a cam-counterweight arrangement and the cam driven masses to keep the mechanism's center of mass fixed.

Shchptil (1968) suggested new construction that physically traces out the center of mass of a planar mechanism. By changing the original mass distribution, the total center of mass is moved to a rotating point of the proportional auxiliary mechanism. It allows the introduction of a counterweight which causes the final center of mass to be reduced to stationary point and the rotating part being not the part of the original linkage. It simultaneously generates a moment that may be used to balance the first harmonics of the disturbing moment (shaking moment).

Berkof and Lowen (1969) gave the concept of "Method of Linearly Independent Vectors" that permits the complete force balancing of certain planar linkages. It consists of writing equations, describing the position of total mechanism center of mass so that the coefficient of time dependent term may be set equal to zero. It makes

the center of mass stationary that vanishes the shaking force completely. The equation for four and six-bar planar mechanisms with arbitrary link mass distribution is derived by them. In this method, the links masses are redistributed in such a way that it eliminates the time-dependent terms coefficients in an equation thereby representing the trajectory of the total center of mass of the mechanism.

Kaufman and Sander (1971) applied the concept of "Method of Linearly Independent Vectors" in RSSR and RSSP spatial mechanisms. Shaking force is eliminated by distributing the link masses so that the time dependent terms are eliminated in the equation which describes the motion of the overall center of mass of the linkages. This process makes the total center of mass stationary.

Tepper and lowen (1972) proposed the contour theorem that differentiates between the mechanisms in which the shaking force can be fully balanced and those in which cannot be achieved. Complete force balancing of planar linkage is possible using simple counterweights provided that from every point on the linkage there exists a contour to the ground through revolute joints only. Generalization of the method of linearly independent vectors for single degree freedom mechanism is presented, and it is proved that the counterweights required for the complete force balance of an *n*-link planar mechanism are half of the total number of the links. It was shown that the pinned planar mechanisms can always be force balanced as they do not have the time-dependent coefficient in the center of the mass equation.

Lowen et al. (1974) found that the complete force balance increases the shaking moment and driving torque for the mechanism. *Therefore, only force balancing is not useful and the moment balance is also needed to balance the mechanism completely.* Smith (1975) developed a computer program for designing the counterweights to

balance the shaking force completely in the planar mechanisms using the "Method of Linearly Independent Vectors".

Walker and Oldham (1978, 1979) proposed a general theory of balancing shaking force using counterweights. Three equations are derived by them from which the force balance condition of multi-degree freedom n-bar planar linkages with revolute and prismatic joints can be obtained. They presented the criteria for deciding the number of the counterweights required for complete force balancing and for the selection of the links to which the counterweight are to be attached.

Bagci (1979) presented the shaking force balancing of planar linkages with force transmission irregularities encountered in spatial mechanisms where the links have a connection to fixed link through pairs permitting linear freedom only. In such cases, the shaking force balancing is achieved using the method of linearly independent mass vectors and balancing idler loops concept.

Bagci (1983) presented the method of balancing shaking forces completely in space mechanisms using real vectors. Design equations for force balancing RSSR, RSRC, CSC and RCRC screw generator are developed. It is shown that SC and SRC dyads in spatial mechanism also introduce force transmission irregularity and are balanced by attaching a force balancing RRR dyad or a linearly moving counter balancer driven by gear rack drive. Note that R, S, and C denote Revolute, Spherical, and Cylindrical joints.

Chen (1984) presented the partial balancing of shaking force of a spatial 4 bar RCCC linkage using optimization method. Three counterweights were attached to the 4 bar RCCC linkage and the optimal vectors of the position of counter weights were computed using optimization to achieve balancing.

Kochev (1987) proposed the general method of force balancing applicable to both spatial and planar mechanism. Here, the three sets of general force balancing conditions in X, Y and Z directions are derived. Thus, the linear balancing conditions for some spatial and planar linkages are presented in the Cartesian form in this method.

Park and Kwak (1987) proposed optimal design formulation to reduce the undesirable dynamic effect due to clearance at joints. The optimization function to be minimized is the maximum ratio of the rate of change of force direction to the magnitude of the joint force. The magnitude and location of added mass (counterweight) to each link is computed optimally. It is applied to offset slider crank mechanism.

Segla et. al. (1998) proposed Statistical Balancing of a Robot Mechanism with the aid of a Genetic Algorithm. Static balancing of robot mechanism reduces the motor power. The average gripper force in the working area is considered as an objective function and the link lengths, angle between links and spring force are considered as design variables. An industrial robot with 6 degrees of freedom is considered as an example. The balancing system should produce such forces that should be able to eliminate, or at least essentially reduce the static gravity forces at powered joints. The balancing using springs is proposed in this study.

2.2 Shaking force and shaking moment balancing, and driving torque reduction in mechanisms and robotic manipulators

The shaking moment is also to be balanced apart from balancing the shaking force to achieve the dynamic balance in the mechanisms. Enormous work has been reported on the balancing of shaking force and shaking moment either partially or completely particularly for planar linkages. Some work on spatial linkages has also been reported

and lately some work has been reported on balancing using advanced evolutionary optimization techniques as well.

Lowen et. al. (1983) surveyed literature on force and moment balancing of linkages. It confines to the full or partial balancing of shaking forces and shaking moments using internal mass redistribution or counterweight addition.

Lee and Chang (1984) proposed an analytical and computer-aided procedure for balancing of high-speed linkages. It involves a trade-off between shaking force, shaking moment, bearing reactions and input torque fluctuations by mass distribution of the links or counter-weighting the linkage. Analytical mechanics and heuristic optimization techniques are used to achieve the trade-off. This method has been demonstrated on a four-bar linkage.

Yu (1987a, b) presented the partial/optimum balancing of shaking force and shaking moment of RSSR spatial linkages by using a dyad (or link) between output link and the frame. By the addition of counterweights to the input link, balancing of shaking force and shaking moment is further improved. It is observed that the complete balancing of spatial mechanism is not possible because their kinematics and dynamics is more complex as compared to planar linkages.

Kochev (1992) presented the active balancing of the frame shaking moment in high-speed planer machines. The total moment comprising of the shaking moment and the driving torque is reduced based on mass redistribution and using one or more than one balancer revolving in a prescribed way in association with the geometry and the masses of the original linkage. Elimination of the overall reaction moment (shaking + driving) is achieved rather than its component which allows uniform rotation of the crank or the use of one balancer instead of three balancers.

Rahman S. (1996) presented reduction of inertia induced forces in a general spatial mechanism. In this study, the computer-aided design procedure has been developed for minimization of inertia-induced forces in CSSP mechanism. Here also, the concept of a dynamically equivalent system of point masses is used, and the point masses are kept positive. It is applied to generalized three-dimensional slider crank mechanism containing a different kind of joints such as cylindrical, spherical and prismatic type. However, the quantum of reduction in the average optimized value of shaking force and shaking moment is 0.73 % and 5.39% respectively, which is not very significant.

Chiou et. al. (1997) proposed the two rotating mass balancers for partial balancing of spatial mechanisms. It is concerned with the partial balancing of spatial mechanisms by the use of counterweights mounted on shafts that rotate at cycle frequency and multiple of that frequency. In this, an equivalent system with only two rotating force vectors of any one frequency term of the shaking force and shaking moment of the spatial mechanism is found. That eliminates the term of the shaking effects with a two rotating mass balancers.

Wawrzecki (1998) proposed a method of balancing spatial mechanism of the needle arm drive on a knitted fabric over lock sewing machine using the addition of masses at the design stage. It is suggested that each structural group of mechanism in the machine should be balanced separately.

Papakostas et. al. (1998) reported on the genetic design of dynamically optimal robotic manipulators. The procedure is task oriented and minimizes the reaction forces and moments induced by the manipulator during the execution of specified trajectories. The objective function incorporates these forces and moments, which are

15

reduced by using genetic algorithms to calculate the balance weight and the associated eccentricity of each link for which the base reaction is minimized. The dynamic performance is measured by the mean-squared value of the reaction forces and moments generated during one cycle of trajectory execution. Reduction of 55% to 64% is reported in objective function value using genetic algorithms for the solution of optimization problem formulated.

Kochev (2000) provided a critical review of the methods employing additional members for complete shaking moment balancing. The techniques used are, direct balancing of shaking moment with the addition of one additional member which may be a cam driven rocker or a counter rotary balancer run by non-circular gear set or the crank itself revolving with a prescribed fluctuation, duplicate mechanism and direct balancing of individual members.

Feng et. al. (2000) proposed optimum balancing of shaking force and shaking moment for spatial RSSR mechanism using Genetic Algorithm. A new method, comprehensive mass redistribution method is used for optimal balancing. It consists of two parts i. e. mass redistribution of the link itself and adding weights to the end of the link. This method is better than conventional methods, and the weight of the mechanism is decreased.

 Guo et. al. (2000) proposed the optimum dynamic design of planar Linkage using Genetic Algorithm. Here also, mixed mass redistribution method is used. It is demonstrated that using genetic algorithms we can obtain optimum dynamic characteristics more efficiently than by the traditional non-linear optimization techniques. The mixed redistribution method reduces shaking force, shaking moment and driving torque more effectively.

Arkalin and Dahan (2001) presented partial shaking moment balancing of fully force balanced planar and spatial linkages. It is achieved by the displacement of the axis of rotation of the input link connected with the counterweight.

Attia (2001) presented a simplified recursive formulation for the dynamic analysis of planar linkages replacing the rigid body by a dynamically equivalent constrained system of particles (i. e. point masses). Geometric constraints that fix the distance between particles are introduced. The concepts of linear and angular momentums are used to formulate dynamic equations for planar systems. However, these are expressed in terms of rectangular Cartesian coordinates of a dynamically equivalent system of particles. It results in the reduced system of differential algebraic equations without introducing any rotational coordinates.

Attia and Quasseem (2003) presented the matrix formulation for the dynamic analysis of spatial mechanisms with a common type of kinematic joints using point coordinates and velocity transformation. Here also, the rigid body is replaced by the dynamically equivalent system of particles. The equations of motion are derived in terms of relative joint coordinates using velocity transformation matrix. The velocity transformation matrix relates the relative joint velocities to the Cartesian velocities.

Ouyang et. al. (2003) presented an integrated approach to the design of robotic mechanisms for force balancing and trajectory tracking. The robotic manipulators are real-time controllable (RTC) mechanisms. A new approach termed as adjusting kinematic parameter (AKP) for the force balancing of RTC mechanism is described. It reduces joint forces and torques in servo motors and improves their trajectory tracking performance.

Alici and shirinzadeh (2004) presented a methodology for optimum dynamic balancing of two degrees of freedom planar parallel manipulator articulated with revolute joints. The optimization selects a set of parameters for mass distribution of moving links. The addition of counterweights is employed by them.

Korayem and Ghariblu (2004) established the load carrying capacity of a mobile base manipulator operated by limited force or torque actuators. It is shown that the maximum allowable load on a given trajectory is a function of base position. The recursive Newton-Euler method is used to compute the dynamic effects of the load and manipulator on each joint actuator, then the load carrying capacity of the mobile manipulator at each base point is computed by considering the manipulator joint and torque constraints.

Arakalin and Smith (2005) presented the review of work on shaking force and shaking moment balancing of planar mechanisms by different methods based on the generation of movements of counterweights. Methods based on copying properties of pantograph system that carry counterweights (formed by gear or toothed belt transmissions) are proposed. It executes a movement exactly opposite to the movement of the total center of movable link masses. Such solution provides dynamic balancing with a relatively small increase of total mass of the movable link.

Marcelin (2005) examined the possibility of using genetic algorithms for the optimization of the loads transmitted through the connections of the mechanisms. The objective function is the square root of the quadratic sum of all the components of loads and moments of all the connections (joints). The design variables are the relative positions of various connections.

Kuckus and Bingul (2006) reported on link mass optimization using genetic algorithms for industrial robot manipulators. It is applied to optimize the link masses of a three link robot manipulator with two revolute joint and one prismatic joint to obtain minimum energy performance.

Kim (2006) presented the task based kinematic design of a two degree of freedom robot with a parallelogram five-bar link mechanism. Task-based design determines the kinematic and dynamic design parameters such as the dimensions and the mass of each link and DOF using optimality criteria. Further, the type of a manipulator is also decided based on task and manipulator specifications using the optimality criteria. The optimality criteria used are dexterity and cost. The genetic algorithm with excellent convergence criteria is used for optimization.

Nguyen (2007) presented the balancing conditions for a spatial mechanism. The balancing conditions for shaking force and shaking moment of spatial one DOF mechanisms are derived algebraically. The balancing conditions for shaking force and shaking moment of slider crank mechanism are presented in this research.

Chaudhary and Saha (2007) presented minimization of constraint forces in industrial manipulators. The minimization of constraint forces improves the dynamic performance of an industrial manipulator. An optimization method is proposed using the concept of dynamically equivalent system of point masses. A seven point-mass model in parallelepiped configuration is used. It is applied to six DOF PUMA robot to demonstrate that the constraint forces are substantially reduced.

Chaudhary and Saha (2007) presented balancing of four bar linkage using the maximum recursive dynamic algorithm. The technique presented is simple and computationally efficient for optimum balancing of four-bar linkages. It is based on

the maximum recursiveness of the dynamic equations for the evaluation of bearing forces. Mass distribution of linkage is embedded in constraints. Dynamically equivalent system of a rigid link comprises of two point masses.

Verschuure (2008) proposed the optimization of counter weight parameters for balancing of spatial mechanisms that result in minimal forces and moments under constrained driving torque. The optimization problem can be reformulated as a convex problem using voxel -based discretizations. It results in counter weight shapes that can be easily implemented. It is applied to RSSR four bar spatial mechanism.

Chaudhary and Saha (2008) presented balancing of shaking forces and shaking moments for planar mechanisms using the equimomental systems. The concept of a dynamically equivalent system of point masses is used here to represent the rigid links. A set of three equimomental point masses is used for each link. In order to determine shaking forces and shaking moments, the dynamic equations of motion are formulated in terms of point mass parameters. It leads to optimization for mass distribution to improve the dynamic performance of the mechanisms.

Arakelian and Smith (2008) presented the design of a planar 3 DOF 3-RRR reaction less parallel manipulators. Design equations and techniques are proposed which allows the dynamic substitution of the moving platform of a parallel manipulator by three concentrated masses. The total angular momentum of the manipulator can be reduced to zero using either counter rotations or inertia flywheel rotating with prescribed velocity.

Chaudhary and Saha (2008) presented optimization technique for the balancing of spatial mechanisms. The shaking forces and shaking moments induced due to inertia forces are optimized for a spatial mechanism. For a given link, the inertia forces

20

induced are dependent on the mass distribution of the link and its speed of operation. The equimomental system of seven point masses in parallelepiped configuration is used to represent inertial properties of links and to identify optimizing variables. It is applied on spatial RSSR mechanism. Mass redistribution of links offers the advantage over counterweight balancing without weight addition.

Wijk et. al. (2009) presented the comparison of various dynamic balancing principles regarding additional mass and inertias. It is stated that the major disadvantage of existing balancing principles is that a considerable amount of mass and inertia is added to the system. The existing balancing principles are applied to double pendulum for comparison, both analytically and numerically. It is reported that the duplicate mechanism principle offers the dynamic balancing with minimum addition of mass and inertia to the system if available space is not a limiting factor. Using the force balancing counter masses as moment balancing counter inertias leads to less mass addition compared to use of separate counter rotations. Balancing the mechanism altogether is more advantageous.

Briot and Arakelian (2009) presented the complete shaking force and shaking moment balancing of the position oriented decoupled PAMINSA manipulator. The dynamic reaction forces on the frame are eliminated by making the mass center of moving links stationary. The reaction moments are eliminated by optimal control of end effector, which rotates with prescribed velocity.

Farmani et. al. (2011) presented the multi-objective optimization for force and moment of a four -bar linkage using evolutionary algorithms. The concept of inertia counterweights and physical pendulum are used completely to balance the mass effects independent of input angular velocity. The particle swarm optimization and

non-dominated genetic algorithm are applied to minimize multi-objective functions subjected to design constraints. Optimal solution minimizes the counter weights and eliminates the shaking forces and shaking moments transmitted to the ground.

Wijk et. al. (2012) presented the comparative analysis for low-mass and low-inertia dynamic balancing of a mechanism. The main disadvantage of dynamic balancing is the considerable increase in mass and inertia. Evaluation of a balanced rotatable link is most crucial for comparison. A rotatable link is balanced by either of, duplicate mechanism, counter mass, separate counter rotation (SCR) and counter rotary counter mass (CRCM). The duplicate mechanism offers the best compromise for low-mass and low-inertia but requires a considerable space. Though, CRCM and SCR balanced link are more compact. However, there is a trade-off between mass and inertia for which CRCM balanced link is the better of the two.

Nehemiah et. al. (2012) proposed the complete shaking force and shaking moment balancing of complex planar mechanisms. Shaking force is balanced by the redistribution of mass and shaking moment by adding gear inertia counterweights. The conditions for shaking moment balancing are formulated by copying properties of pantograph linkage and the method of dynamic substitution of distribution masses with concentrated point masses. It is applied to complex Stephenson's linkage.

Erkaya (2013) investigated the balancing of a planar mechanism using the genetic algorithm. Balancing of a four-bar mechanism is formulated as an optimization problem. Optimization function consists of sub-components of shaking force and shaking moment, and the design variables are kinematic and dynamic parameters of linkage. A Genetic algorithm is used to solve the optimization problem.

The major research gaps revealed based on literature survey are as follows:

1. The different point-mass configurations to provide positive value to equimomental point masses not explored.

2. Shaking moment/force minimization is an optimization problem. Industrial manipulators requiring least constraint moment/force at different joints are needed to develop economic manipulators for industrial use.

3. Dynamic balancing by internal mass redistribution can be more effective than adding devices like gears, mechanism etc.

4. Recently developed evolutionary optimization technique such as Teaching-Learning-based- Optimization (TLBO) is not explored for optimization of industrial manipulators.

2.3 Teaching-learning-based-optimization technique

Rao et al. (2011, 2012, 2013) proposed a novel method called "Teaching- learning-based optimization" (TLBO) for designing mechanical components. It does not require any algorithm parameter to be tuned, as required in the evolutionary algorithm such as a genetic algorithm. It makes the implementation simpler. TLBO uses the best solution of the current iteration to change the existing solution in the population, thereby increasing the convergence rate. It is newly developed optimization algorithm that has been used for various optimization problems like constrained mechanical design optimization, multi-objective unconstrained & constrained functions, to solve complex benchmark functions & difficult engineering problems.

Tayfun (2013, 2014) presented the use of TLBO for discrete optimization of truss structures and optimal design of grillage structures. Satpathy et. al. (2013) presented the use of TLBO based orthogonal design for solving the global optimization problem.

Kunjir Yu (2014) proposed an improved TLBO for solving numerical and engineering optimization problems. In this, a feedback phase, mutation crossover operation of differential evolution algorithms, and chaotic perturbation mechanism are incorporated to improve the performance of algorithm significantly.

Debai Chen et. al. (2014) proposed TLBO with Producer-Scrounger (PS) model for global optimization. In this study, the swarm is divided in three parts: producer, scroungers, and remainders. The producer is the best individual selected from the current population, and it exploits new solution with a random angle and maximum radius. Some individuals different from the producer are randomly selected according to pre-defined probability as scroungers. The scroungers update their position with an area-copying operator which is used in PS model. Computation cost of this modified TLBO is less than that of original TLBO.

Panwar and Rao (2013), Rao and Kalyankar (2014), Keesari and Rao (2013), used TLBO for optimizing process parameters and also to solve the job shop scheduling problem. Yeldiz (2013) presented Optimization of multi-pass turning operations using hybrid teaching-learning approach. Adil et. al.(2014) and Yu et. al. (2015) reported using TLBO to solve the job shop scheduling problem.

2.4 Research Objectives

Based on the gaps revealed by literature survey, the following major research objectives are identified.

1. Exploring different point-mass configuration that ensures positive value to equimomental point-masses to facilitate link shape formulation.

2. Optimization scheme to minimize shaking moment/force in industrial manipulators using internal mass redistribution.

3. Explore use of recently developed evolutionary optimization technique such as TLBO for optimization of industrial manipulators.

2.5 Summary

Dynamic balancing of shaking force and its effect on other dynamic quantities are reviewed in Section 2.1. It is observed by many researchers that balancing of shaking force alone is not useful as it increases shaking moment and driving torque in the mechanism. Dynamic balancing of shaking force and shaking moment, and driving torque reduction in mechanisms and robotic manipulators is reviewed in Section 2.2.Some reviews on dynamic balancing show that there will be no clear-cut method for static and dynamic balancing. Several works of literature are very specific (generally with the addition of weight as balancers) and applicable to the mechanisms (mostly planar mechanism). A generalized methodology is not available which can be applied to all types of mechanisms, particularly open loop spatial mechanisms. Therefore, various optimization methods for simultaneous minimization of the shaking force and the shaking moment are also explored and reviewed in section 2.2. However, the methods used for balancing the flexible mechanisms are excluded in this section. It is observed that relatively less literature is reported on the generalized methodology for dynamic balancing of spatial mechanisms, specifically on industrial manipulators. Even in the literature reported, the dynamic balancing of shaking force and shaking moment adds to mass and inertia of the linkage in most of the cases. However, in very few it is achieved by the redistribution of the mass of the link without adding additional mass. It reduces the shaking moment which is dependent on the inertia of link. The equimomental point masses model suggested in available literature involves negative point mass values. It is likely to result in enormous

difficulty in shape optimization of the link. Equimomental point mass model with the positive value for point masses would be helpful in link shape optimization. Recent literature indicates that evolutionary technique genetic algorithm is used by many researchers in the optimization of spatial and industrial manipulator linkages [17, 27, 29 and 39]. The literature available on the teaching-learning based optimization (TLBO) technique, which is developed recently in 2011, is reviewed in section 2.3. In recent years its use in optimization is reported in different areas [64-74].

Chaudhary and Saha proposed seven point-masses model in parallelepiped configuration, but it involves negative point masses. Further, seven point-masses model with equal point- masses along three coordinate axes is proposed by Rahman for the slider-crank mechanism. However, so far no one has proposed the use of six and five point-masses hexahedron model or four point-masses model for representing a rigid link in terms of the point-mass model with positive point-mass values for spatial linkages. So far there is no literature reported on using TLBO for optimization of dynamic balancing of industrial manipulators. It justifies the research objectives identified in section 2.4.

Point-mass Models

Consideration of the inertia induced shaking force, shaking moment and driving torque of a manipulator are important for designers. These dynamic quantities depend on the mass and inertia of its moving links, thus on the mass, location of its mass center and mass distribution. These inertia properties can be represented more conveniently using the dynamically equivalent system of point masses. The dynamically equivalent system is also referred as the equimomental system. The concept of the dynamically equivalent system is elaborated by Sherwood et al. [23]. In order to dynamically balance industrial manipulators, the concept of the equimomental system of point-mass is introduced, and the various dynamically equivalent point-masses systems possible to represent links of a robot are proposed a new in this chapter. The configurations ensures positive value to all point-masses.

3.1 Equimomental systems for spatial motion
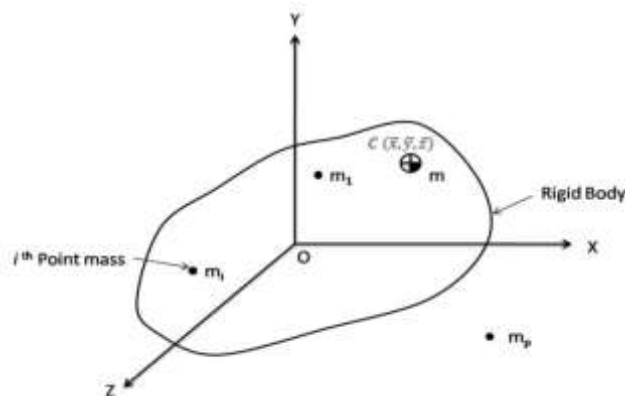
Fig. 3.1 Equimomental system of a rigid body in spatial motion

A rigid body, having mass m, Cartesian coordinates of mass center $(\bar{x}, \bar{y}, \bar{z})$, moments of inertia, I_{xx}, I_{yy}, I_{zz}, and the products of inertia, I_{xy}, I_{yz}, I_{zx} is considered as shown in Fig. 3.1.The coordinates of the mass center location and the inertias are

taken in body fixed frame, OXYZ. Let, the rigid body be discretized in a set of p point-mass, which are rigidly fixed to the body fixed frame at locations (x_i, y, z_i), for $i = 1, 2, ..., p$. There is a set of ten conditions to be satisfied to represent the rigid link dynamically equivalent to the set of point-masses. These conditions are (i) The total mass of all point masses, (ii) The mass center of point- masses, and (iii) The mass moment of inertia and product moment of inertias of the set of point- masses and link must be same. To find the values of point-masses and their location using above ten conditions, the different set of point-mass are explored in this chapter. We can have a minimum of four point masses. The ten equimomental conditions are expressed mathematically as follows:

$$\sum_{i=1}^{p} m_i = m \tag{3.1}$$

$$\sum_{i=1}^{p} m_i x_i = m\,\bar{x} \tag{3.2}$$

$$\sum_{i=1}^{p} m_i y_i = m\bar{y} \tag{3.3}$$

$$\sum_{i=1}^{p} m_i z_i = m\,\bar{z} \tag{3.4}$$

$$\sum_{i=1}^{p} m_i(y_i^2 + z_i^2) = I_{xx} \tag{3.5}$$

$$\sum_{i=1}^{p} m_i(x_i^2 + z_i^2) = I_{yy} \tag{3.6}$$

$$\sum_{i=1}^{p} m_i(x_i^2 + y_i^2) = I_{zz} \tag{3.7}$$

$$\sum_{i=1}^{p} m_i x_i y_i = I_{xy} \tag{3.8}$$

$$\sum_{i=1}^{p} m_i y_i z_i = I_{yz} \tag{3.9}$$

$$\sum_{i=1}^{p} m_i x_i z_i = I_{xz} \tag{3.10}$$

The different point mass configurations presented below represent the dynamically equivalent point-masses systems for a given link.

3.2 Seven point-mass octahedron model

Each link is treated as the dynamically equivalent system of point masses to distribute link masses optimally. A set of seven point masses in octahedron configuration as shown in Figs. 3.2 represent the links dynamically. Body fixed frame $x_i y_i z_i$ is fixed to ith link at its mass center and axes x_i, y_i, z_i are principal axes. It is assumed that six point masses, m_{ij}, are located at the vertices of an octahedron. Subscripts i and j denote the ith link and its jth point mass, respectively. The remaining seventh point mass is assumed to be located at the mass center of the link. The point masses are rigidly fixed to the frame $x_i y_i z_i$. The two systems, rigid link and the system of seven point masses in octahedron configuration, are dynamically equivalent. If (i) the sum of all point-masses equals the mass of link, (ii) the mass center of the set of point masses coincides with the mass center of the rigid link, and (iii) the moment of inertias and product of inertias for distributed point-masses is same as that of rigid link. These conditions are known as equimomental conditions for the ith link.
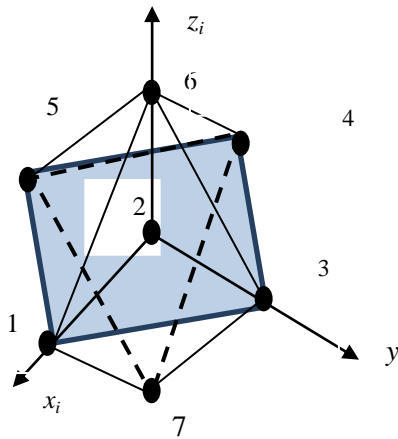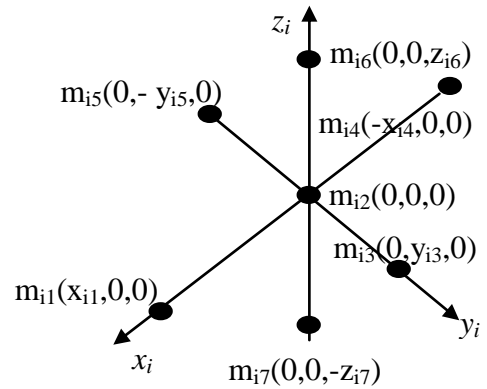
(a) Octahedron model   **(b) Coordinates of point masses**

Figure 3.2: Seven point-mass Octahedron Model

The mass, m_i, mass center coordinates ($\bar{x}_i$, $\bar{y}_i$, $\bar{z}_i$), the moment of inertia ($I_{ixx}, I_{iyy}, I_{izz}$) and the product of inertia ($I_{ixy}, I_{iyz}, I_{izx}$) are defined for the ith link. The coordinates (x_{ij}, y_{ij}, z_{ij}) of point mass m_{ij} are defined for j^{th} point mass of ith link. Assuming equal point masses at equidistance on either side of axes x_i, y_i and z_i, we get

$$m_{i1} = m_{i4}, m_{i3} = m_{i5} and m_{i6} = m_{i7} \tag{3.11}$$

$$x_{i1} = -x_{i4}, y_{i3} = -y_{i5} and z_{i6} = -z_{i7} \tag{3.12}$$

The point mass m_{i2} is placed at the mass center of the link. Since the other point masses are placed on axes, their other coordinates are zeros. These assumptions lead product of inertias zero while x_i, y_i and z_i become principal axes of the ith link. The mass center also is at the origin, i.e., $\bar{x}_i = \bar{y}_i = \bar{z}_i = 0$. This arrangement automatically satisfies the six equimomental conditions about location of center of mass and product of inertias, the remaining four conditions of total mass and inertia about three axes give:

$$m_i = 2m_{i1} + m_{i2} + 2m_{i3} + 2m_{i6} \tag{3.13}$$

$$I_{ixx} = 2m_{i3}y_{i3}^2 + 2m_{i6}z_{i6}^2 \tag{3.14}$$

$$I_{iyy} = 2m_{i1}x_{i1}^2 + 2m_{i6}z_{i6}^2 \tag{3.15}$$

$$I_{izz} = 2m_{i1}x_{i1}^2 + 2m_{i3}y_{i3}^2 \tag{3.16}$$

Eqs.(3.13) – (3.16) contain 7 unknowns, four point masses $m_{i1}, m_{i2}, m_{i3}, m_{i6}$, and three coordinates x_{i1}, y_{i3}, z_{i6}. Assuming $m_{i1} = m_{i3} = m_{i6} = \alpha m_i$, Eqs. (3.13) – (3.16) give:

$$m_{i2} = (1 - 6\alpha)m_i \tag{3.17}$$

$$x_{i1}^2 = (I_{iyy} + I_{izz} - I_{ixx})/4\alpha m_i \tag{3.18}$$

30

$$y_{i3}^2 = (I_{ixx} + I_{izz} - I_{iyy})/4\alpha m_i \tag{3.19}$$

$$z_{i6}^2 = (I_{ixx} + I_{iyy} - I_{izz})/4\alpha m_i \tag{3.20}$$

Where, a constant α must satisfy $1 > (1 - 6\alpha) > 0$, i.e. , $\alpha < 1/6$.

Finally, if we know the mass and inertias of the rigid link, the unknown parameters of the point mass system can be computed using Eqs. (3.17-3.20).Such system of point-mass is dynamically equivalent to the rigid link.

3.3 Six point–mass hexahedron model

Similar to the seven point-mass model in octahedron configuration, six point-mass model is defined in hexahedron configuration as shown in Fig. 3.3.

(a) Hexahedron model   **(b) Coordinates of point-masses**
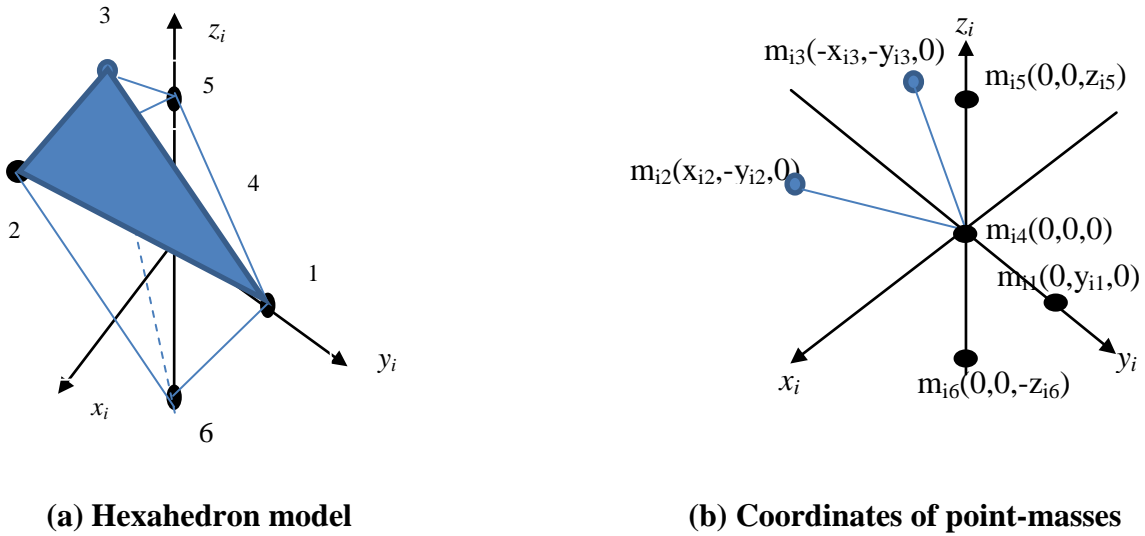
Figure 3.3: Six point – mass hexahedron model

For six point-mass model the following relationships of point masses and their distances along axes x_i y_i and z_i are assumed to place the mass center of six point masses in hexahedron configuration at the mass center of the link .

$$m_{i1} = 2m_{i2} = 2m_{i3} \ and \ m_{i5} = m_{i6} \tag{3.21}$$

$$x_{i2} = -x_{i3} \,, y_{i1} = -y_{i2} = -y_{i3} \ and \ z_{i5} = -z_{i6} \tag{3.22}$$

Since, all other coordinates are zeros for point masses 1,4,5 and 6 as shown in Fig. 3.3 and the location of masses 2 and 3 being symmetric hence the product of inertias become zero. x_i, y_i and z_i are principal axes of the ith link and the mass center is at the origin, i.e., $\bar{x}_i = \bar{y}_i = \bar{z}_i = 0$. This arrangement automatically satisfies the six equimomental conditions about center of mass and product of inertias, the remaining four conditions of total mass and inertia about three axes gives:

$$m_i = 2m_{i1} + m_{i4} + 2m_{i5} \tag{3.23}$$

$$I_{ixx} = 2m_{i1}y_{i1}^2 + 2m_{i5}z_{i5}^2 \tag{3.24}$$

$$I_{iyy} = m_{i1}x_{i2}^2 + 2m_{i5}z_{i5}^2 \tag{3.25}$$

$$I_{izz} = m_{i1}x_{i2}^2 + 2m_{i1}y_{i1}^2 \tag{3.26}$$

Eqs. (3.23) – (3.26) contain 6 unknowns, three point masses m_{i1}, m_{i4}, m_{i5}, and three coordinates x_{i2}, y_{i1}, z_{i5} . Assuming $m_{i1} = 2m_{i5} = \alpha m_i$, Eqs. (3.23) – (3.26) gives :

$$m_{i4} = (1 - 3\alpha)m_i \tag{3.27}$$

$$x_{i2}^2 = (I_{iyy} + I_{izz} - I_{ixx})/2\alpha m_i \tag{3.28}$$

$$y_{i1}^2 = (I_{ixx} + I_{izz} - I_{iyy})/4\alpha m_i \tag{3.29}$$

$$z_{i5}^2 = (I_{ixx} + I_{iyy} - I_{izz})/2\alpha m_i \tag{3.30}$$

Where, a constant α must satisfy, $1 > (1 - 3\alpha) > 0$, i.e. , $\alpha < 1/3$.

Finally, knowing the mass and inertias of the rigid link, Eqs.(3.27) – (3.30) provide unknown parameters of the point mass system. Such a system of point-mass is dynamically equivalent to a rigid link.

3.4 Five point – mass hexahedron model

Similar to the seven point-mass model in octahedron configuration, five point mass model is defined in hexahedron configuration as shown in Fig. 3.4.For five point mass

model the following relationships of point masses and their distances along axes x_i, y_i and z_i, are assumed to place the mass center of five point masses in hexahedron configuration at the mass center of the link .

$$m_{i1} = 2m_{i2} = 2m_{i3} \text{ and } m_{i4} = m_{i5} \tag{3.31}$$

$$x_{i2} = -x_{i3}, y_{i1} = -y_{i2} = -y_{i3} \text{ and } z_{i4} = -z_{i5} \tag{3.32}$$
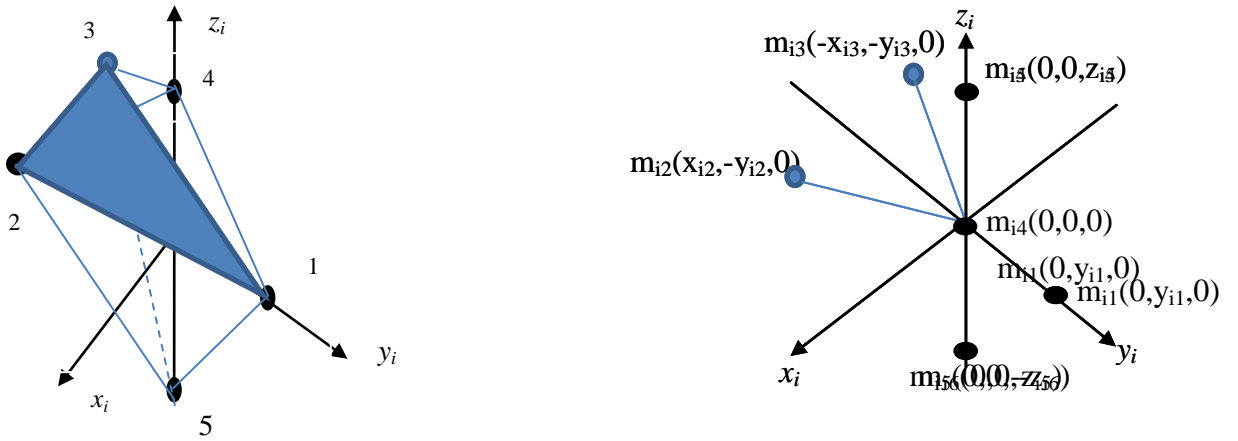
| (a) Hexahedron model | (b) Coordinates of point-masses |

Figure 3.4: Five point – mass hexahedron model

Since, all other coordinates are zeros for point masses 1,4 and 5 as shown in Fig. 3.4 and the location of masses 2 and 3 being symmetric, hence the product of inertias become zero. x_i, y_i and z_i are principal axes of the ith link and the mass center is at the origin, i.e., $\bar{x}_i = \bar{y}_i = \bar{z}_i = 0$. This arrangement automatically satisfies the six equimomental conditions about center of mass and product of inertias, the remaining four conditions of total mass and inertia about three axes give:

$$m_i = 2m_{i1} + 2m_{i4} \tag{3.33}$$

$$I_{ixx} = 2m_{i1}y_{i1}^2 + 2m_{i5}z_{i4}^2 \tag{3.34}$$

$$I_{iyy} = m_{i1}x_{i2}^2 + 2m_{i5}z_{i4}^2 \tag{3.35}$$

$$I_{izz} = m_{i1}x_{i2}^2 + 2m_{i1}y_{i1}^2 \tag{3.36}$$

Eqs. (3.33) − (3.36) contain 5 unknowns, two point masses m_{i1}, m_{i4}, and three coordinates x_{i2}, y_{i1}, z_{i5}. Assuming $2m_{i4} = m_{i1}$, Eq. (3.33) − (3.36) gives:

$$m_{i1} = m_i \div 3 \tag{3.37}$$

$$x_{i2}^2 = 3(I_{iyy} + I_{izz} - I_{ixx})/2m_i \tag{3.38}$$

$$y_{i1}^2 = 3(I_{ixx} + I_{izz} - I_{iyy})/4m_i \tag{3.39}$$

$$z_{i4}^2 = 3(I_{ixx} + I_{iyy} - I_{izz})/2m_i \tag{3.40}$$

Finally, the mass and inertias of the rigid link are known, Eqs. (3.37) − (3.40) provide unknown parameters of the point mass system. Such a system of point-mass is dynamically equivalent to a rigid link.

3.5 Four point–mass model

Four point-mass model is defined in parallelepiped configuration as shown in Fig. 3.5.
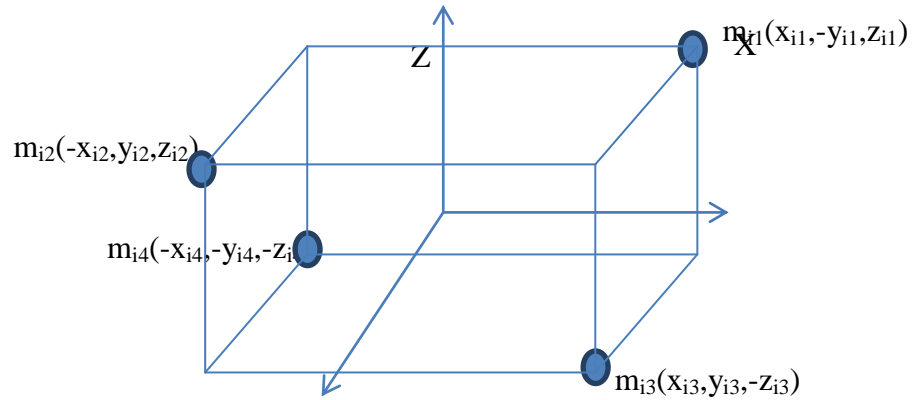
Figure 3.5: Four point – mass model

For four point mass model the following relationships of point masses and their distances along axes x_i, yi and z_i, are assumed to place mass center of four point masses at the mass center of the link .

$$m_{i1} = m_{i2} = m_{i3} = m_{i4} \tag{3.41}$$

$$x_{i1} = -x_{i2} = x_{i3} = -x_{i4}, \quad y_{i1} = -y_{i2} = -y_{i3} = y_{i4}$$

and $z_{i1} = z_{i2} = -z_{i3} = -z_{i4}$ \hfill (3.42)

With above assumptions, the point-masses and their co-ordinates can be expressed as

$,m_{i1}(x_{i1}, -y_{i1}, z_{i1}), m_{i1}(x_{i1}, -y_{i1}, z_{i1}), m_{i1}(x_{i1}, y_{i1}, -z_{i1}), m_{i1}(-x_{i1}, -y_{i1}, -z_{i1})$. It

makes product of inertias zero. The axes x_i y_i and z_i become principal axes for the ith

link and the mass center is at the origin, i.e., $\bar{x}_i = \bar{y}_i = \bar{z}_i = 0$. This arrangement

automatically satisfies the six equimomental conditions pertaining to center of mass

and product of inertias, the remaining four conditions of total mass and inertia about

three axes give:

$$m_i = 4m_{i1} \hspace{4cm} (3.43)$$

$$I_{ixx} = 4m_{i1}y_{i1}^2 + 4m_{i1}z_{i1}^2 \hspace{3cm} (3.44)$$

$$I_{iyy} = 4m_{i1}x_{i1}^2 + 4m_{i1}z_{i1}^2 \hspace{3cm} (3.45)$$

$$I_{izz} = 4m_{i1}x_{i1}^2 + 4m_{i1}y_{i1}^2 \hspace{3cm} (3.46)$$

Eqs. (3.43) – (3.46) contain 4 unknowns, one point masses m_{i1} and three coordinates

x_{i1}, y_{i1}, z_{i1}, we get:

$$m_{i1} = m_i / 4 \hspace{4cm} (3.47)$$

$$x_{i1}^2 = (I_{iyy} + I_{izz} - I_{ixx})/2m_i \hspace{2.5cm} (3.48)$$

$$y_{i1}^2 = (I_{ixx} + I_{izz} - I_{iyy})/2m_i \hspace{2.5cm} (3.49)$$

$$z_{i1}^2 = (I_{ixx} + I_{iyy} - I_{izz})/2m_i \hspace{2.5cm} (3.50)$$

Finally, the mass and inertias of rigid link are known, Eqs. (3.47) – (3.50) provide

unknown parameters of the point mass system. Such a system of point-masses is

dynamically equivalent to a rigid link.

3.6 Example for Equimomental point masses
We take six degree of freedom PUMA Robot, whose details are available in the

published literature [43], as an example. The masses and inertias of six different links

of the robot are as given below:

Table 3.1: Mass and inertias about center of mass for six degree of freedom PUMA

robot

Link	Link Mass (kg)	I_{xx} (kg-m^2)	I_{yy} (kg-m^2)	I_{zz} (kg-m^2)	I_{xy} (kg-m^2)	I_{yz} (kg-m^2)	I_{xz} (kg-m^2)
1	10.521	1.612	1.612	0.5091	0.0	0.0	0.0
2	15.761	0.4898	8.0783	8.2672	0.0	0.0	0.0
3	8.767	3.3768	3.3768	0.3009	0.0	0.0	0.0
4	1.052	0.1810	0.1273	0.1810	0.0	0.0	0.0
5	1.052	0.0735	0.1273	0.0735	0.0	0.0	0.0
6	0.351	0.0071	0.0071	0.0141	0.0	0.0	0.0

Table 3.2: Equimomental Point masses for 7 point mass model taking α = 1/8 (in Kg)

Link	Link mass	m_{i1}	m_{i2}	m_{i3}	m_{i4}	m_{i5}	m_{i6}	m_{i7}	Point mass sum
1	10.52	1.315	2.630	1.315	1.315	1.315	1.315	1.315	10.52
2	15.76	1.970	3.940	1.970	1.970	1.970	1.970	1.970	15.76
3	8.77	1.096	3.192	1.096	1.096	1.096	1.096	1.096	8.77
4	1.052	0.131	0.263	0.1315	0.1315	0.1315	0.1315	0.1315	1.052
5	1.052	0.131	0.263	0.1315	0.1315	0.1315	0.1315	0.1315	1.052
6	0.351	0.088	0.175	0.0877	0.0877	0.0877	0.0877	0.0877	0.351

Table 3.3: Coordinates of the Point masses for 7 point mass model (in meters)

Link	x_{i1}	y_{i3}	z_{i6}	x_{i4}	y_{i5}	z_{i7}
1	0.31109	0.31109	0.71839	-0.31109	-0.31109	-0.71839
2	1.41846	0.29347	0.19540	-1.41846	-0.29347	-0.19540
3	0.26200	0.26200	1.21328	-0.26200	-0.26200	-1.21328
4	0.49195	0.66798	0.49195	-0.49195	-0.66798	-0.49195
5	0.49195	0.66798	0.49195	-0.49195	-0.19353	-0.49195
6	0.28345	0.28345	0.02387	-0.28345	-0.28345	-0.02387

Table 3.4: Equimomental Point masses for 6 point mass model taking α =1/4 (in Kg)

Link	Link mass	m_{i1}	m_{i2}	m_{i3}	m_{i4}	m_{i5}	m_{i6}	Point mass sum
1	10.521	2.6302	1.3151	1.3151	2.6302	1.3151	1.3151	10.521
2	15.761	3.9402	1.9701	1.9701	3.9402	1.9701	1.9701	15.761
3	8.767	3.1918	1.0959	1.0959	3.1918	1.0959	1.0959	8.767
4	1.052	0.2630	0.1315	0.1315	0.2630	0.1315	0.1315	1.052
5	1.052	0.2630	0.1315	0.1315	0.2630	0.1315	0.1315	1.052
6	0.351	0.1754	0.0877	0.0877	0.1754	0.0877	0.0877	0.351

Table 3.5: Coordinates of the Point masses for 6 point mass model (in meters)

Link	x_{i2}	y_{i1}	z_{i5}	x_{i3}	$y_{i2} = y_{i3}$	z_{i6}
1	0.31109	0.21997	0.50798	-0.31109	-0.21997	-0.50798
2	1.41846	0.20751	0.14490	-1.41846	-0.20751	-0.14490
3	0.26200	0.18526	0.87769	-0.26200	-0.18526	-0.87769
4	0.49195	0.47233	0.34786	-0.49195	-0.47233	-0.34786
5	0.49195	0.47233	0.34786	-0.49195	-0.13684	-0.34786
6	0.28345	0.20043	0.01688	-0.28345	-0.20043	-0.01688

Table 3.6: Equimomental Point masses for 5 point mass model (in Kg)

Link	Link mass	m_{i1}	m_{i2}	m_{i3}	m_{i4}	m_{i5}	Point mass sum
1	10.521	3.5070	1.7535	1.7535	1.7535	1.7535	10.521
2	15.761	5.2537	2.6268	2.6268	2.6268	2.6268	15.761
3	8.767	2.9223	1.4612	1.4612	1.4612	1.4612	8.767
4	1.052	0.3507	0.1753	0.1753	0.1753	0.1753	1.052
5	1.052	0.3507	0.1753	0.1753	0.1753	0.1753	1.052
6	0.351	0.1170	0.0585	0.0585	0.0585	0.0585	0.351

Table 3.7: Coordinates of the Point masses for 5 point mass model (in meters)

Link	x_{i2}	y_{i1}	z_{i4}	x_{i3}	$y_{i2} = y_{i3}$	z_{i5}
1	0.26941	0.19050	0.62215	-0.26941	-0.19050	-0.62215
2	1.50352	0.17971	0.16922	-1.50352	-0.17971	-0.16922
3	0.22690	0.16044	1.05073	-0.22690	-0.16044	-1.05073
4	0.42604	0.40905	0.42604	-0.42604	-0.40905	-0.42604
5	0.42604	0.40905	0.42604	-0.42604	-0.11851	-0.42604
6	0.24547	0.17357	0.02067	-0.24547	-0.17357	-0.02067

Table 3.8: Equimomental Point masses (in kg) and Coordinates (in meters) of the four

point mass model

Link	Link mass	$m_{i1} = m_{i2} = m_{i3} = m_{i4}$	x_{i1}	y_{i1}	z_{i1}
1	10.521	2.6302	0.15555	0.15555	0.35920
2	15.761	3.9402	0.70923	0.14345	0.10246
3	8.767	2.1918	0.13100	0.13100	0.60664
4	1.052	0.2630	0.24597	0.33399	0.24597
5	1.052	0.2630	0.24597	0.09676	0.24597
6	0.351	0.1754	0.20085	0.20085	0.01194

3.7 Summary

In this chapter, the equimomental point-mass values, and their locations are obtained for various point-mass configurations i.e. seven point-mass octahedron model, six point-mass hexahedron model, five point mass hexahedron model, and four point-mass model. Finally, the equimomental point-mass values and their locations for PUMA robot is obtained and tabulated for these four types of models.

Dynamic Analysis

Mechanical systems are generally classified as open-loop (serial and/or tree type) and closed-loop type based on their composition/architecture. Industrial manipulators fall under the category of the open-loop type system. In this chapter, the dynamic formulation, i.e., the equations of motion for the robot (open-loop system) is presented that is used to compute reaction forces and moments at the joints. It is based on Newton-Euler equations of motion being derived with respect to the links frame. Since, we have represented rigid links in terms of equimomental point-masses systems in chapter 3, the dynamic formulation for point-masses system is presented here. Further, dynamic analysis of n degrees of freedom serial manipulator is done and the expressions for shaking forces and shaking moments are derived.

4.1 Dynamic analysis of a serial industrial manipulator

An n-link, n-DOF, open-loop serial-chain robot manipulator, such as PUMA robot, can be represented as open-loop (serial type) system shown in Fig. 4.1.
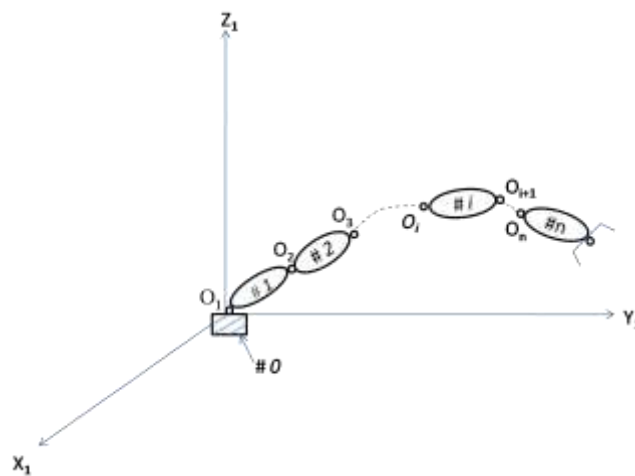
Fig. 4.1: Serial Open-loop System, Manipulator

If m_i is the mass of the ith link and $\mathbf{I_i^c}$ denotes the 3x3 inertia tensor of the ith link about its mass center C_i, the Newton-Euler (NE) equations of motion for the ith link are written as

Newton's Equation: $\mathbf{f}_i^c = m_i \dot{\mathbf{v}}_i^c$ \hfill (4.1)

Euler's Equation: $\quad \mathbf{n}_i^c = \mathbf{I}_i^c \dot{\boldsymbol{\omega}}_i + \tilde{\boldsymbol{\omega}}_i \mathbf{I}_i^c \boldsymbol{\omega}_i$ \hfill (4.2)

Where $\mathbf{n}_i^c$ is the resultant of all external moments about its mass center C_i, and $\mathbf{f}_i^c$ is the resultant force acting at C_i. The cross-product of angular velocity with any vector $\vec{X}$ is defined as $\tilde{\boldsymbol{\omega}}_i = \vec{\boldsymbol{\omega}}_i \times \vec{X}$.

The velocity $\mathbf{v}_i$ and acceleration $\dot{\mathbf{v}}_i$ of origin O_i are then obtained from velocity and acceleration of mass center as:

$$\mathbf{v}_i = \mathbf{v}_i^c + \tilde{\mathbf{d}}_i \boldsymbol{\omega}_i \hfill (4.3)$$

$$\dot{\mathbf{v}}_i = \dot{\mathbf{v}}_i^c + \tilde{\mathbf{d}}_i \dot{\boldsymbol{\omega}}_i + \tilde{\boldsymbol{\omega}}_i \tilde{\mathbf{d}}_i \boldsymbol{\omega}_i \hfill (4.4)$$

Where vector $\mathbf{d}_i$ is from origin O_i to mass center C_i .

The applied moment and force, $\mathbf{n}_i$ and $\mathbf{f}_i$ w.r.t O_i respectively are then obtained from that w.r.t. C_i as:

$$\mathbf{n}_i = \mathbf{n}_i^c + \mathbf{d}_i \times \mathbf{f}_i^c \hfill (4.5)$$

$$\mathbf{f}_i = \mathbf{f}_i^c \hfill (4.6)$$

Where, $\boldsymbol{\omega}_i$, $\mathbf{v}_i$, $\mathbf{n}_i$ and $\mathbf{f}_i$, are the angular velocity, linear velocity, the resultant moment, and the resultant force acting on the ith link, respectively, at O_i of the link.

Using Eqs. 4.1, 4.3 and 4.6, we get

$$\mathbf{f}_i = m_i \dot{\mathbf{v}}_i - m_i \tilde{\mathbf{d}}_i \dot{\boldsymbol{\omega}}_i - m_i \tilde{\boldsymbol{\omega}}_i \tilde{\mathbf{d}}_i \boldsymbol{\omega}_i \hfill (4.7)$$

Using Eqs. 4.2, 4.5 and 4.6, and $\mathbf{I}_i = \mathbf{I}_i^c - m_i \tilde{\mathbf{d}}_i^2$, we get

$$\mathbf{n}_i = \mathbf{I}_i \dot{\boldsymbol{\omega}}_i + \tilde{\boldsymbol{\omega}}_i \mathbf{I}_i \boldsymbol{\omega}_i + m_i \tilde{\mathbf{d}}_i \dot{\mathbf{v}}_i \hfill (4.8)$$

In order to represent the mass m_i, in terms of the parameters of the point-masses, the ith rigid link is modeled as different point-mass models.
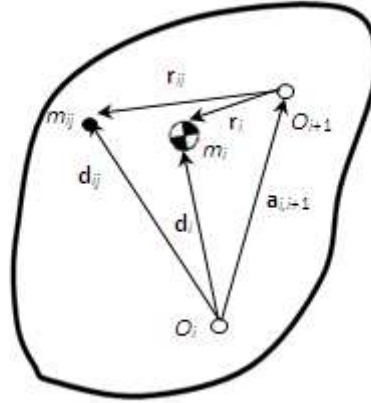
Fig. 4.2 Definitions of vectors

Referring to Fig. 4.2, the vectors, $\mathbf{d}_{ij}$ and $\mathbf{r}_{ij}$, are the positions of the point-mass, m_{ij}, from the origins O_i and O_{i+1}, respectively. Vector $\mathbf{d}_i$ locates the link's mass center. Using the equimomental conditions, i.e. the mass center of point mass system to coincide with mass center of rigid link along all three axes, $\mathbf{d_i}$ is obtained in terms of $\mathbf{d}_{ij}$ as :

$$\mathbf{d}_i = \frac{1}{m_i}\sum_{j=1}^{n} m_{ij}\mathbf{d}_{ij} \tag{4.9}$$

Denoting, $\mathbf{d}_{ij} = [d_{ijx} \quad d_{ijy} \quad d_{ijz}]^{\mathrm{T}}$, the 3×3 skew-symmetric matrix, $\tilde{\mathbf{d}}_i$, associated with the vector, $\mathbf{d}_i$ is given by

$$\tilde{\mathbf{d}}_i = \frac{1}{m_i}\begin{bmatrix} 0 & -\sum_{j=1}^{7} m_{ij}d_{ijz} & \sum_{j=1}^{7} m_{ij}d_{ijy} \\ \sum_{j=1}^{7} m_{ij}d_{ijz} & 0 & -\sum_{j=1}^{7} m_{ij}d_{ijx} \\ -\sum_{j=1}^{7} m_{ij}d_{ijy} & \sum_{j=1}^{7} m_{ij}d_{ijx} & 0 \end{bmatrix} \tag{4.10}$$

Using the conditions of equality for each component of the inertia tensor for the point mass system and the rigid link, the inertia tensor, $\mathbf{I}_i$, about O_i, in terms of the point mass parameters has the following representation:

$$\mathbf{I}_i = \begin{bmatrix} \sum_{j=1}^{n} m_{ij}\left(\mathrm{d}_{ijy}^2 + \mathrm{d}_{ijz}^2\right) & \sum_{j=1}^{n} m_{ij}\mathrm{d}_{ijx}\mathrm{d}_{ijy} & \sum_{j=1}^{n} m_{ij}\mathrm{d}_{ijx}\mathrm{d}_{ijz} \\ \sum_{j=1}^{n} m_{ij}\mathrm{d}_{ijx}\mathrm{d}_{ijy} & \sum_{j=1}^{n} m_{ij}\left(\mathrm{d}_{ijx}^2 + \mathrm{d}_{ijz}^2\right) & \sum_{j=1}^{n} m_{ij}\,\mathrm{d}_{ijy}\mathrm{d}_{ijz} \\ \sum_{j=1}^{n} m_{ij}\,\mathrm{d}_{ijx}\mathrm{d}_{ijz} & \sum_{j=1}^{n} m_{ij}\,\mathrm{d}_{ijy}\mathrm{d}_{ijz} & \sum_{j=1}^{n} m_{ij}\left(\mathrm{d}_{ijx}^2 + \mathrm{d}_{ijy}^2\right) \end{bmatrix} \quad (4.11)$$

4.2 Shaking force and shaking moment

The dynamic balancing of mechanisms is necessary to reduce the amplitude of vibrations of the frame on which the mechanism is mounted due to shaking force and shaking moment. Further, the balancing also helps to obtain the constant speed of the mechanism through smoothening of the high fluctuations in the driving torque/force. We know that the vibration of any system leads to noise, wear, and fatigue, etc. Therefore there is a challenge to reduce all these three quantities, i.e., shaking force, shaking moment, and input torque fluctuations. Shaking force and shaking moment can be balanced, if the mass center of moving link lies at their point of rotation by using counterweights to the moving links. However, it increases the overall mass and inertia of the mechanism. It results in the increase in driving torque and reactions at the joints. Hence, to improve the overall performance, a trade-off between all dynamic quantities is to be made which can be better achieved by reducing the inertia of links through proper mass distribution by treating balancing problem as an optimization problem.

The shaking force is defined as the reaction of the vector sum of all the inertia forces of moving links of the manipulator, and the shaking moment is the reaction of the resultant of the inertia moments and the moment of the inertia forces [43]. The free body diagram of the ith link is given in Fig. 4.3. The shaking force and shaking moment in a manipulator having *n* moving links are given by
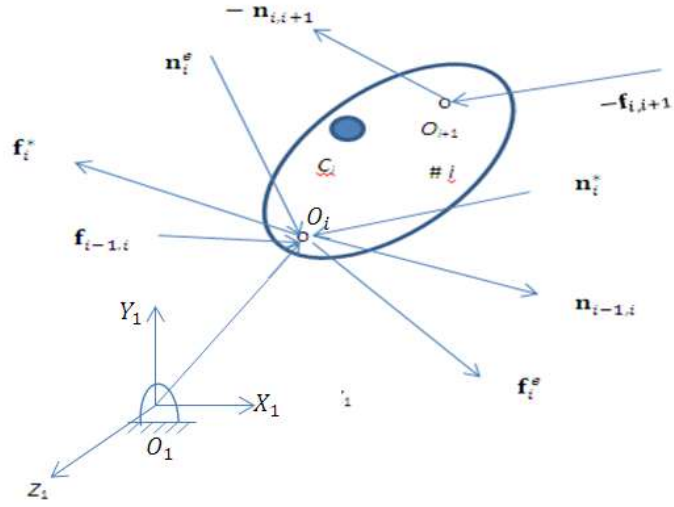
Fig. 4.3 : Free body diagram of the ith Link

$$\mathbf{f}_{sh} = - \sum_{i=1}^{n} \mathbf{f}_i^* \tag{4.12}$$

$$\mathbf{n}_{sh} = - \sum_{i=1}^{n}(\mathbf{n}_i^* + \tilde{\mathbf{a}}_{1,i}\mathbf{f}_i^*) \tag{4.13}$$

Where $\mathbf{f}_i^*$ and $\mathbf{n}_i^*$ are the 3-vectors of inertia force and inertia moment of the ith link acting at and about origin O_i, respectively. The 3×3 matrix, $\tilde{\mathbf{a}}_{1,i}$, is the skew-symmetric matrix corresponding to three vectors, $\mathbf{a}_{1,i}$, from O_1 to O_i. The point O_1 is the origin of the frame, $X_1Y_1Z_1$, attached to the fixed link about which the shaking moment is defined. The equilibrium of forces and moments are expressed as (Fig. 4.3).

$$\mathbf{f}_i^e + \mathbf{f}_{i-1,i} - \mathbf{f}_{i,i+1} = \mathbf{f}_i^* \tag{4.14}$$

$$\mathbf{n}_i^e + \mathbf{n}_{i-1,i} - \mathbf{n}_{i,i+1} + \tilde{\mathbf{a}}_{i,i+1}\mathbf{f}_{i,i+1} = \mathbf{n}_i^* \tag{4.15}$$

Where the 3-vectors, $\mathbf{f}_{i-1,i}, \mathbf{n}_{i-1,i}$, and $\mathbf{f}_{i,i+1}, \mathbf{n}_{i,i+1}$, are the constraint forces and moments at the origins, O_i and O_{i+1}, respectively and 3-vectors, $\mathbf{f}_i^e$ and $\mathbf{n}_i^e$, are the external force and moment acting on the ith link at and about O_i, respectively.

Eqs. (4.14) and (4.15) are used to find constraint forces and moments from distant link to the first link.

4.3 Summary

In this chapter, the dynamic analysis of a serial industrial manipulator is established and the equations for shaking forces and shaking moments for the ith link are given. Using these recursive relations, we can find the shaking forces and shaking moments for other links moving in the backward direction from the end effector.

Optimization Problem Formulation

An optimization problem is formulated in this chapter to minimize shaking force and shaking moment simultaneously. In our case, the objective function is to minimize the shaking force and shaking moment on the base frame of the manipulator. The expressions for shaking force and shaking moment given in chapter 4 are used. This formulation is simplified by representing the inertial properties of the links in terms of the equimomental point-mass parameters. The point-mass parameters are used as design variables for the proposed optimization problem formulation, and associated constraints are formulated.

5.1 Optimization problem and optimality criteria

Two most commonly used optimization techniques to reduce the shaking force and shaking moment are (i) counterweighing the moving links and (ii) redistribution of the mass of moving links. In the case of counterweight balancing, counterweights are attached to the moving links such that the shaking force and shaking moment transmitted to the mechanism frame is minimized. We can formulate it as an optimization problem. Since the shaking force and shaking moment are the resultants of the inertia forces and moments of the moving links, when the link length and trajectory of motion that governs speed are given, the inertia forces depend only on the mass distribution of the links. Hence, mass distribution is the obvious choice to balance spatial mechanisms.

There are many possible criteria by which the shaking force and shaking moment transmitted to the frame/fixed link of the mechanism can be minimized. One of the criteria can be based on the root mean square (RMS) values of shaking force, and

shaking moment for a given trajectory of motion. Besides the RMS values, there are other criteria like maximum values, The amplitude of specified frequency and amplitude at some specified point during the motion cycle. The choice of criteria depends on the requirements. Here, the RMS value is preferred as it gives equal emphasis to the result of all time instances and every harmonic component.

Our objective is to demonstrate the effectiveness of proposed point-mass models (Positive equimomental point-mass values are offered for all masses by keeping the masses in such configurations) and optimization techniques (TLBO and GA) in the dynamic balancing of industrial manipulators through reduction of shaking moments and shaking forces. The equations of motion (NE equations) and expressions for shaking forces and moments have been derived in Chapter 4. Since the shaking moments and shaking forces at the different joint of the manipulator are dependent on velocities and acceleration of links apart from other parameters, their values are time dependent. Therefore the RMS values of shaking force $\tilde{f}_{sh}$ and shaking moment $\tilde{n}_{sh}$ at δ discret positions of the manipulator link are given by:

$$\tilde{f}_{sh} = \sqrt{\sum f_{sh}^2/\delta} \; ; \text{ and } \tilde{n}_{sh} = \sqrt{\sum n_{sh}^2/\delta} \qquad (5.1)$$

Then optimality criteria is considered as

$$z = w_1 \tilde{f}_{sh} + w_2 \tilde{n}_{sh} \qquad (5.2)$$

Where w_1 and w_2 are weighing factors whose value depends on the application. If we take $w_2 = 1$ and $w_1 = 0,$ it minimizes shaking moment alone. Similarly, by taking, $w_2 = 0,$ and $w_1 = 1,$ it minimizes shaking force alone. Here, $w_2 = 1,$ and $w_1 = 1$ is taken, to give equal weights to the reduction of shaking force and shaking moment.

We intend to reduce inertia induced forces and moments through mass redistribution of links i.e. by finding the values of different point-masses. It makes point-masses of different links as the design variables. For manipulator having n moving links, with each link modeled by p equimomental point masses, then we will have pn design variables. The pn-vector of design variables is expressed as:

$$\mathbf{x} = [m_{11}, m_{12}, \dots, m_{1p}, \dots, m_{n1}, m_{n2}, \dots, m_{np}] \qquad (5.3)$$

For existing robot/manipulator, we intend to keep the total mass of each link same or more thus it becomes a constraint, apart from individual point mass of each link to be more than zero being the other constraint. Thus the optimization problem for the manipulator is stated as below.

$$\text{Minimize } z(\mathbf{x}) = w_1 \tilde{f}_{sh} + w_2 \tilde{n}_{sh} \qquad (5.4a)$$

Subject to $\sum_{j=1}^{p} m_{ij} \geq m_i$ for all n links, i.e., $i = 1,2,3,\dots.. n$ $\qquad (5.4b)$

$m_{ij} \geq 0$ for all point-masses of all links, i.e., $i = 1,2,3,\dots.. n$ and $j = 1,2,\dots.p$ $\quad (5.4c)$

As discussed in Chapter 3, on point-mass models, all equimomental point masses of the links are assumed positive to satisfy conditions of product moment of inertias to be zero and also to avoid the practical implementation problem associated with 7 points parallelepiped negative point mass model. Since, the load carrying capacity that is the design parameter of robot/manipulator which depends on dimensions and material of the links (i.e. mass of the links). Therefore, the total mass of each link is kept same for the existing manipulator. However, in the case of a new design of the robot, it can have a different value with load capacity and stresses in the link being the constraints.

5.2 Application problem- PUMA robot

The greater use of the robot is being made, these days, in the industrial system compared to human for repetitive and non-conducive tasks in the industry. For instance, unlike the human, robots are able to work tirelessly and do repetitive tasks with high speed and accuracy. PUMA offers 200, 500, and 700 Series of Robots. PUMA 500 Series Robots are of 5 or 6 revolute axes. PUMA 560 Robot is a well-known industrial robot with six degrees of freedom. It is an RRRRRR robot type which can do various tasks such as point welding in the automotive industry and similar industries. This robot has six degree of freedom, three of them (waist rotation, shoulder rotation, elbow rotation) are related to a manipulator that offers positioning of the arm and the remaining (wrist bend, flange rotation) offers orientation to the arm and are related to end effector. The schematic diagram of PUMA 500 series is shown in Fig. 5.1. Gripper or End effector is mounted at gripper mounting location. Specialized tools like welding electrode, paint brush, a gas cutting torch, a de-burring tool, or a grinding wheel attached at the end of manipulator's arm to perform special tasks are also considered as end-effectors. In this study, dynamic balancing of PUMA robot is considered as a problem to demonstrate the application/use of proposed point-mass models and optimization techniques. PUMA robot is considered because the parameters like masses of different links, their inertias, and DH parameter are available in the published literature for PUMA robot.
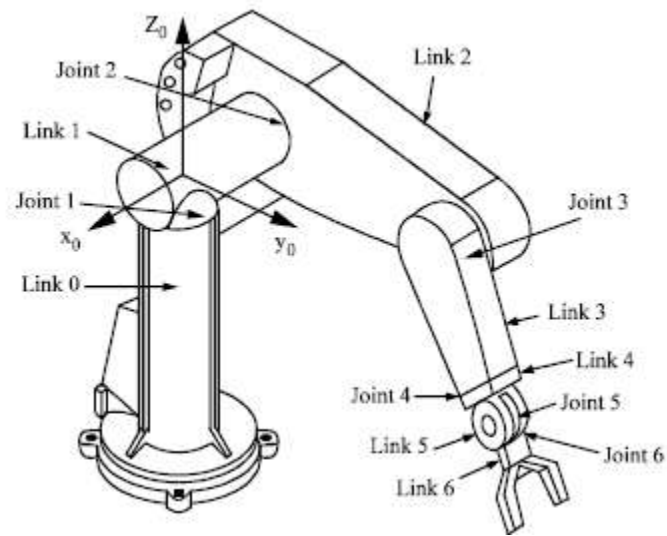
Figure 5.1 Schematic of PUMA 500 series Robot [57]

The DH parameters, link's masses, and inertias of the manipulator given in [43] are taken here for analysis and comparison purposes. The frame convention and notations of DH parameters are shown in Fig. 5.2. The architecture of a PUMA robot is shown in Fig. 5.3 whose DH parameters, mass, and inertia about the mass center of each link are given in Table 5.1.
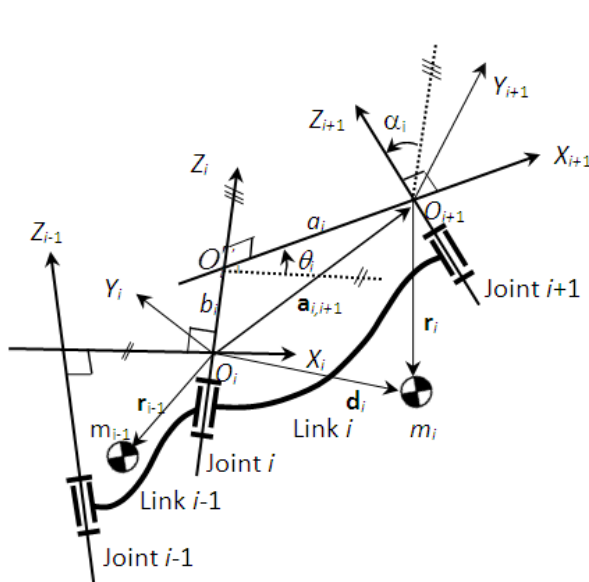
Fig. 5.2 Coordinate frames and DH parameters (Saha,57)
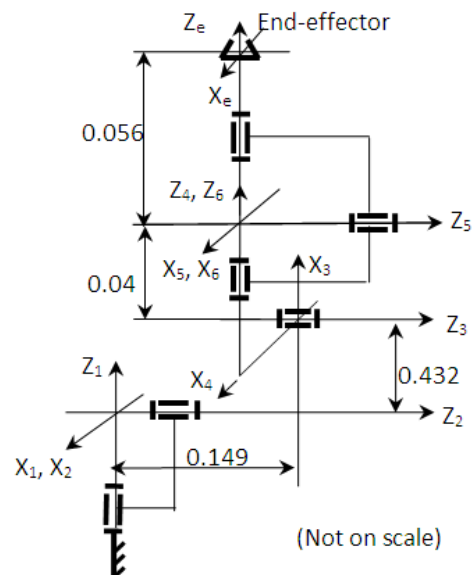
Fig. 5.3 Architecture of a PUMA Robot (Saha,57)

49

Inertias of the links are given in the local frame, and off-diagonal terms of inertias are all zero. Note that X_{i+1} Y_{i+1} $Z_{i+1}$is fixed to the ith link in this notation. The joint trajectories are taken as:-

$$\theta_i = \theta_i(0) + \frac{\theta_i(T) - \theta_i(0)}{T} \left[t - \frac{T}{2\pi} \sin\left(\frac{2\pi}{T} t\right) \right]$$, where T=10 Secs,

$$\theta_i(0) = 0, \theta_i(T) = 180^o$$

TABLE 5.1: DH parameters, and mass and inertia properties of links

I	a_i	b_i	α_i	θ_i	m_i	r_{ix}	r_{iy}	r_{iz}	I_{ixx}	I_{iyy}	I_{izz}
	(m)	(m)	(deg)	(deg)	(Kg)		(m)			(Kg-m^2)	
1	0	0	-90	θ_1	10.521	0	0	-0.054	1.612	1.612	0.5091
2	0.432	0.149	0	θ_2	15.761	-0.292	0	0	0.4898	8.0783	8.2672
3	0.02	0	90	θ_3	8.767	-0.02	0	0.197	3.3768	3.3768	0.3009
4	0	0.432	-90	θ_4	1.052	0	-0.057	0	0.181	0.1273	0.181
5	0	0	90	θ_5	1.052	0	0	0.007	0.0735	0.1273	0.0735
6	0	0.056	0	θ_6	0.351	0	0	-0.019	0.0071	0.0071	0.0141

The equimomental point masses for each link are obtained for different point-masses configurations (i.e. 7/6/5/4 point-masses to represent rigid links of the manipulator) in chapter 3. The values of point masses and their locations for 7, 6, 5 and 4 point mass configurations are given in Tables 3.2 to 3.8.

5.3 Summary

In this chapter, the optimization problem is formulated giving objective function and associated constraints. Weight factors are used for shaking force and shaking moment in the objective function. RMS value of the shaking forces and shaking moments, DH parameters and other details of PUMA robot are given which shall be used in solving the optimization problem formulated using different optimization techniques.

Optimization Techniques - GA and TLBO

The difficulties associated with mathematical optimization like Linear Programming and Dynamic Programming etc. to solve engineering problems having a large number of variables and non-linear objective functions led to the development of several modern heuristic algorithms for searching near-optimal solutions to such problems. Some of the evolutionary and swarm intelligence based algorithms are Genetic Algorithm (GA), Particle Swarm Optimization (PSO), Ant Colony Optimization (ACO), Artificial Bee Colony (ABC). All these algorithms are population-based. Recently, population-based algorithm, Teaching Learning based algorithm has been added to this group of evolutionary and swarm intelligence based algorithms. All these are population based probabilistic algorithms and require common controlling parameters like population size, the number of generations, elite size, etc. Apart from these controlling parameters, each algorithm requires its algorithm-specific parameters. Genetic Algorithm, which is based on Darwin's principle of survival of fittest, require mutation rate and crossover rate. Similarly, PSO uses inertia weight, social and cognitive parameters. However, the TLBO algorithm does not require any such algorithm-specific parameter. Hence, it is relatively simpler in its coding and implementation. Recently, TLBO has been used for solving the optimization problem in wide engineering applications.

6.1 Genetic algorithm tool box

A built-in standard tool box is available in MATLAB for solving constrained linear optimization problem with linear constraints. We can change population size, crossover probability, mutation probability, elite count and tolerance function as per

our requirements. However, there is a default setting in the built-in software for these parameters. The default setting, for population size, is 20, crossover probability is 0.8, elite count 2, tolerance function 1e -6 and performs mutation operation on remaining single parents i.e. 2 giving mutation probability of 0.10. Stopping criteria can be generation count, function tolerance, fitness limit, etc.

At each step the GA uses current population to create the children that make up the next generation. The algorithm selects a group of individuals in the population called parents who contribute their genes - the entries of their vectors - to their children. The algorithm selects individuals that have better fitness value/function value as parents. One can specify the function that algorithm uses to select the parents in the selection function. GA generates initial population randomly or if the range is known we can define/give the initial population as input.

GA creates three types of children for next generation

- Elite children are individuals in the current generation with best fitness values. These individuals automatically survive to the next generation.

- Crossover children are created by combining the vectors of their parents.

- Mutation children are created by introducing random changes or mutation to a single parent.

6.2 Teaching learning based optimization

The Teaching-Learning-Based Optimization (TLBO) method developed recently by R. V. Rao et al. (2011) is also a nature inspired population-based method. It is based on acquiring knowledge/learning through teacher and self- learning through fellow colleagues so as to perform better in the evaluation. The subject knowledge can be acquired better through teachers, who are possessing subject related knowledge better.

Further refinements in terms of introducing elite, mutation and crossover concepts as prevailing in GA; feedback phase and chaotic perturbation mechanism that helps to improve significantly the performance of basic algorithm has been introduced in basic TLBO model very recently by Kunjie Yue (2014).

The TLBO method is based on the effect of the influence of a teacher on the output of learners in the class. Here, the output is considered in terms of results or grades. The teacher is considered as a highly learned person who shares his or her subject knowledge with the learners. The quality of a teacher affects the outcome of the learners. It is obvious that a good teacher trains learners such that they can have better results in terms of their marks or grades in the subject taught.

Considering that two different teachers, T_1 and T_2, teach a subject with the same content to the same merit level students/learners in two different classes. On evaluation by the teachers with the same set of questions and with same time allotment to answer these questions, the distribution of marks obtained by the students/learners of two different classes would be different. The plot of the distribution of marks by the students in a class is generally observed to follow a normal distribution pattern though it might be skewed somewhat.

If the mean of marks obtained by students who learned from teacher T_2 is better compared to mean marks of students who learned from teacher T_1, then it can be said that teacher T_2 is better than teacherT_1 in terms of teaching. The main difference between the results is their mean (M_2 for teacher T_2 and M_1 for teacher T_1), i.e. a good teacher produces a better mean for the results of the students/learners. Further, the students/learners also learn from the interaction among themselves, which also helps

in their results. The optimization technique called "Teaching–Learning-Based Optimization" (TLBO) is based on this teaching–learning process.
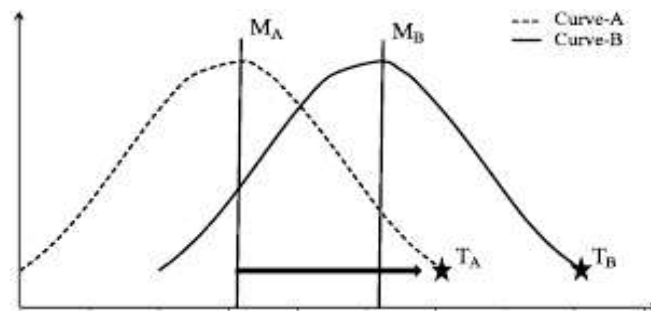
Fig. 6.1: Distribution of marks obtained by a group of learners [Rao et. al.,59]

Since the teacher is considered as the most knowledgeable person in the society, so the best learner in the population of learners is considered as a teacher, which is shown by T_A in Fig. 6.3. The teacher tries to disseminate knowledge among learners, which will, in turn, increase the knowledge level of the whole class and help learners to get good marks or grades. So a teacher increases the mean of the class according to his or her capability. In Fig. 6.3, teacher T_A tries to move mean M_A towards his/her level according to his or her capability thereby increasing the learners' level to a new mean M_B. Teacher T_A will put maximum effort to teach that subject to his or her students, but students will gain knowledge according to the quality of teaching and the quality of students present in the class. The quality of the students is judged from the mean value of the population. Teacher T_A puts in the effort so as to increase the quality of the students from M_A to M_B where $M_B > M_A$ at this stage the students require a new teacher, of superior quality than themselves, i.e. in this case the new

teacher is T_B. Hence, there will be a new curve-B with new teacher T_B. Like other nature-inspired algorithms, TLBO is also a population-based method that uses a population of solutions to proceed to the global solution. For TLBO, the population is considered as a group of learners or a class of learners. In optimization algorithms, the population consists of different design variables. In TLBO, different design variables are analogous to different subjects offered to learners and the learners' result is analogous to the 'fitness', as in other population-based optimization techniques. The teacher is considered as the best solution obtained so far. The process of TLBO is divided into two parts. The first part consists of the 'Teacher Phase' and the second part consists of the 'Learner Phase'. The 'Teacher Phase' means learning from the teacher and the 'Learner Phase' means learning through the interaction among learners

6.2.1. Teacher phase

A good teacher is one who brings his or her learners up to his or her level in terms of knowledge. In this phase, the teacher tries to increase the mean result of the class from any value M1 to his or her level. However, practically this is not possible, and a teacher moves the mean of class from M1 to any other value M2 (M2 > M1).It follows a random process depending on many factors.

The new value of design variable is obtained by adding a fraction, lying between 0 and 1, of the difference between the mean of the population and variable value of the teacher to the old value of design variable. Only the fraction of difference is added because the knowledge transferred may lie between 0 to 100 %. If the objective function value for the new solution is better than that of old, new solution is accepted otherwise the old one is retained. It completes the "Teacher's Phase".

6.2.2 Learner Phase

In "Learner Phase", learners increase their knowledge by interaction among themselves. A learner learns new things if the other learner has more knowledge than him/her. A learner improves his/her knowledge through interaction with any other learner from the population. Suppose the learner 1 learns from learner 5 than the new value of the decision variable is dependent on the objective function value of learner 1 and 5, whether it is minimization or maximization problem, i.e., the improvement is based on maximization/ minimization case and the comparison of their objective function values.

The new value of design variable is obtained by adding a fraction, lying between 0 and 1, of the difference between old design variable values of learner 1and 5, if the objective function value of learner 1 is less than that of 5 in the case of the minimization problem. However, if the objective function value of 1 is greater than that of 5 then the difference is subtracted.

If the objective function value for the new solution is better than that of old, new solution is accepted otherwise the old one is retained. This process completes one cycle of iteration. The process from the computation of variable mean onwards is repeated if the termination criteria remain unsatisfied. The design vector for which the objective function is minimum represents the optimal solution. It would be another way round for maximization problem. We can understand the use of TLBO better through the following example which is same as that taken for GA.

Maximize: $Z = 30(Y_1)^2 - Y_2$ where Y_1 & Y_2 lies between 0 and 1.

Step 1: We generate initial population randomly for each Y_1 and Y_2, in the range of 0 and 1. Selecting population size N of 8. Eight random numbers are generated for each

of Y_1 and Y_2 (Col. 2 and 3 of Table 6.1). The function value FV is then computed using the initial population of variables (Col. 4 of Table 6.1).

Teacher Phase

The maximum FV equals to 27.1680 is the best solution $Y_1 = 0.96$ and $Y_2 = 0.48$. The best student i.e. Learner number 7 with variable values that gives best FV acts as the teacher. The mean value of each variable is computed by summing up the value of the variable for each learner, then dividing it by the number of learners. The mean value of variables Y_1 and Y_2 is 0.591 and 0.626 respectively (Last row of Table 6.1). The difference between the variable value of teacher and the mean value of variable multiplied by the random number between 0 and 1 is obtained. The random number generated for variable Y_1 and Y_2 is0.2055 and 0.9384 respectively. The new value of variables is then obtained by adding the difference obtained to the old value of variables. However, the new/ modified value of the variable is to be restricted within their upper and lower limits (Col. 5 and 6 of Table 6.1). The FV with the modified value of variables is then obtained (Col. 7 of Table 6.1). If new FV (Col 7 value) is better than old FV (Col. 4 value), variables value is modified else old value (of Col. 2 and 3) is retained (Col. 8 and 9 of Table 6.1). It completes teachers phase. In this case, FV for all sets is improved in teachers phase.

Learner Phase

In learner phase, we select any two learners randomly for each learner from whom the learner learns (Col. 10 of Table 6.1). It indicates that the learner 1 learns from learner 7 and 3. Since our objective function is of maximization type, we have to modify the variables value suitably depending on old objective function value of learner 1 to be less than or more than old objective function value of learner 7 and 3. Generate a

random number between 0 and 1 for all variables (The last row under learners phase of Table 6.1, it is 0.8147 and 0.9058).

The new value of the variable is obtained by subtracting a fraction, lying between 0 and 1, of the difference between old variable values of learner 1 and 7, if the objective function value of learner 1 is less than that of 7 in the case of maximization problem. However, if the objective function value of 1 is greater than that of 5 then the difference is added.

We get $Y_{new,1} = 0.9785$, $Y_{new,2} = 0.3866$ and FV = 28.3373 for learning by 1 from 7 and $Y_{new,1} = 0.9304$, $Y_{new,2} = 1.4617$ (i.e. 1.0 which is upper limit) and FV = 24.9693 for learning by 1 from 3. Both FV's are more than FV achieved after teacher's phase (22.666). Hence variable value is modified (Col. 14, 15 and 16 of Table 6.1). Similarly, the variable values are modified during learners phase for other learners. It gives the population and its FV after one iteration. It consists of "Teachers Phase" and "Learners Phase" (Col. 14, 15 and 16).

The average value of FV after the first iteration is 25.3630 i.e. there is a significant improvement over initial population average of 13.0880. Subsequent generations/iterations improve the new population average further. Even after first iteration two of the variable set pertains to exact solution value of 30.00 and three sets pertains to FV lying between ~ 28.3 to 29.3 close to exact solution value. We can use penalty function combined with objective function to handle constraints in the optimization problem. The second iteration starts with the above variable value and continues till the termination criterion is satisfied.

Table 6.1: Initial Population (Pop.), Modified Pop./Variable value and Function Value

after Teachers Phase, Learners Phase and after one generation of TLBO Algorithm

S. No.	Initial Pop.			Teachers			Mod. Var		Le ar	Learners			Mod.Var(Final)		Fval after 1 cycle
	Y_1	Y_2	Fval	Y_{1new}	Y_{2new}	Fval New	Y_1	Y_2		Y_1	Y_2	Fval	Y_1	Y_2	
1	0.81	0.90	18.783	0.8838	0.767	22.666	0.8838	0.7670	7	0.9785	0.3866	**28.337**	0.9785	0.3866	28.337
									3	0.9304	(1.0)	24.969			
2	0.13	0.91	-0.403	0.2038	0.777	**0.469**	0.2038	0.777	1	0.6926	0.6864	13.704	0.7496	0.1430	16.714
									8	0.7496	0.1430	**16.714**			
3	0.63	0.10	11.807	0.7038	(0.0)	**14.860**	0.7038	0.0	7	0.9451	0.3143	26.482	0.9889	0.0	29.338
									4	0.9889	(0.0)	**29.338**			
4	0.28	0.55	1.802	0.3538	0.417	**3.338**	0.3538	0.417	8	0.7774	0.0547	**18.0766**	0.7774	0.0547	18.076
									2	0.4760	0.0909	706			
5	0.96	0.96	26.688	(1.0)	0.827	**29.173**	1.0	0.827	4	(1.0)	(1.0)	29.000	1.0	0.8180	29.182
									6	(1.0)	0.8180	**29.182**			
6	0.16	0.97	-0.202	0.2338	0.837	**0.803**	0.2338	0.837	5	0.8580	0.8280	**21.2572**	0.8580	0.8280	21.257
									4	0.3315	0.4566	840			
7	**0.96**	**0.48**	**27.168**	(1.0)	0.347	**29.653**	1.0	0.347	8	(1.0)	0.6550	29.345	1.0	0.0	30.000
									3	(1.0)	(0.0)	**30.000**			
8	0.80	0.14	19.060	0.8738	0.007	**22.899**	0.8738	0.007	7	0.9766	0.3150	28.297	1.0	0.0	30.000
									6	(1.0)	(0.0)	30.000			
Sum	4.73	5.01	104.704	R. No.	R. No.	123.661				R. No.	R. No.			Sum	202.904
Avg	0.591	0.626	13.088	0.2055	0.9384	15.433				0.8147	0.9058			Avg.	25.363

6.3 Summary

In this chapter, the basic methodologies of Genetic Algorithm and Teaching-Learning-Based-Optimization are discussed. Maximization problem is solved step by step using TLBO.

The step by step solution of same maximization problem using GA is given in Appendix-A. Comparing the results obtained using TLBO and GA demonstrates the effectiveness of TLBO over GA.

Optimization Using Genetic Algorithm

This chapter gives the results in the form of optimized mass distribution for each link of the manipulator. PUMA robot is considered as a problem for illustration of the proposed methodology on the dynamic balancing of Industrial manipulator using different point-masses model developed in chapter 3 and equation of motion given in chapter 4. The optimization problem is formulated in chapter 5 while optimization technique GA is discussed in chapter 6. Using GA, the values of optimization function, i.e., the sum of RMS values of constraint moments and constraint forces at each joint of the manipulator is computed by varying the decision variables i.e. point-masses.

Optimized function values for 5 cases are obtained using GA. Their mean, optimized point-mass values of each link for minimum function value, constraint moment and constraint force at each joint of manipulator for minimum function value is presented in tabular form. The variation of constraint moment and constraint force at each joint of the manipulator over one cycle of operation is then graphically represented.

Finally, the comparison of results for different point-mass models is made and discussed. Further, the driving torque values are also given to demonstrate that the optimization reduces the driving torque.

7.1 Shaking moments and shaking forces using GA

The genetic algorithm toolbox of MATLAB 2008a is used to solve the optimization problem formulated through equations 5.4a to 5.4c. The objective function is computed using equations of motions derived in Chapter 4 for dynamically equivalent point-masses system. Equations of motion call for the value of equimomental point-

masses and their locations. These are computed using expressions derived in Chapter 3 for six degrees of freedom PUMA Robot and are given in Tables 3.2 to 3.8.

MATLAB coding has been done, to evaluate the value of objective/fitness function, to define constraints given in equations 5.4b to 5.4c and to develop main GA optimization function program defining various input parameters like initial population, the number of variables, population size, elite count, the number of generations and function tolerance. The default settings for crossover probability and mutation probability available in built-in GA program, are used.

7.1.1 Seven point-mass parallelepiped model

The shaking forces and shaking moments value for seven point mass parallelepiped model of Puma robot has been found using "fmincon" optimization toolbox of MATLAB by Chaudhary & Saha [43]. The optimization function values for this model using equimomental point mass values given in [43] are found using GA tool available in GA toolbox of MATLAB – version 8 for validation purposes. GA solutions were obtained for this point-masses model with different population size, elite children count to be retained in next generation, termination criteria (tolerance function and the number of generations), and defining initial population(if required). There is a default setting for these parameters in the algorithm. It calls for input information on number of variables, fitness/objective function (sum of RMS values of constraint forces as given in problem formulation) and constraints (lower and upper bound on the sum of different point masses of a link as given in problem formulation). Equimomental point-masses values and their locations for the original (unbalanced) robot are considered as initial population for better convergence of objective function

in less number of generations. We obtained a number of solutions (some feasible and some non-feasible) by having variations on these parameters. The best feasible solution reported here was obtained with population size of 1680, 25 generation count, elite count of 40, 0.8 crossover fraction(default setting), 10^{-90} tolerance function and defining point masses for the unbalanced robot as initial population (it was used as an initial solution in optimization using fmincon).The values of the minimum objective function obtained using GA and those reported by Chaudhary & Saha [43] are tabulated in Table 7.1 for comparison and validation purposes.

Table 7.2 shows the mass, inertia about link origin and inertia about the center of mass for the optimized point masses obtained using fmincon and Genetic Algorithm. The total mass values for all six link is same for the fmincon & GA optimal solutions. It results in the same moment of inertia about origin for both cases. However, the optimal point mass values being different, it gives different MI values about the center of mass. Even though the optimal solution using GA does not reduce constraint moment particularly for link 2, it gives the positive value of I_{xx}^c, I_{yy}^c, and I_{zz}^c for all the six links that make a feasible solution. I_{xx}^c, I_{yy}^c, and I_{zz}^c values for links 1,2 and 4 are negative in case of fmincon. The optimal solution due to high negative point mass values that reduces constraint moments further, but it makes solution infeasible. Few more solutions close to the one whose details are given in Table 7.1 & 7.2 were obtained using GA which gives positive moment of inertia values about the center of mass for all the six links. Therefore for validation purposes for our mass models (7/6/5/4) optimized solutions are obtained using GA and newly developed optimization method TLBO.

Table 7.1: Constraint forces and Constraint moments at various Joints of PUMA with

GA and fmincon solution

Constraint moment	$\tilde{n}_1$	$\tilde{n}_2$	$\tilde{n}_3$	$\tilde{n}_4$	$\tilde{n}_5$	$\tilde{n}_6$	Total
Original PUMA	73.12	75.61	14.47	5.43	0.111	0.076	168.817
Optimized PUMA (GA)	4.79	28.48	4.28	3.67	0.11	0.076	41.406
Optimized PUMA (fmincon) [43]	1.95	1.87	1.23	1.05	0.24	0.067	6.407
Constraint force	$\tilde{f}_1$	$\tilde{f}_2$	$\tilde{f}_3$	$\tilde{f}_4$	$\tilde{f}_5$	$\tilde{f}_6$	Total
Original PUMA	367.97	264.79	110.22	24.138	13.797	3.452	784.367
Optimized PUMA (GA)	367.91	264.71	110.13	24.118	13.797	3.452	784.117
Optimized PUMA (fmincon) [43]	367.91	264.70	110.12	24.089	13.797	3.452	784.068

Table 7.2: Optimized mass and inertia using fmincon & GA

Link i	Case 1, fmincon					Case 2, GA			
	m_i^*	link inertia	I_{ixx}^*	I_{iyy}^*	I_{izz}^*	m_i^*	I_{ixx}^*	I_{iyy}^*	I_{izz}^*
	kg	kg/m^2	kg/m^2	kg/m^2	kg/m^2	Kg	kg/m^2	kg/m^2	kg/m^2
1	10.	I_1	1.6423	1.6423	0.5088	10.	1.6423	1.6423	0.5488
	521	I_1^c	0.0199	1.6415	**-1.1128**	521	0.8465	0.8606	0.4923
2	15.	I_2	0.4896	9.4224	9.6112	15.	0.4896	9.4224	9.6112
	761	I_2^c	**-0.5419**	**-0.2165**	1.0038		0.4317	0.8445	1.0549
3	8.	I_3	3.7168	3.7203	0.3044	8.	3.7168	3.7203	0.3044
	767	I_3^c	3.7138	3.7127	0.2976		3.7026	3.7093	0.3004
4	1.	I_4	0.1844	0.1273	0.1844	1.	0.1844	0.1273	0.1844
	052	I_4^c	**-0.9597**	0.1271	**-0.9599**		0.0433	0.1273	0.0433
5	1.	I_5	0.0736	0.1274	0.0735	1.	0.0736	0.1274	0.0735
	052	I_5^c	0.0735	0.1273	0.0735		0.0735	0.1273	0.0735
6	0.	I_6	0.0072	0.0072	0.0141	0.	0.0072	0.0072	0.0141
	351	I_6^c	0.0059	0.0059	0.0141		0.0071	0.0071	0.0141

7.1.2 Seven point-mass octahedron model

GA solutions were obtained for this point-mass model with different population size, elite count, tolerance function and termination criteria –the number of generations. Equimomental point-masses values and their locations for the original (unbalanced)

robot are considered as initial population for better convergence of objective function in lesser generations. The value of objective function obtained is presented in Table 7.3. It is observed that the average function value (FV) obtained, for N=7200; EC=72; tolerance function 1e-90, is 830.37. The reduced tolerance function permits iteration for the larger number of generations before terminating the solution. Elite count of 10% of population size is observed to be satisfactory. If the population size is increased to N=9000, the improved function value is obtained with 19 generations. Since the number of design variables (42) is large, the increase in population size improves the value of objective function.

Table 7.3: Objective function values with GA for octahedron point-masses model

population size	elite count	tolerance function	generation	generation termination	objective function value
7200	72	1e -90	20	14	830.37
7200	72	1e -200	20	19	829.33
9000	90	1e -200	20	19	825.08
9000	180	1e -90	20	14	832.47
9000	**180**	**1e -200**	**20**	**19**	**824.02**

The details of improvement in function value, for the solution in row 5 of Table 7.3 (marked bold) are given in Table 7.4. These results are obtained for different generations with population size (N) = 9000, Elite count (EC) = 180 and Tol fun= 1e-200 is given in Table 7.4. The Point mass values obtained for optimized function value of 824.02 for all links 1 to 6 are provided in Table 7.5. The optimized values of shaking moments and shaking forces at different joints of original and optimized PUMA robot obtained using seven-point octahedron point-masses model are given in Table 7.6.

Table 7.4: Improvement in FV during generations for the minimum, FV = 824.02

generation	f-count	best f(x)	max. constraint	stall generation	generation	f-count	best f(x)	max. constraint	stall generation
1	198132	953.221	2.22e-016	0	11	2088132	827.035	2.22e-016	0
2	387132	928.727	2.22e-016	0	12	2277132	826.505	2.22e-016	0
3	576132	868.974	2.22e-016	0	13	2466132	826.505	2.22e-016	1
4	765132	852.634	2.22e-016	0	14	2655132	826.245	2.22e-016	0
5	954132	842.692	2.22e-016	0	15	2844132	826.181	2.22e-016	0
6	1143132	835.504	2.22e-016	0	16	3033132	825.789	2.22e-016	0
7	1332132	834.674	2.22e-016	0	17	3222132	824.924	2.22e-016	0
8	1521132	833.160	2.22e-016	0	18	3411132	824.707	2.22e-016	0
9	1710132	832.757	2.22e-016	0	19	3600132	824.021	2.22e-016	0
10	1899132	827.480	2.22e-016	0					

Table 7.5: Point mass values for Optimized FV of 824.02

Link, i	m_{i1}	m_{i2}	m_{i3}	m_{i4}	m_{i5}	m_{i6}	m_{i7}
1	1.5230	2.7320	0.2567	1.6719	1.1403	0.3106	2.8883
2	0.4073	3.1891	0.7520	5.3442	0.6879	0.1228	5.2584
3	0.1678	1.1920	1.0725	0.9323	3.1433	0.1627	2.0967
4	0.1308	0.1238	0.3115	0.1315	0.0922	0.1315	0.1315
5	0.1315	0.2630	0.1315	0.1315	0.1315	0.1315	0.1315
6	0.0439	0.0878	0.0439	0.0439	0.0437	0.0439	0.0439

The optimized constraint moment values at different joints are reduced significantly. The shaking moment is reduced from 168.817 to 39.838 due to the proper mass distribution of links that affects its inertia and thus shaking moment. The constraint forces that depends on the total mass of the link remains nearly the same because the total mass of the links is retained same. However, the peak value of constraint forces

at different joints is reduced somewhat as demonstrated by various graphs of constraint forces from Fig. 7.7-7.12.

Table 7.6: Constraint moments and constraint forces for original and optimized

PUMA with FV of 824.02

Constraint moment	$\tilde{n}_1$	$\tilde{n}_2$	$\tilde{n}_3$	$\tilde{n}_4$	$\tilde{n}_5$	$\tilde{n}_6$	Total
Original PUMA	73.120	75.610	14.470	5.430	0.111	0.076	168.817
Optimized PUMA	6.086	22.244	6.694	4.627	0.111	0.076	39.838
Constraint force	$\tilde{f}_1$	$\tilde{f}_2$	$\tilde{f}_3$	$\tilde{f}_4$	$\tilde{f}_5$	$\tilde{f}_6$	
Original PUMA	367.970	264.790	110.220	24.138	13.797	3.452	784.367
Optimized PUMA	367.947	264.719	110.129	24.136	13.797	3.452	784.180
Driving Torque	Jt. 1	Jt. 2	Jt. 3	Jt. 4	Jt. 5	Jt. 6	
Original PUMA	5.049	78.856	25.691	0.121	0.122	0.022	109.861
Optimized PUMA	4.601	3.438	1.659	0.174	1.357	0.089	11.318

Fig. 7.1: Constraint moments of original and optimally balanced PUMA at joint 1 with 7 point-mass model

Fig. 7.2: Constraint moments of original and optimally balanced PUMA at joint 2 with 7 point-mass model

Fig. 7.3: Constraint moments of original and optimally balanced PUMA at joint 3 with 7 point-mass model
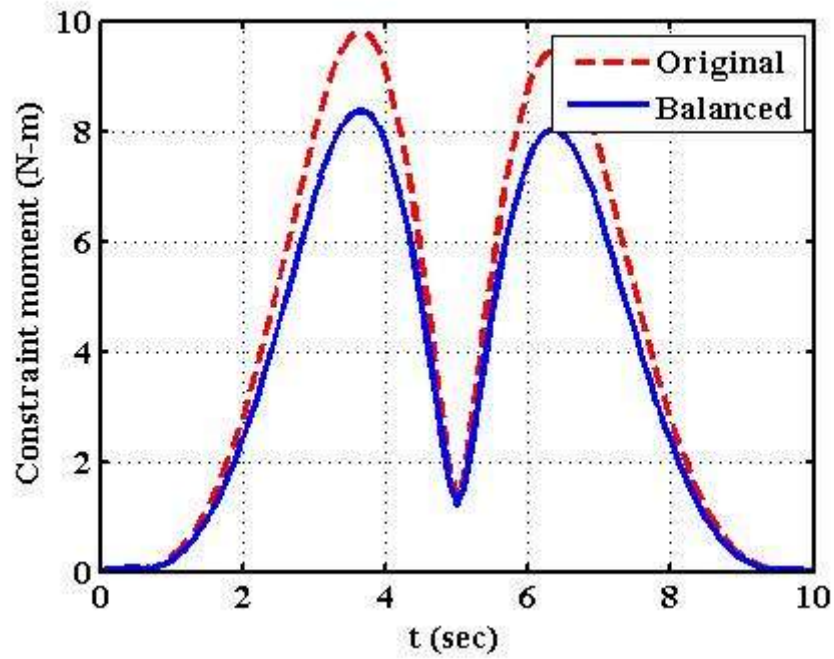
Fig. 7.4: Constraint moments of original and optimally balanced PUMA at joint 4 with 7 point-mass model
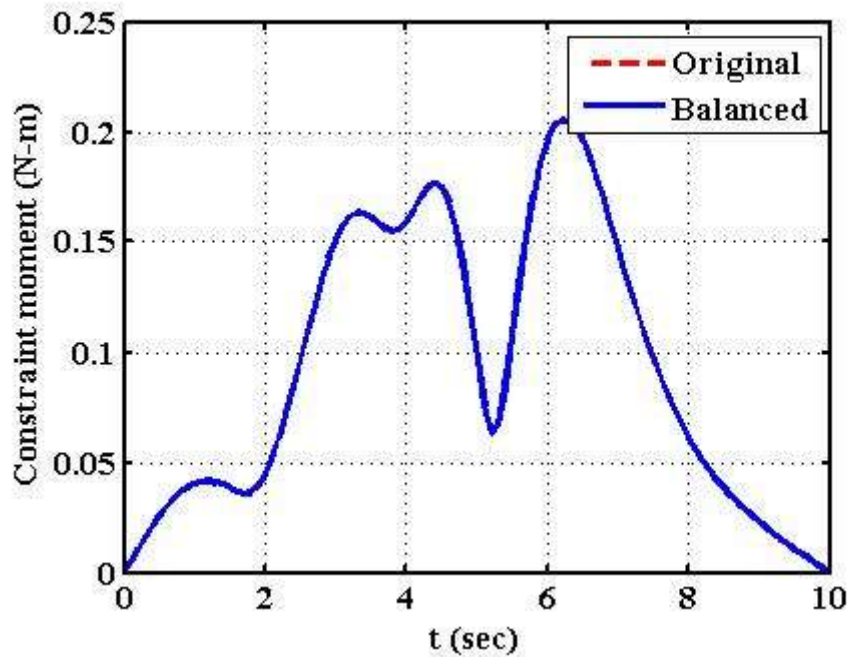
Fig. 7.5: Constraint moments of original and optimally balanced PUMA at joint 5 with 7 point-mass model
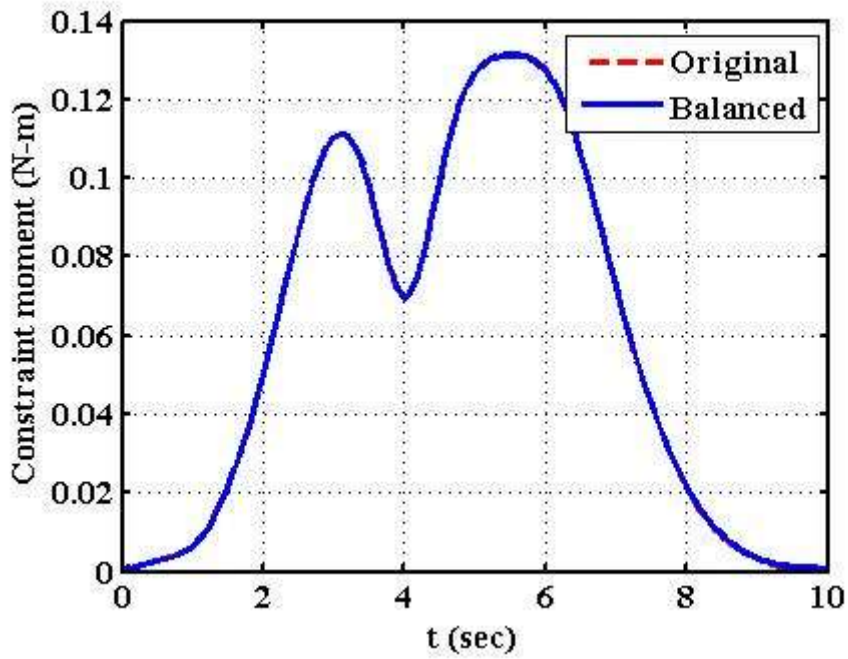
Fig. 7.6: Constraint moments of original and optimally balanced PUMA at joint 6 with 7 point-mass model
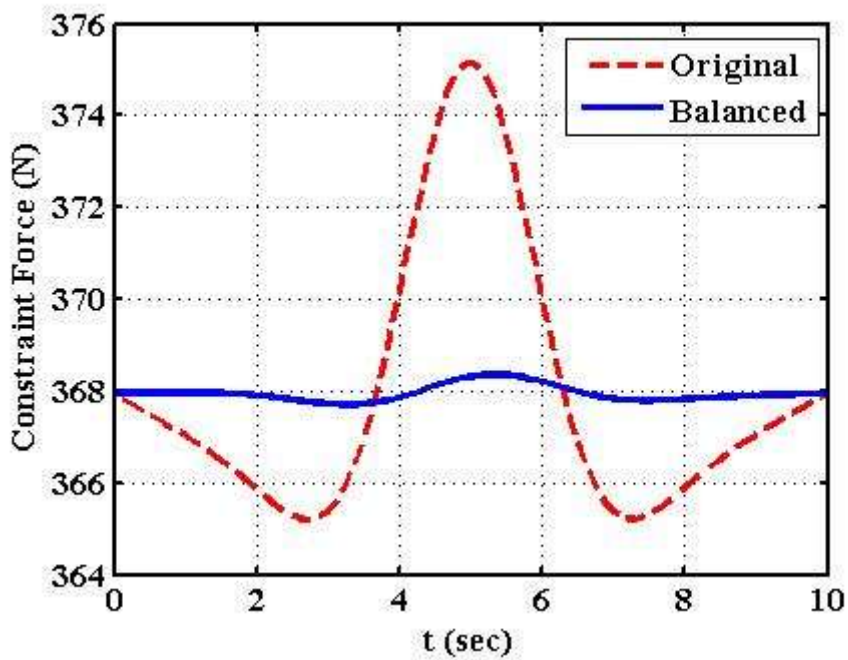
Fig. 7.7: Constraint forces of original and optimally balanced PUMA at joint 1 with 7 point-mass mod

69
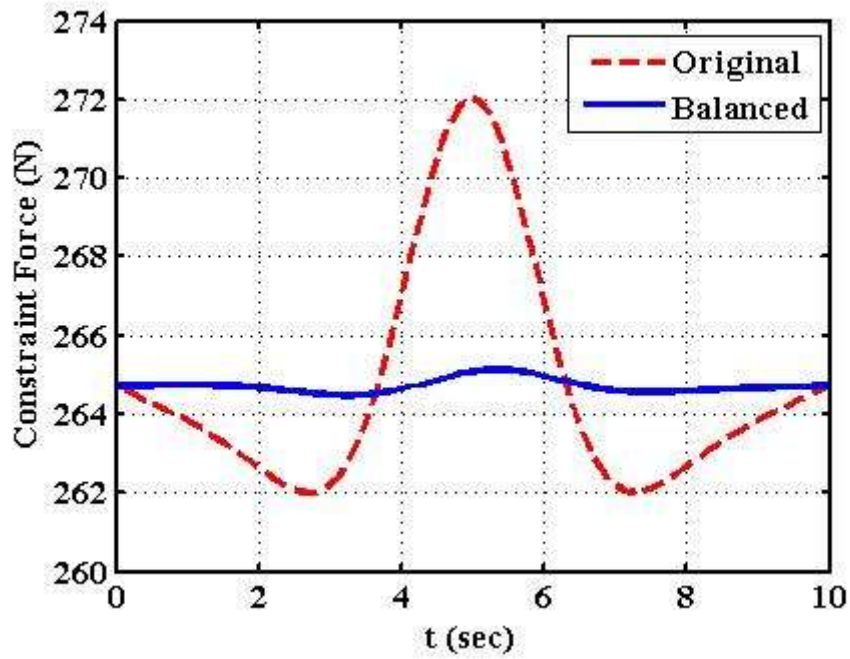
Fig. 7.8: Constraint forces of original and optimally balanced PUMA at joint 2 with 7 point-mass model
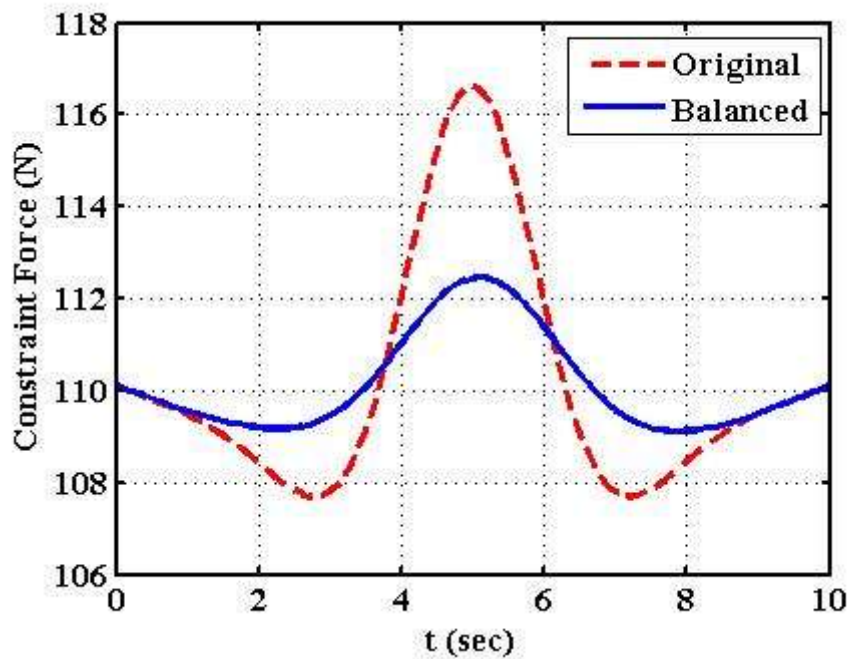
Fig. 7.9: Constraint forces of original and optimally balanced PUMA at joint 3 with 7 point-mass model
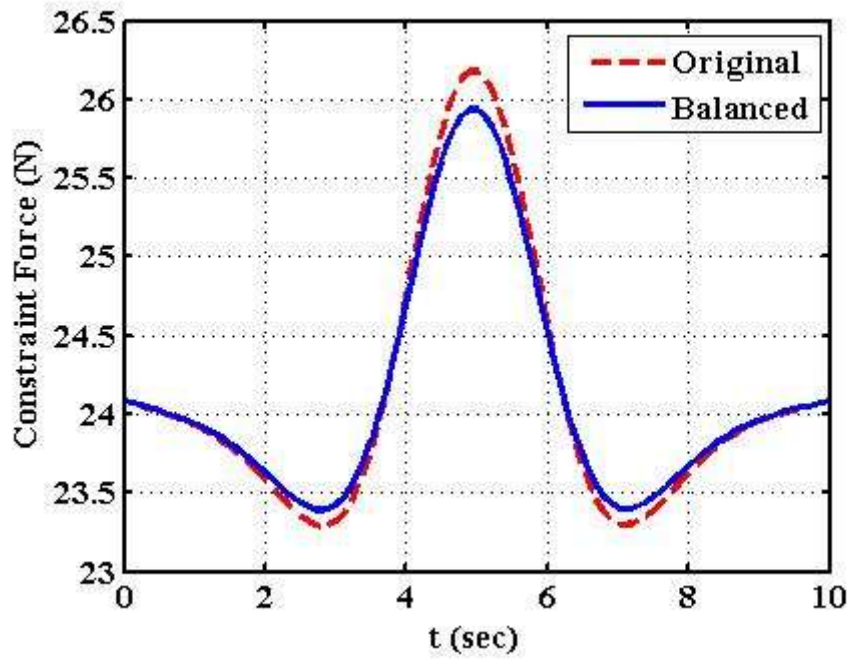
Fig.7.10: Constraint forces of original and optimally balanced PUMA at joint 4 with 7 point-mass model
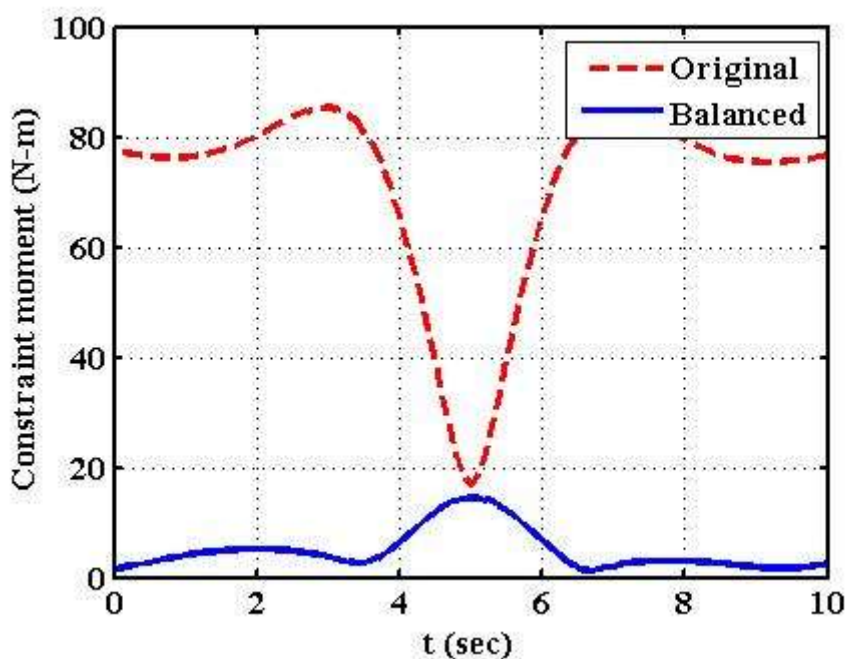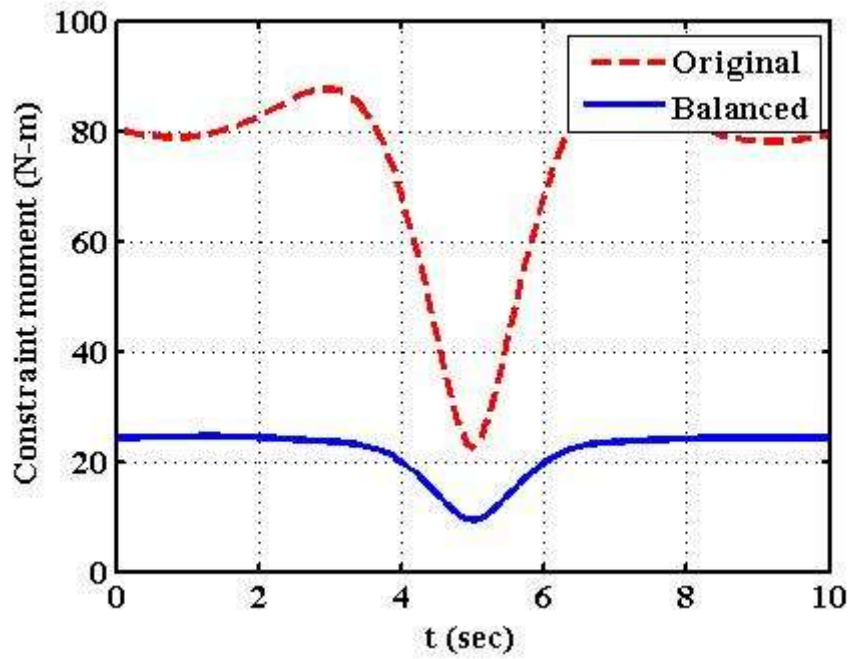

Fig.7.11: Constraint forces of original and optimally balanced PUMA at joint 5 with 7 point-mass model

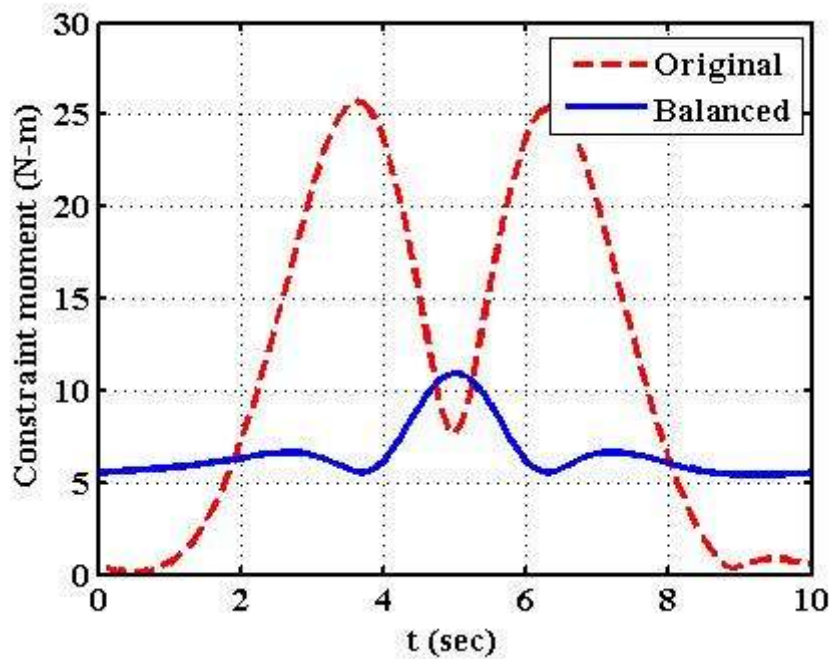**Fig.7.12: Constraint forces of original and optimally balanced PUMA at joint 6 with 7 point-mass model**

Links 5 and 6 posses very low mass and very small size due to which the constraint force of optimal and original link is same (Figs. 7.11 and 7.12)

7.1.3 Six point-mass hexahedron model

GA solutions were obtained for this point-mass model with the population size of 7200, elite count of 72, tolerance function and termination criteria –the number of generations. Equimomental point-masses values and their locations for the original (unbalanced) robot are considered as initial population for better convergence of objective function in less number of generations. The value of objective function obtained is presented in Table 7.7. It is observed that the average function value (FV) obtained, for N=7200; EC=72; tolerance function 10^{-90}, is 826.86. Elite count of 10% of population size is observed to be satisfactory. The population size of 7200 is observed to be satisfactory as the solution is terminated at 20th generation even with tolerance function of 10^{-90}.

Table 7.7: Objective function values using GA with hexahedron point-masses model

population size	elite count	tolerance function	genera tion	generation termination	objective function value
7200	72	1e -90	20	20	827.83
7200	**72**	**1e -90**	**20**	**20**	**823.02**
7200	72	1e -90	20	20	828.76
7200	72	1e -90	20	20	825.80
7200	72	1e -90	20	20	828.90

The details of improvement in function value for the solution at row 2 of above table 7.7 (marked bold) are given in Table 7.8. These results are obtained for different generations with population size (N) = 7200, Elite count (EC)= 72 and Tol fun= 1e-200. The Point mass values obtained for optimized function value of 823.02 for all link's 1 to 6 are provided in Table 7.9.

Table 7.8: Improvement in FV during generations for the minimum FV = 823.02

Gen erati on	f-count	best f(x)	max. constra int	stall genera tion	gen erati on	f-count	best f(x)	max. constr aint	stall genera tion
1	158514	953.2 28	0	0	11	1670514	826.2 89	0	0
2	309714	896.2 47	0	0	12	1821714	824.9 93	0	0
3	460914	864.5 44	0	0	13	1972914	824.7 94	0	0
4	612114	845.3 34	0	0	14	2124114	824.4 71	0	0
5	763314	842.8 87	0	0	15	2275314	824.1 12	0	0
6	914514	835.6 86	0	0	16	2426514	824.1 12	0	1
7	1065714	834.6 04	0	0	17	2577714	823.0 52	0	0
8	1216914	834.4 71	0	0	18	2728914	823.0 21	0	0
9	1368114	830.6 99	0	0	19	2880114	823.0 21	0	1
10	1519314	827.3 28	0	0	20	3031314	823.0 21	0	2

Table 7.9: Point mass values for Optimized FV of 823.02

Link, i	m_{i1}	m_{i2}	m_{i3}	m_{i4}	m_{i5}	m_{i6}
1	1.0650	2.2696	2.7853	1.2845	0.0044	3.1123
2	0.1389	1.7836	3.5002	4.9608	0.2230	5.1545
3	1.0337	2.1918	1.9514	1.5744	0.0790	1.9369
4	0.0501	0.1483	0.5861	0.0203	0.1266	0.1207
5	0.1315	0.2630	0.2630	0.1315	0.1315	0.1315
6	0.0438	0.0878	0.0878	0.0439	0.0439	0.0439

The optimized values of constraint moments and constraint forces at different joints of original and optimized Puma robot obtained using six point hexahedron point-masses model are given in Table 7.10. The optimized constraint moment values at different joints are reduced significantly. The shaking moment is reduced from 168.817 to 38.897 due to the proper mass distribution of links that affects its inertia and thus shaking moment. The constraint forces that depends on the total mass of the link remains nearly the same because the total mass of the links is retained same. However, the peak value of constraint forces at different joints is reduced somewhat as demonstrated by various graphs of constraint forces, Fig. 7.19 - 7.24.

Table 7.10: Constraint moments and Constraint forces for original and optimized PUMA with FV of 823.02

Constraint moment	$\tilde{n}_1$	$\tilde{n}_2$	$\tilde{n}_3$	$\tilde{n}_4$	$\tilde{n}_5$	$\tilde{n}_6$	Total
Original PUMA	73.12	75.61	14.47	5.43	0.111	0.076	168.817
Optimized PUMA	5.102	26.812	2.663	4.132	0.112	0.076	38.897
Constraint force	$\tilde{f}_1$	$\tilde{f}_2$	$\tilde{f}_3$	$\tilde{f}_4$	$\tilde{f}_5$	$\tilde{f}_6$	
Original PUMA	367.97	264.79	110.22	24.138	13.797	3.452	784.367
Optimized PUMA	367.92	264.71	110.128	24.123	13.798	3.453	784.14

Fig.7.13: Constraint moments of original and optimally balanced PUMA at joint 1 with 6point-mass model

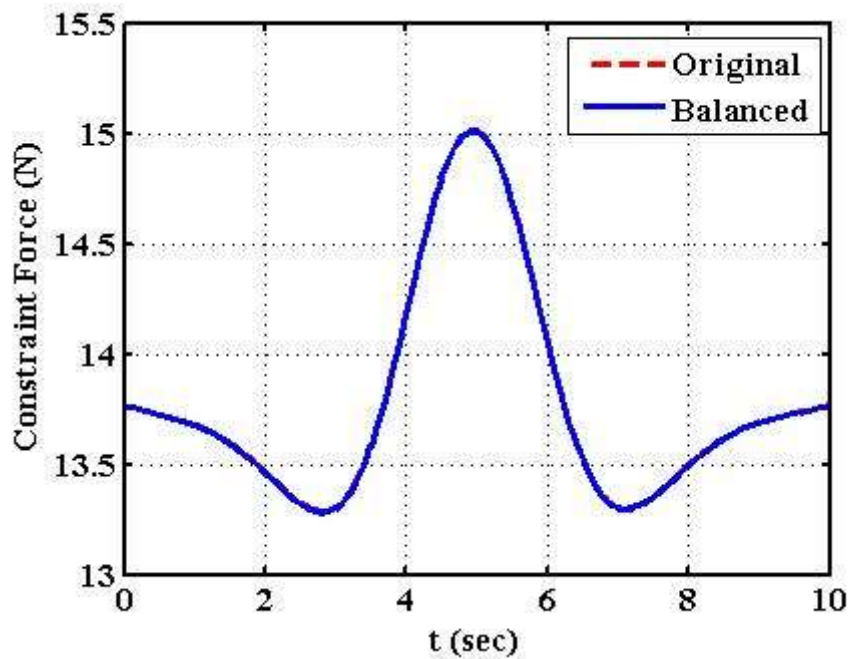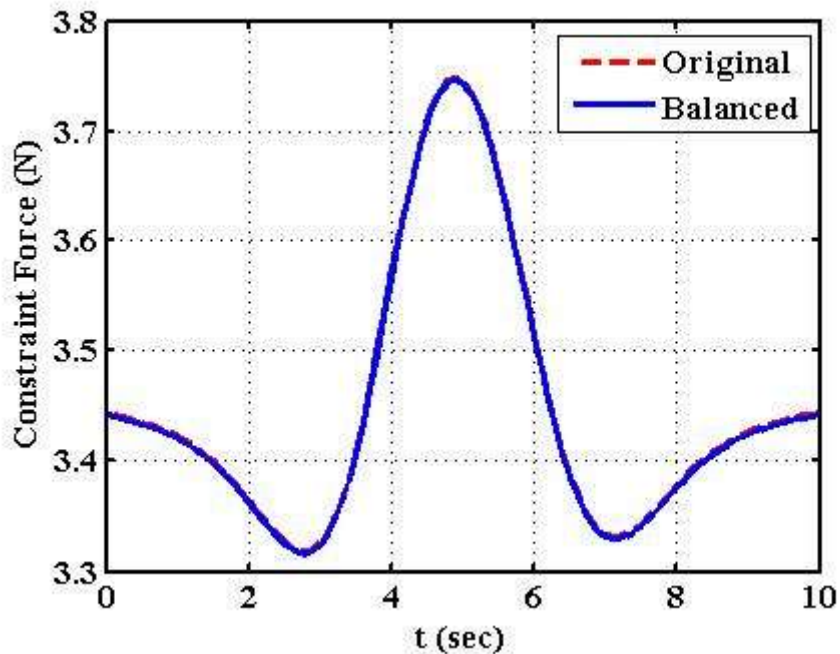**Fig.7.14: Constraint moments of original and optimally balanced PUMA at joint 2 with 6point-mass model**

Fig.7.15: Constraint moments of original and optimally balanced PUMA at joint 3 with 6point-mass model

Fig.7.16: Constraint moments of original and optimally balanced PUMA at joint 4 with 6point-mass model
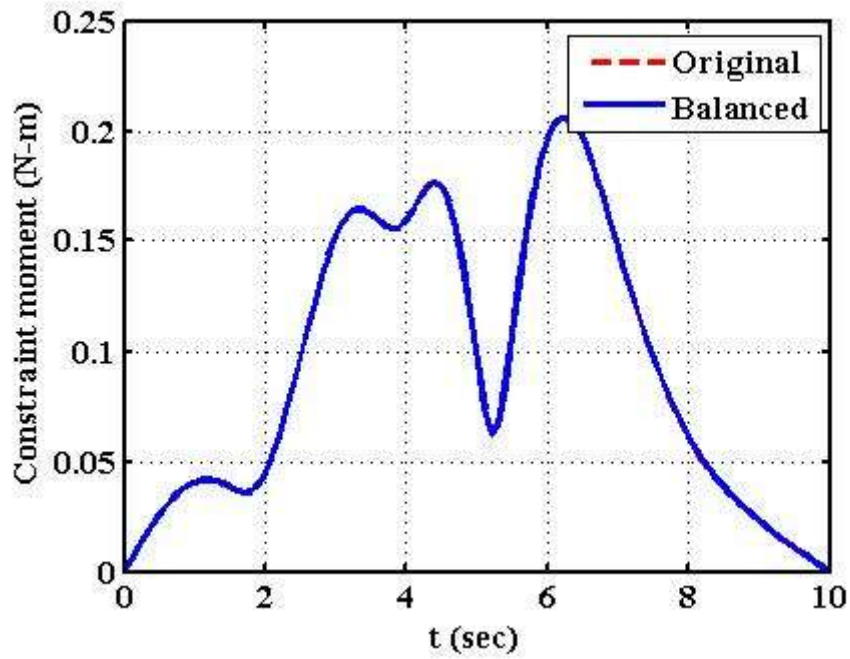
Fig.7.17: Constraint moments of original and optimally balanced PUMA at joint 5 with 6point-mass model
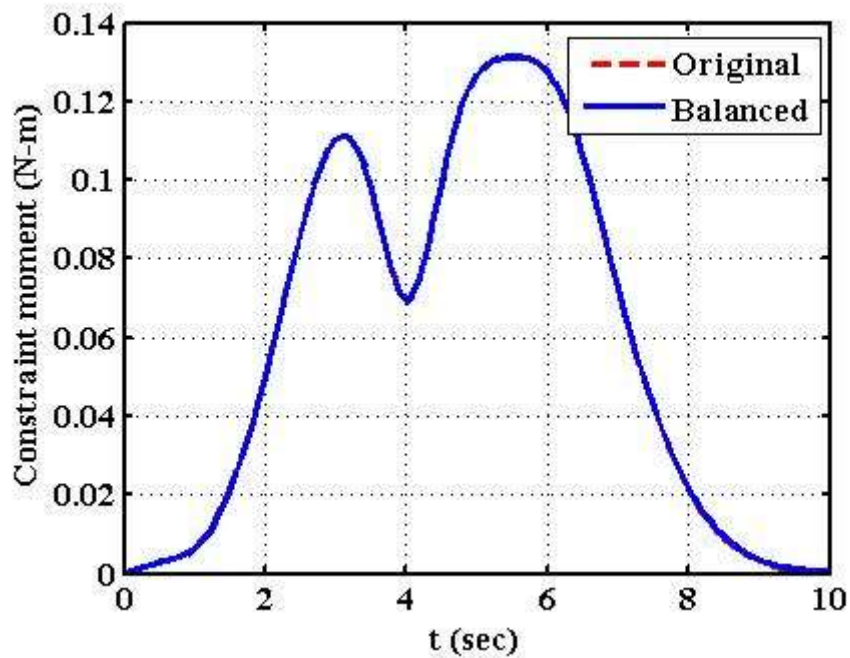
Fig.7.18: Constraint moments of original and optimally balanced PUMA at joint 6 with 6point-massmodel
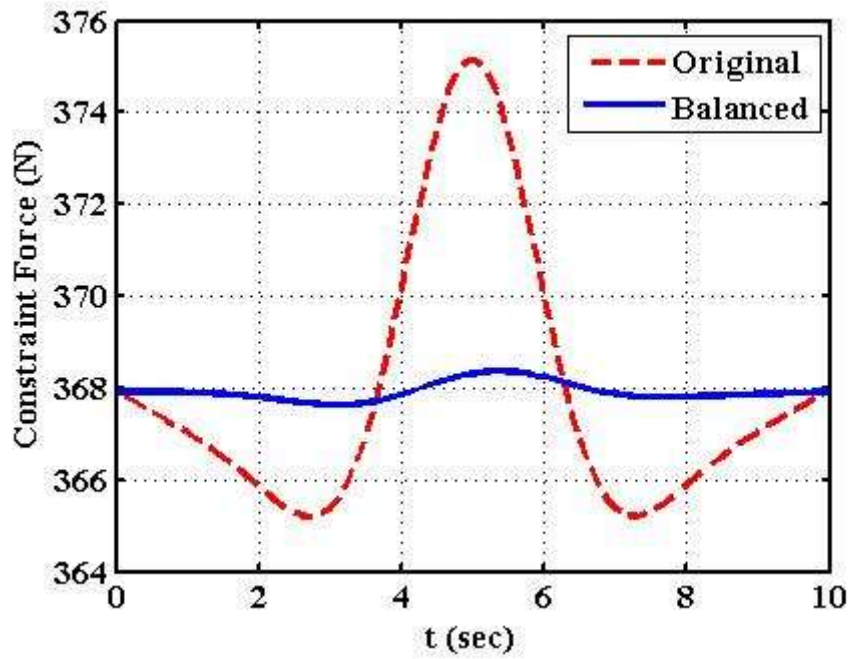
Fig.7.19: Constraint forces of original and optimally balanced PUMA at joint 1 with 6point-mass model
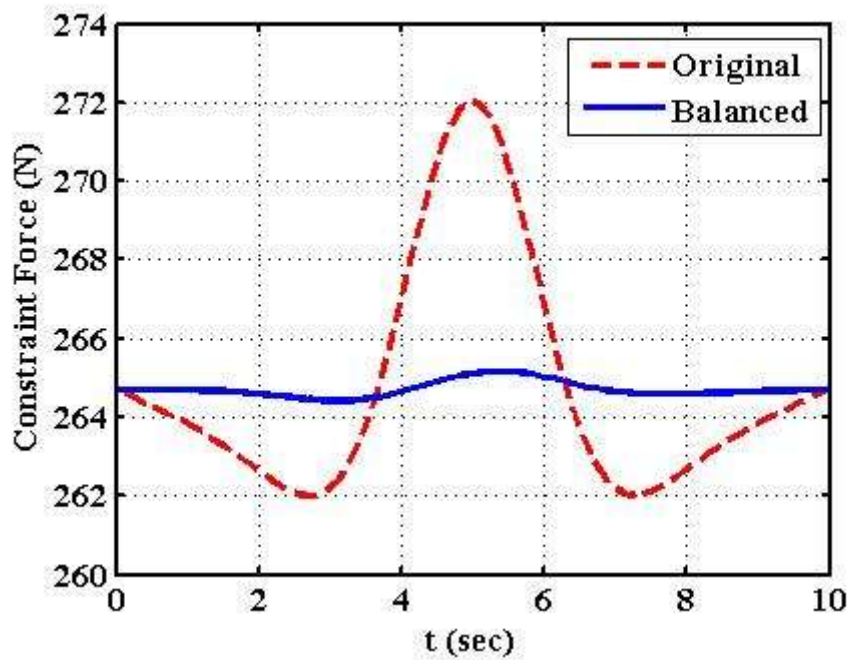
Fig.7.20: Constraint forces of original and optimally balanced PUMA at joint 2 with 6point-mass model
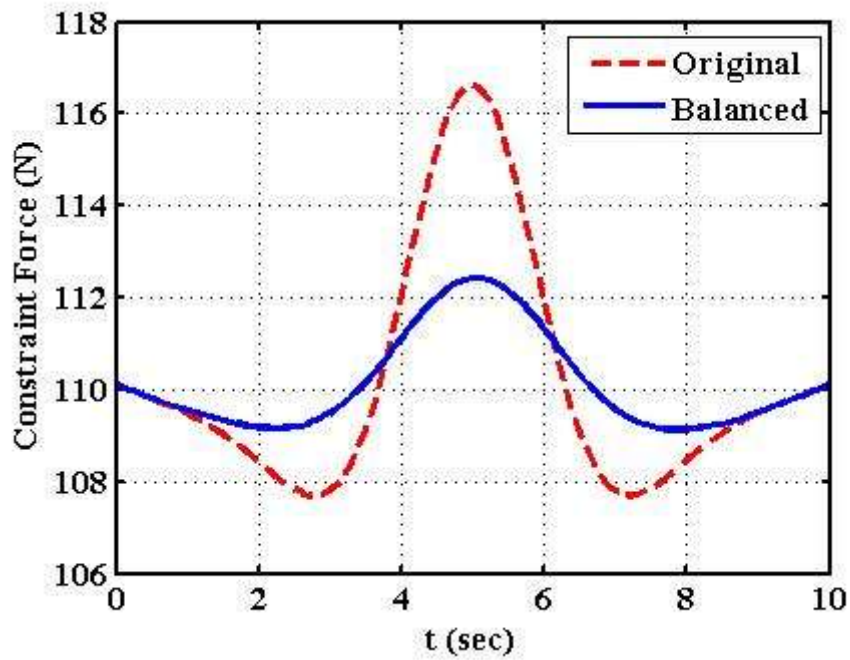
Fig.7.21: Constraint forces of original and optimally balanced PUMA at joint 3 with 6point-mass model
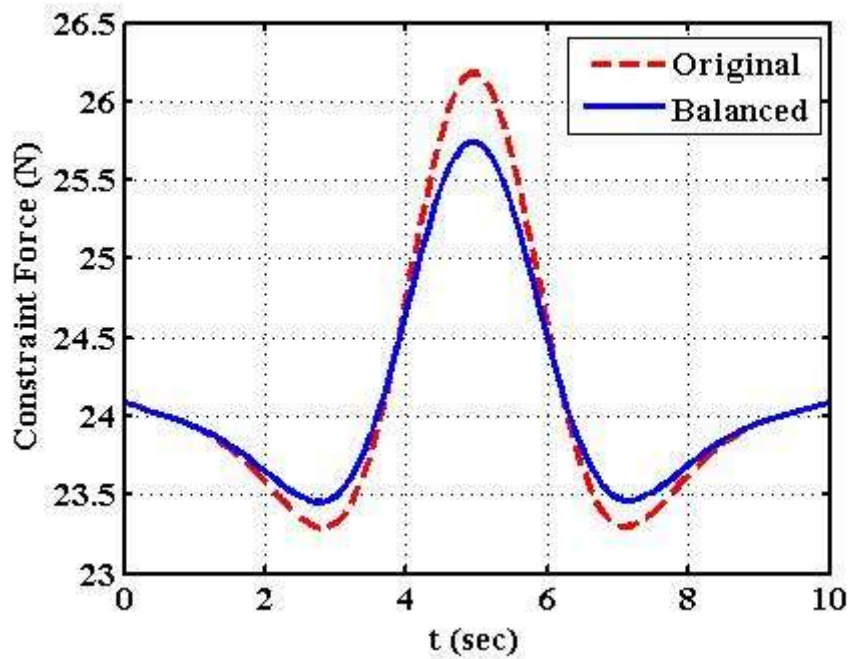
Fig.7.22: Constraint forces of original and optimally balanced PUMA at joint 4 with 6point-mass model
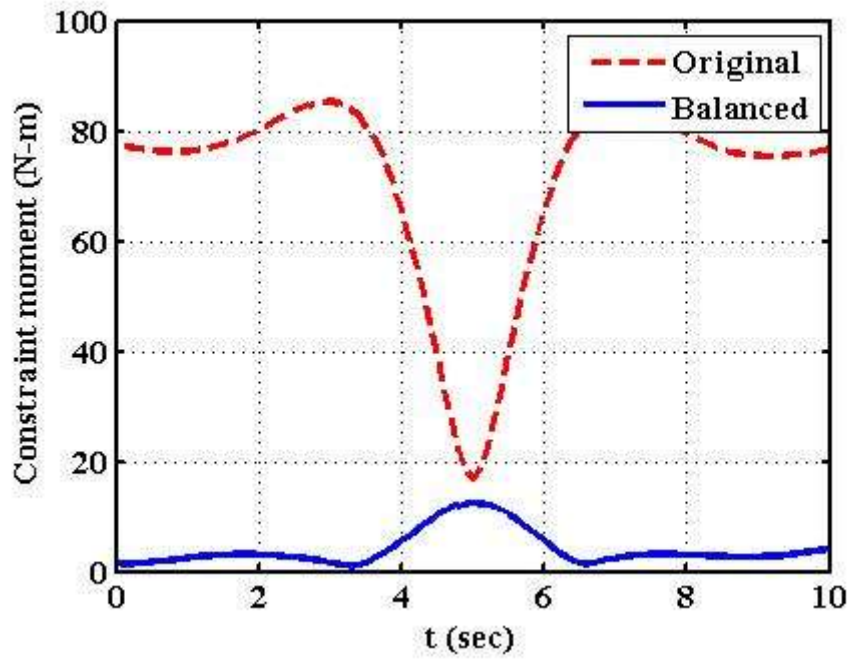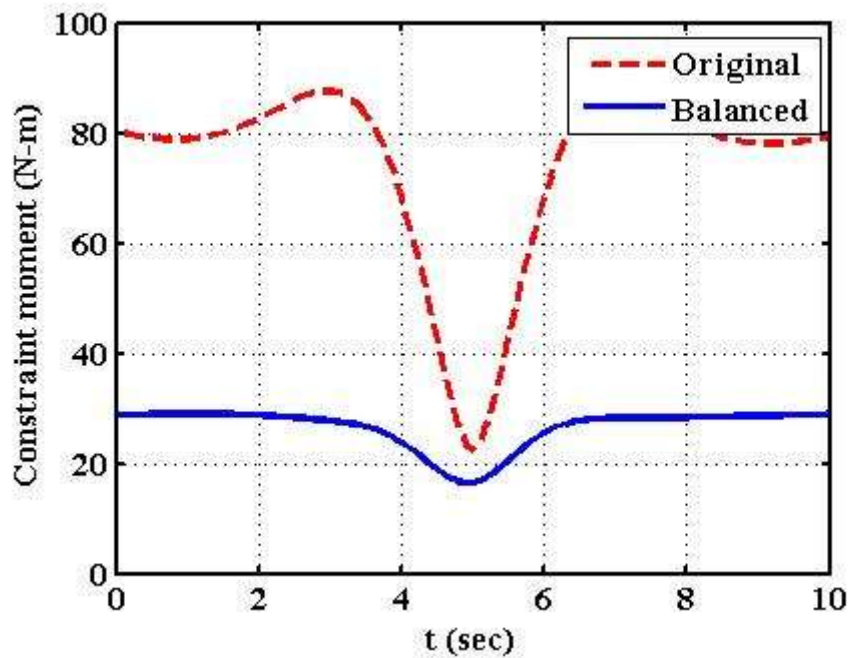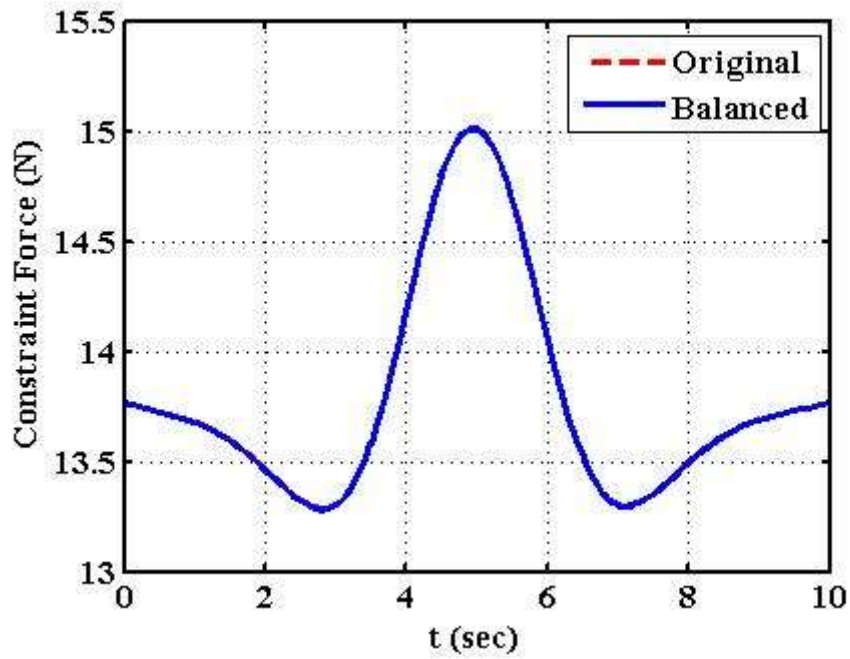
Fig.7.23: Constraint forces of original and optimally balanced PUMA at joint 5 with 6point-mass model
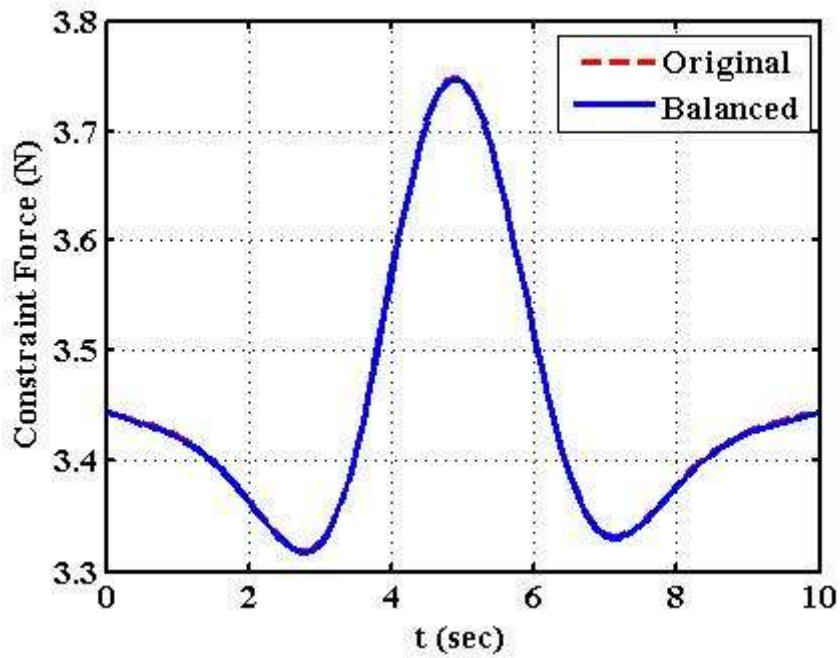
Fig.7.24: Constraint forces of original and optimally balanced PUMA at joint 6 with 6point-mass model
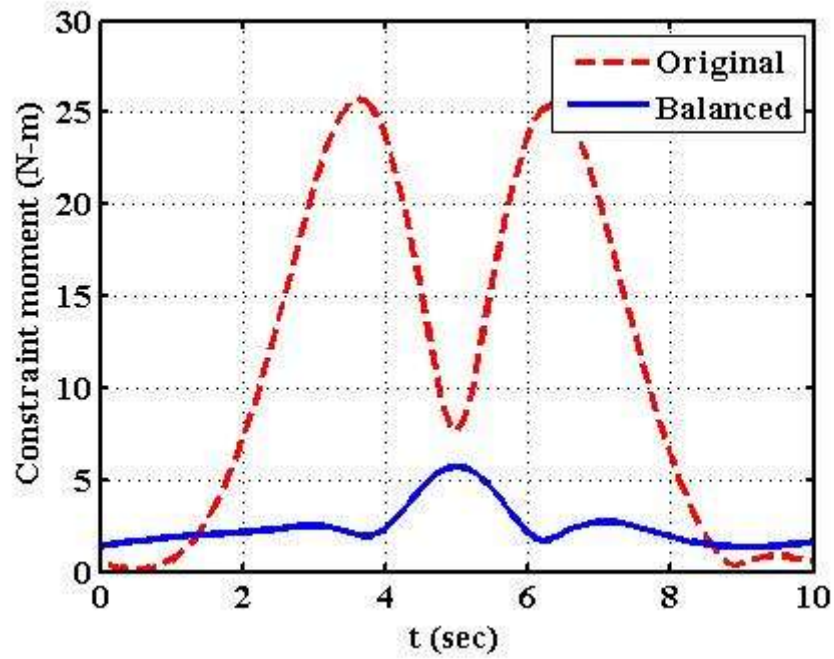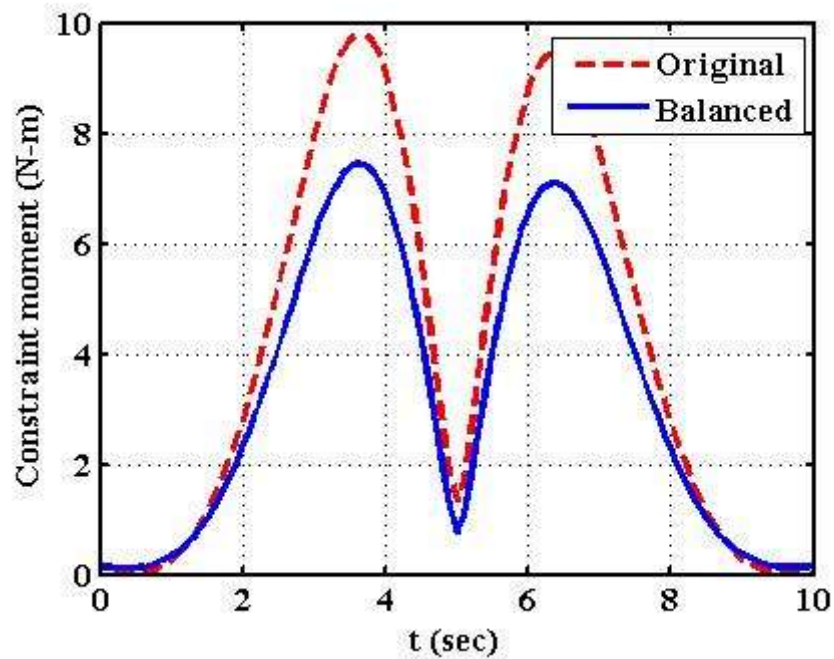
7.1.4 Five point-mass model

GA solutions were obtained for this point-masses model with the population size of 7200, elite count 72, different tolerance function and termination criteria –the number of generations. Equimomental point-masses values and their locations for the original (unbalanced) robot are considered as initial population for better convergence of objective function in lesser generations. The value of objective function obtained is presented in Table 7.11. It is observed that the average function value (FV) obtained, for N=7200; EC=72; tolerance function 1e-200, is 828.08. Elite count of 10% of population size is observed to be satisfactory. The population size of 7200 is observed to be satisfactory as the solution is terminated at the 19th generation with increased tolerance function of 1e-200.

Table 7.11: Objective function values using GA with five point-masses model

population size	elite count	tolerance function	gener ation	generation termination	objective function value
7200	72	1e -200	20	19	831.16
7200	**72**	**1e -200**	**20**	**19**	**825.47**
7200	72	1e -200	20	19	827.25
7200	72	1e -200	20	19	827.99
7200	72	1e -200	20	19	828.53

The details of improvement in function value for the solution at row 2 of Table 7.11 (marked bold) are given in Table 7.12. These results are obtained for different generations with population size (N) = 7200, Elite count (EC) = 72 and Tol fun= 1e-200. The point mass values obtained for optimized function value of 825.47 for all link's 1 to 6 are provided in Table 7.13.

Table 7.12: Improvement in FV during generations for the minimum FV = 825.47

Generation	f-count	best f(x)	max. constraint	stall generation	generation	f-count	best f(x)	max. constraint	stall generation
1	158496	953.213	3.185e-012	0	11	1670496	831.182	1.318e-012	0
2	309696	914.630	1.318e-012	0	12	1821696	831.114	1.318e-012	0
3	460896	885.484	1.318e-012	0	13	1972896	829.778	1.318e-012	0
4	612096	866.020	1.318e-012	0	14	2124096	829.114	1.318e-012	0
5	763296	859.662	1.318e-012	0	15	2275296	828.851	1.318e-012	0
6	914496	842.566	1.318e-012	0	16	2426496	827.993	1.318e-012	0
7	1065696	837.549	1.318e-012	0	17	2577696	826.719	1.318e-012	0
8	1216896	833.823	1.318e-012	0	18	2728896	825.496	1.318e-012	0
9	1368096	832.077	1.318e-012	0	19	2880096	825.474	1.318e-012	0
10	1519296	831.926	1.318e-012	0					

Table 7.13: Point mass values for optimized FV of 825.47

Link, i	m_{i1}	m_{i2}	m_{i3}	m_{i4}	m_{i5}
1	0.5888	2.3594	1.8019	1.1750	4.5964
2	0.4065	3.4948	6.0053	0.7075	5.1477
3	2.6632	1.6427	1.6937	0.2213	2.5461
4	0.1753	0.5116	0.0226	0.1753	0.1672
5	0.1753	0.3506	0.1753	0.1753	0.1753
6	0.0585	0.1170	0.0585	0.0585	0.0585

The optimized values of constraint moments and constraint forces at different joints of original and optimized PUMA robot obtained using five point-masses model are given in Table 7.14. The optimized constraint moment values at different joints are reduced significantly. The shaking moment is reduced from 168.817 to 41.328 due to the proper mass distribution of links that affects its inertia and thus shaking moment. The constraint forces that depends on the total mass of the link remains nearly the same because the total mass of the links is retained same. However, the peak value of

constraint forces at different joints is reduced somewhat as demonstrated by various

graphs of constraint forces, from Fig. 7.31-7.36.

Table 7.14: Constraint moments and Constraint forces for original and optimized
PUMA with FV of 825.47

Constraint moment	$\tilde{n}_1$	$\tilde{n}_2$	$\tilde{n}_3$	$\tilde{n}_4$	$\tilde{n}_5$	$\tilde{n}_6$	Total
Original PUMA	73.12	75.61	14.47	5.43	0.111	0.076	168.817
Optimized PUMA	4.508	26.186	5.573	4.873	0.112	0.076	41.328
Constraint force	$\tilde{f}_1$	$\tilde{f}_2$	$\tilde{f}_3$	$\tilde{f}_4$	$\tilde{f}_5$	$\tilde{f}_6$	Total
Original PUMA	367.97	264.79	110.22	24.138	13.797	3.452	784.367
Optimized PUMA	367.925	264.71	110.12	24.126	13.795	3.452	784.128
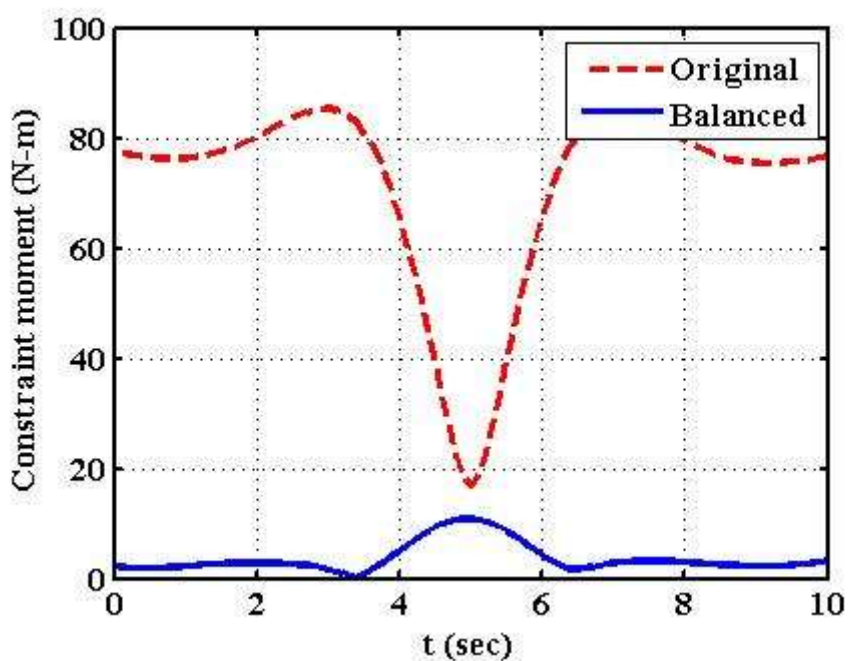
**Fig.7.25: Constraint moments of original and optimally balanced PUMA at joint
1 with 5point-mass model**
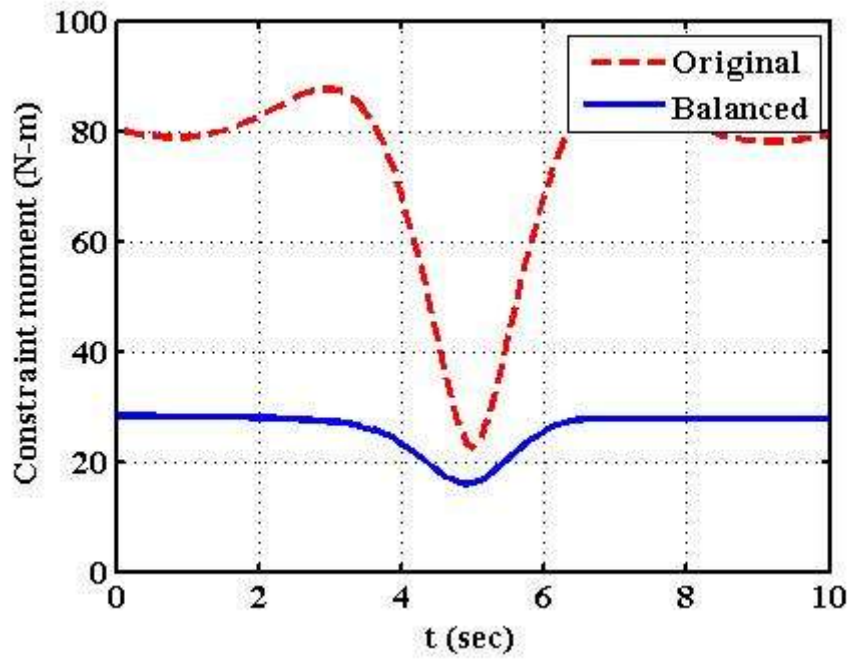
Fig.7.26: Constraint moments of original and optimally balanced PUMA at joint 2 with 5point-mass model
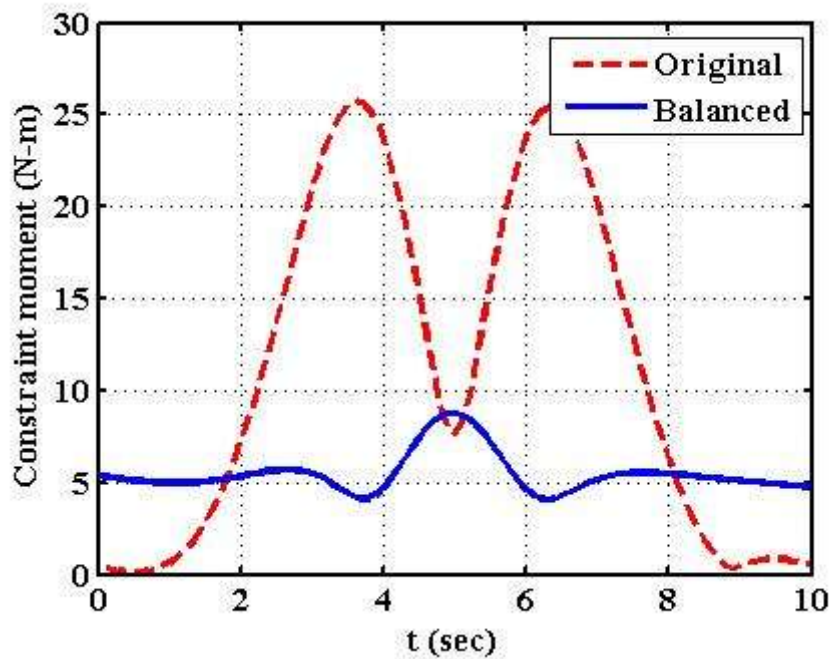
Fig.7.27: Constraint moments of original and optimally balanced PUMA at joint 3 with 5point-mass model

84
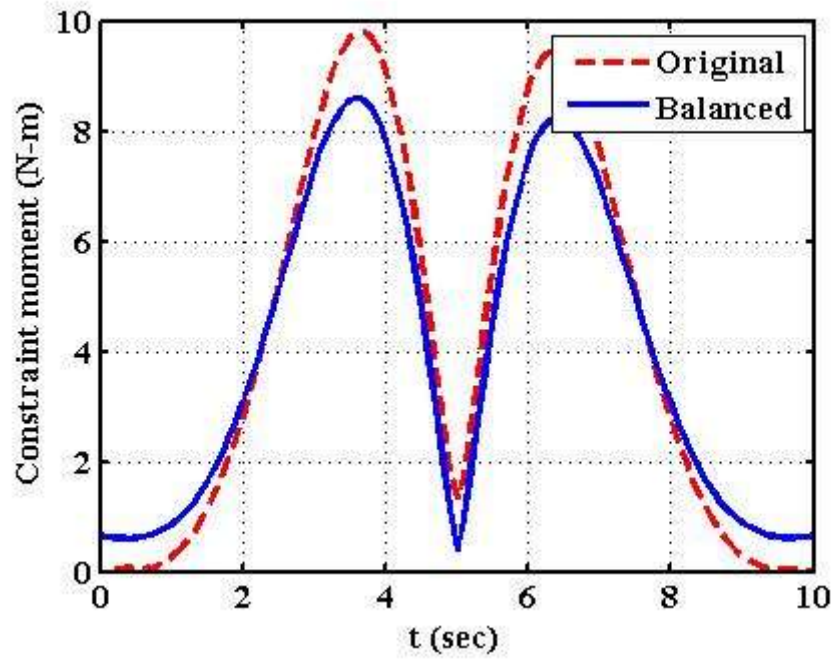
Fig.7.28: Constraint moments of original and optimally balanced PUMA at joint 4 with 5point-mass model
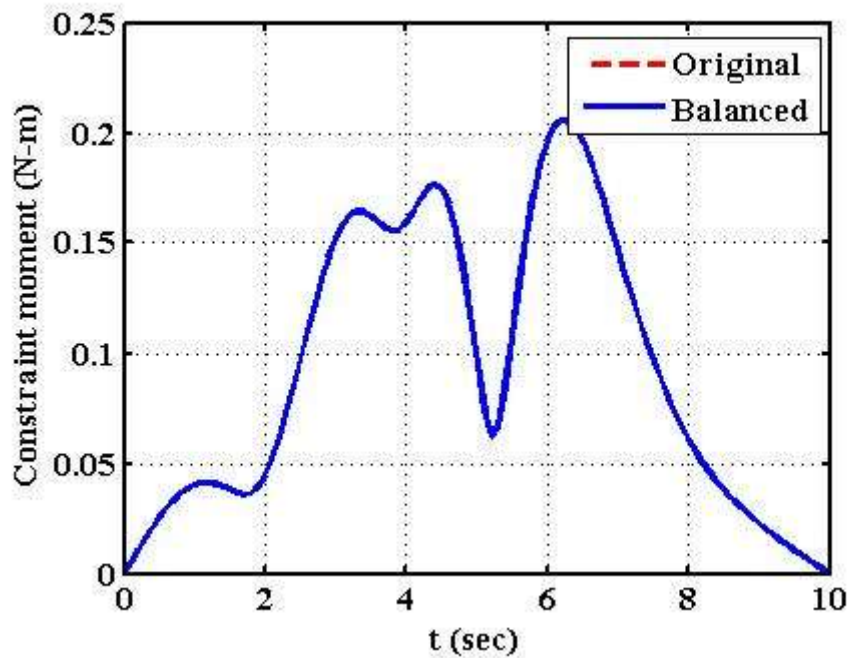
Fig.7.29: Constraint moments of original and optimally balanced PUMA at joint 5 with 5point-mass model
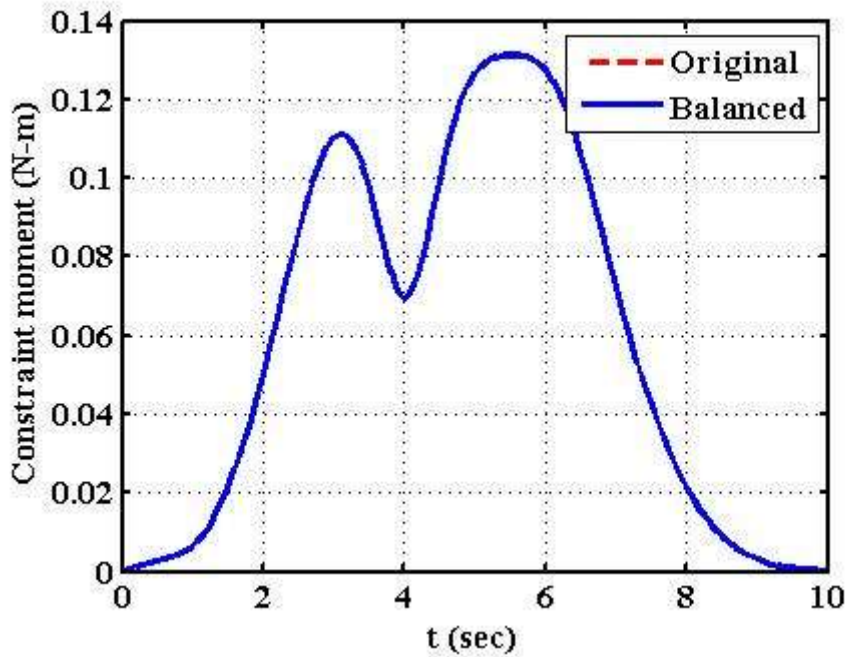
Fig.7.30: Constraint moments of original and optimally balanced PUMA at joint 6 with 5point-mass model

Fig.7.31: Constraint forces of original and optimally balanced PUMA at joint 1 with 5point-mass model

Fig.7.32: Constraint forces of original and optimally balanced PUMA at joint 2 with 5point-mass model

Fig.7.33: Constraint forces of original and optimally balanced PUMA at joint 3 with 5 point-mass model

Fig.7.34: Constraint forces of original and optimally balanced PUMA at joint 4 with 5point-mass model

Fig.7.35: Constraint forces of original and optimally balanced PUMA at joint 5 with 5 point-mass model

Fig.7.36: Constraint forces of original and optimally balanced PUMA at joint 6 with 5 point-mass model

7.1.5 Four point mass model

GA solutions were obtained for this point-masses model with different population size, elite count, tolerance function and termination criteria –the number of generations. Equimomental point-masses values and their locations for the original (unbalanced) robot are considered as initial population for better convergence of objective function in less number of generations. The value of objective function obtained is presented in Table 7.15. It is observed that the average function value (FV) obtained, for N=7200; EC= 72; tolerance function 10^{-90}, is 826.54. Elite count of 10% of population size is observed to be satisfactory. The population size of 7200 is observed to be satisfactory as the solution is terminated at the 20th generation even with tolerance function of 10^{-90}.

Table 7.15: Objective function values using GA with four point-mass model

population size	elite count	tolerance function	gener ation	generation termination	Objective function value
7200	72	1e -90	20	20	826.46
7200	72	1e -90	20	20	828.09
7200	**72**	**1e-90**	**20**	**20**	**825.70**
7200	72	1e -90	20	20	826.90
6000	60	1e-200	20	20	826.27

The details of improvement in function value for the solution at row 3 of Table 7.15 (marked bold) are given in Table 7.16. These results are obtained for different generations with population size (N) = 7200, Elite count (EC) of 72 and Tol fun of 1e-90. The Point mass values obtained for optimized function value of 825.7 for all links 1 to 6 are presented in Table 7.17.

Table 7.16: Improvement in FV during generations for the minimum FV = 825.7

gen erati on	f-count	best f(x)	max. constra int	stall gener ation	gen erati on	f-count	best f(x)	max. constra int	stall gene ratio n
1	158478	953.2 21	4.395e-012	0	11	1670478	829.2 14	0	0
2	309678	936.2 75	0	0	12	1821678	828.3 77	0	0
3	460878	898.8 77	3.480e-012	0	13	1972878	827.4 80	0	0
4	612078	861.9 00	3.480e-012	0	14	2124078	827.2 72	0	0
5	763278	847.4 85	0	0	15	2275278	827.0 21	0	0
6	914478	837.3 53	0	0	16	2426478	826.9 63	0	0
7	1065678	831.4 80	0	0	17	2577678	826.9 56	0	0
8	1216878	831.1 24	0	0	18	2728878	826.3 72	0	0
9	1368078	830.6 75	0	0	19	2880078	825.9 87	8.458e-007	0
10	1519278	829.8 00	0	0	20	3031278	825.7 01	8.485e-007	0

Table 7.17: Point mass values for optimized FV of 825.7

Link, i	m_{i1}	m_{i2}	m_{i3}	m_{i4}
1	3.8121	0.5948	1.4327	4.6831
2	3.0117	4.2440	0.0351	8.4705
3	2.4844	1.0167	1.3208	3.9451
4	0.3594	0.2630	0.2599	0.1703
5	0.2630	0.2630	0.2630	0.2630
6	0.0878	0.0878	0.0878	0.0877

The optimized values of constraint moments and constraint forces at different joints of original and optimized PUMA robot obtained using four point-mass model are given in Table 7.18. The optimized shaking moment values at different joints are reduced significantly. The shaking moment is reduced from 168.817 to 41.524 due to the proper mass distribution of links that affects its inertia and thus shaking moment. The constraint forces that depends on the total mass of the link remains nearly the same because the total mass of the links is retained same. However, the peak value of constraint forces at different joints is reduced somewhat as demonstrated by various graphs of constraint forces, from Fig. 7.43-7.48.

Table 7.18:- Constraint moments and Constraint forces for original and optimized PUMA with FV of 825.7

Constraint moment	$\tilde{n}_1$	$\tilde{n}_2$	$\tilde{n}_3$	$\tilde{n}_4$	$\tilde{n}_5$	$\tilde{n}_6$	Total
Original Puma	73.12	75.61	14.47	5.43	0.111	0.076	168.817
Optimized Puma	4.158	28.495	3.516	5.169	0.111	0.076	41.524
Constraint force	$\tilde{f}_1$	$\tilde{f}_2$	$\tilde{f}_3$	$\tilde{f}_4$	$\tilde{f}_5$	$\tilde{f}_6$	Total
Original Puma	367.97	264.79	110.22	24.138	13.797	3.452	784.367
Optimized Puma	367.94	264.715	110.129	24.140	13.798	3.453	784.175
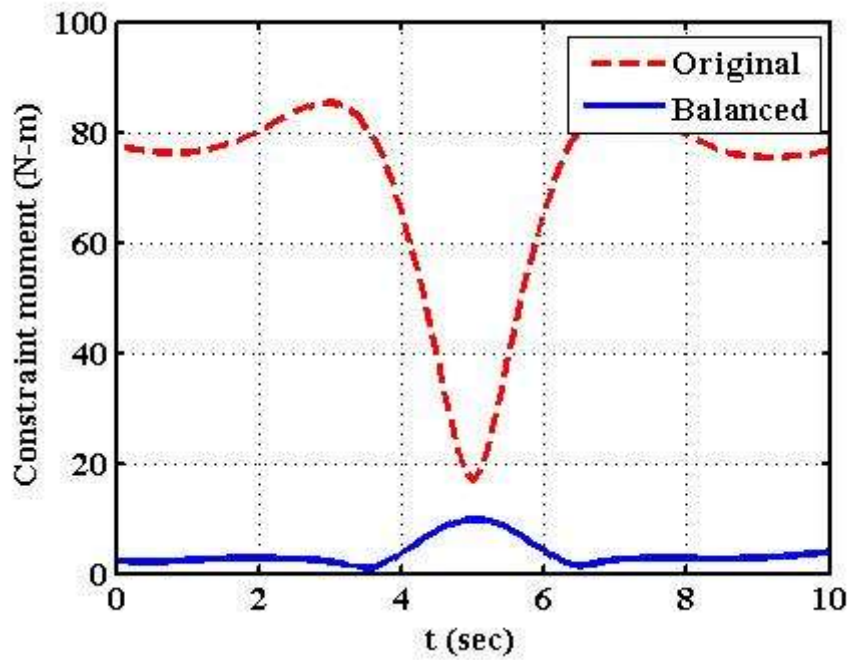
Fig.7.37: Constraint moments of original and optimally balanced PUMA at joint 1 with 4point-mass model
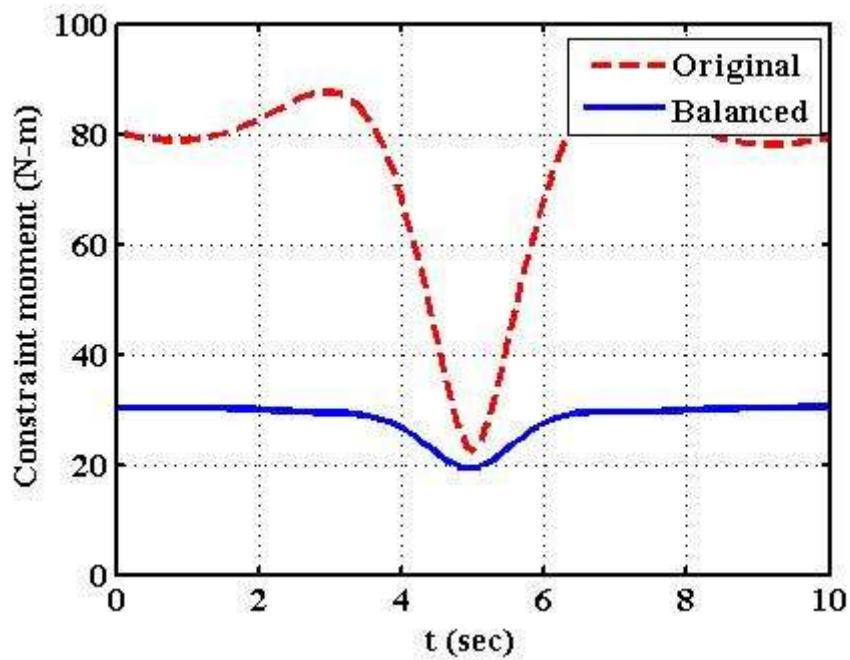
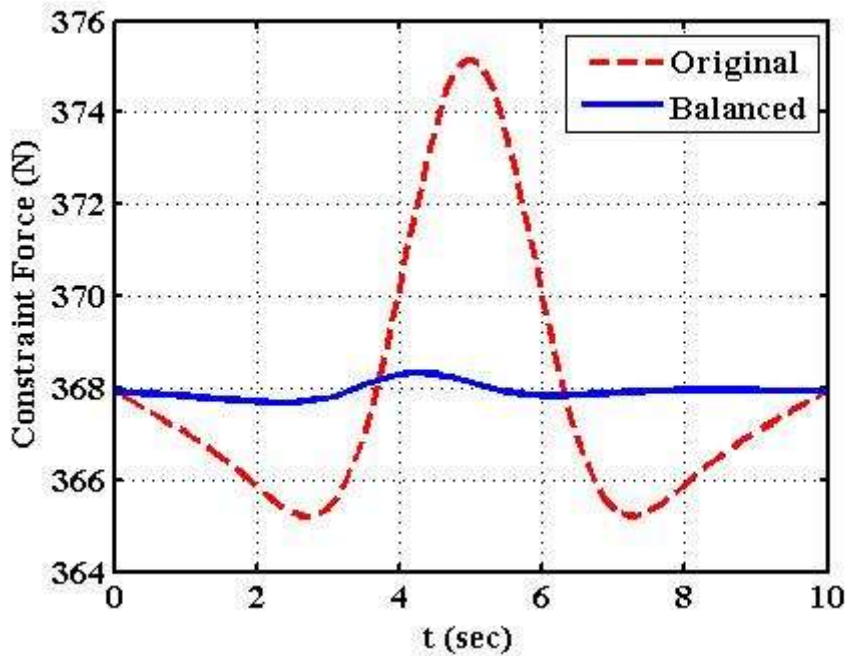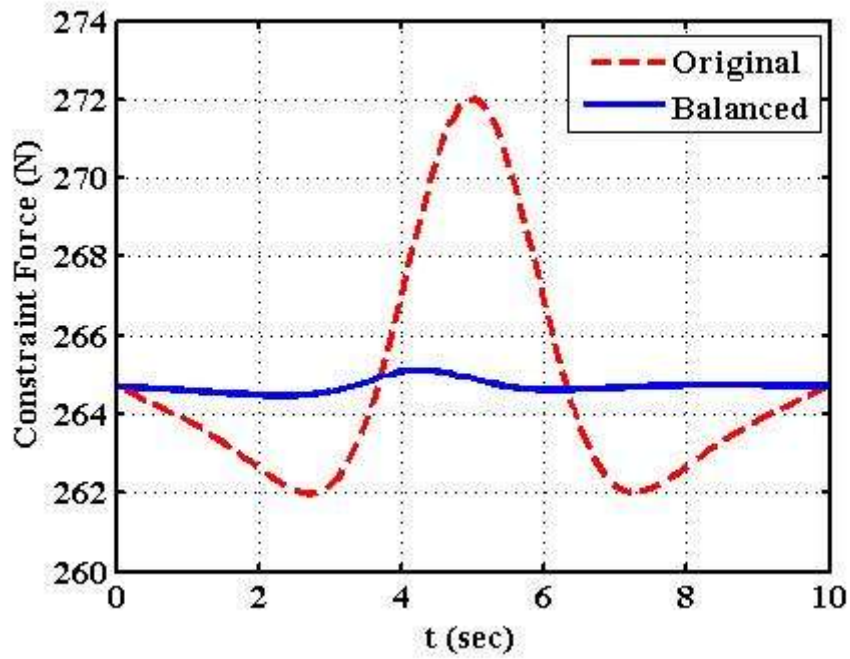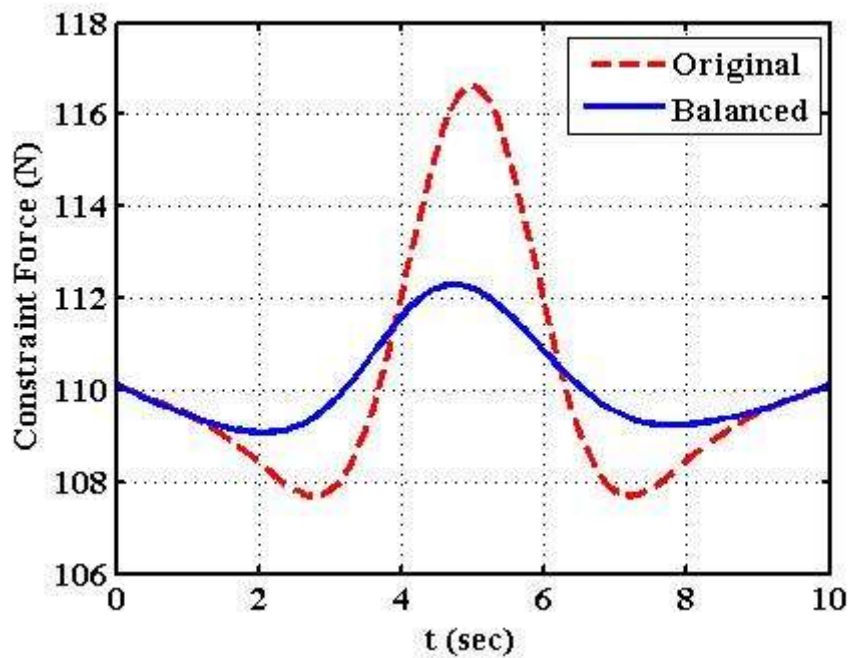**Fig.7.38: Constraint moments of original and optimally balanced PUMA at joint 2 with 4point-mass model**
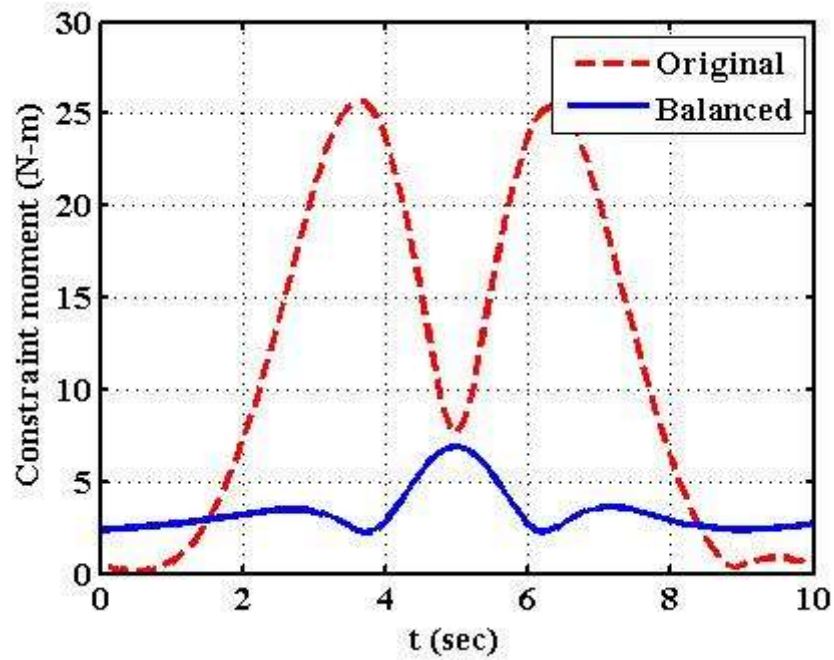
Fig.7.39: Constraint moments of original and optimally balanced PUMA at joint 3 with 4 point-mass model
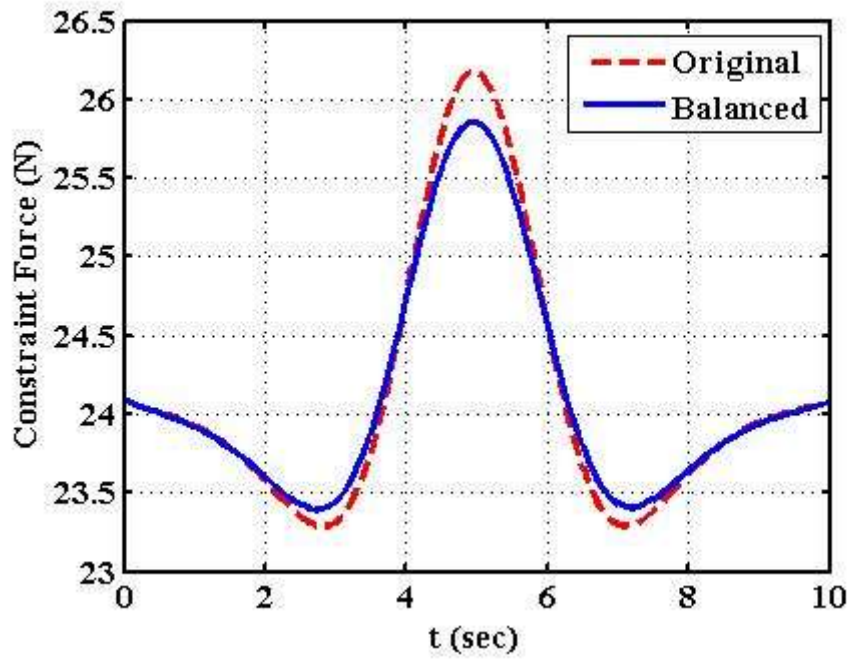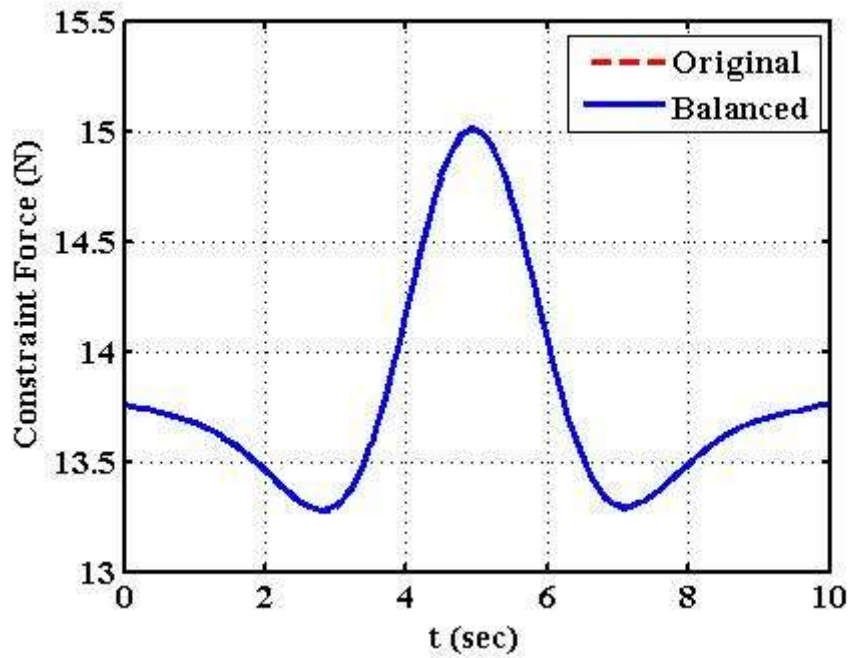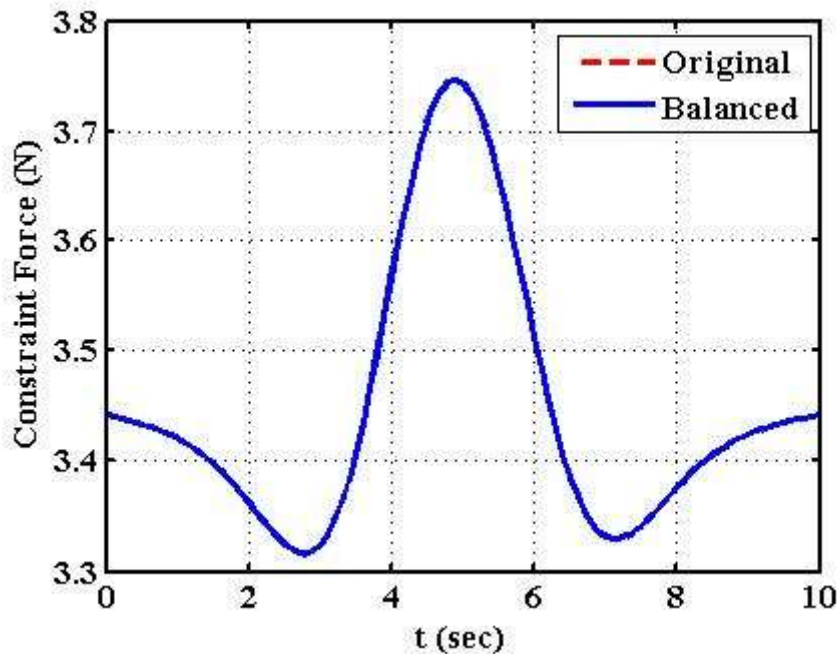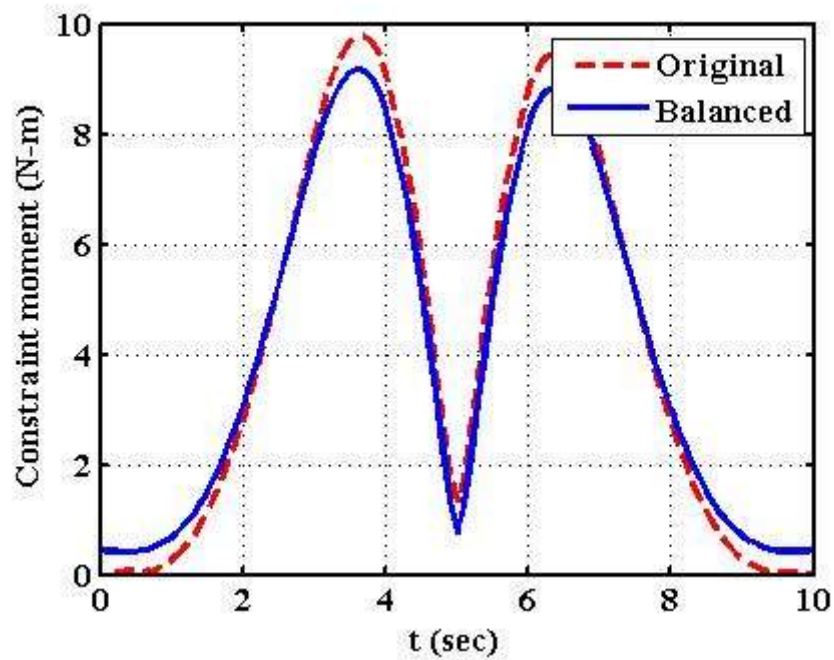

Fig.7.40: Constraint moments of original and optimally balanced PUMA at joint 4 with 4 point-mass model
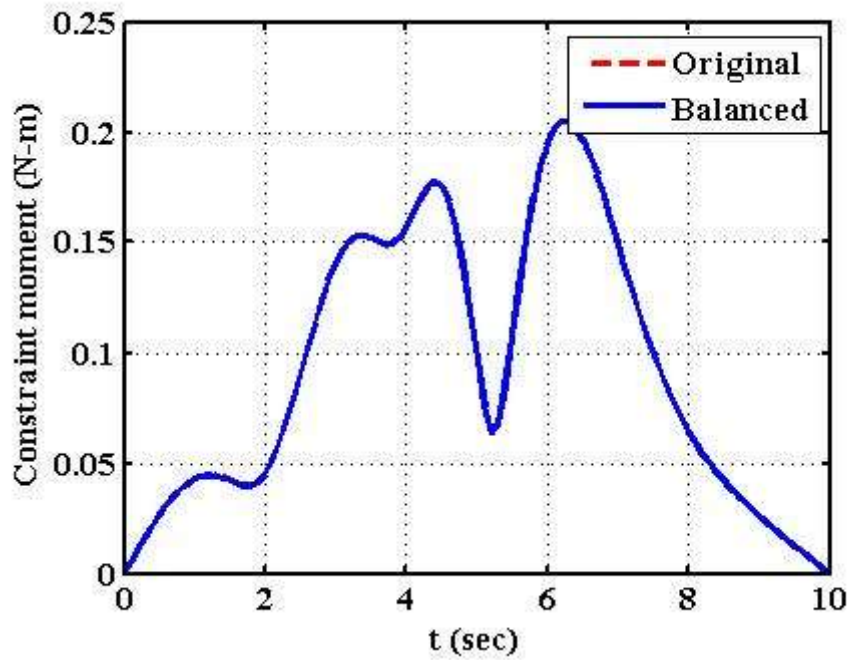
Fig.7.41: Constraint moments of original and optimally balanced PUMA at joint 5 with 4 point-mass model
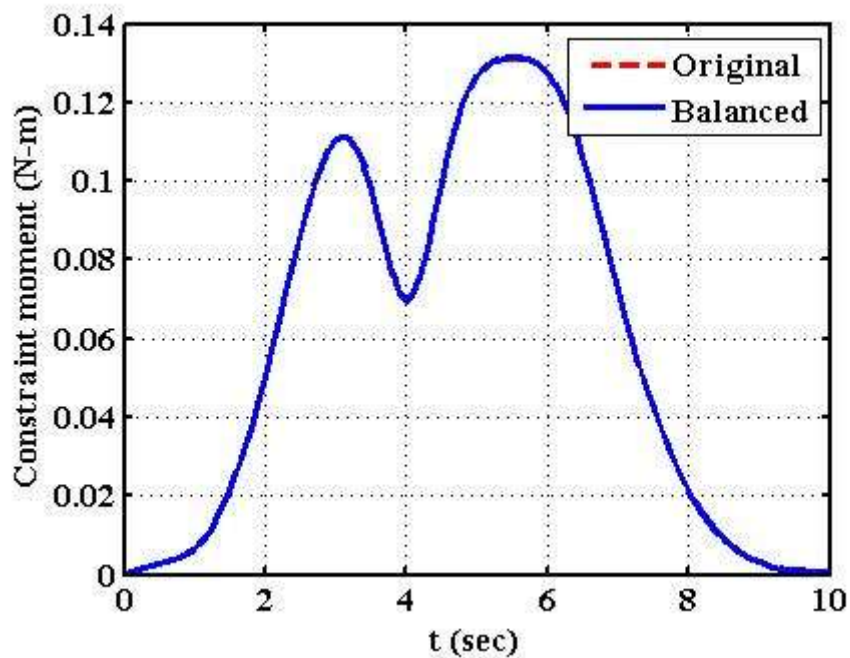
Fig.7.42: Constraint moments of original and optimally balanced PUMA at joint 6 with 4 point-mass model
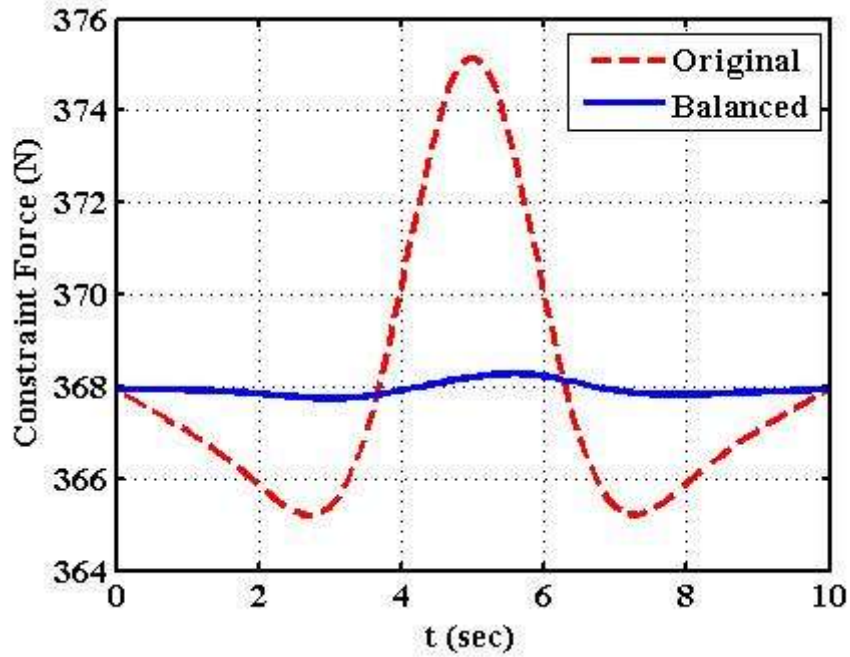
Fig.7.43: Constraint forces of original and optimally balanced PUMA at joint 1 with 4 point-mass model
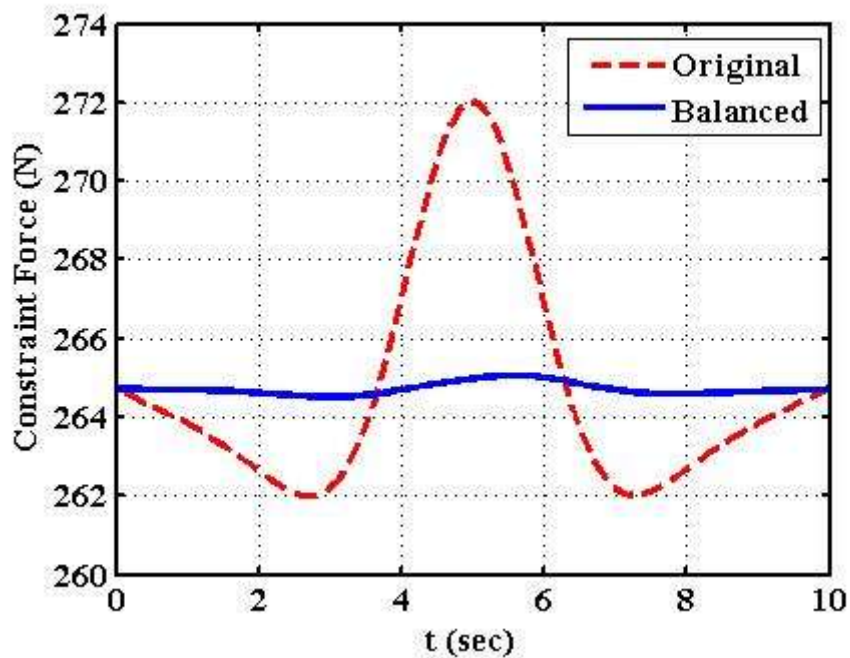
Fig.7.44: Constraint forces of original and optimally balanced PUMA at joint 2 with 4 point-mass model
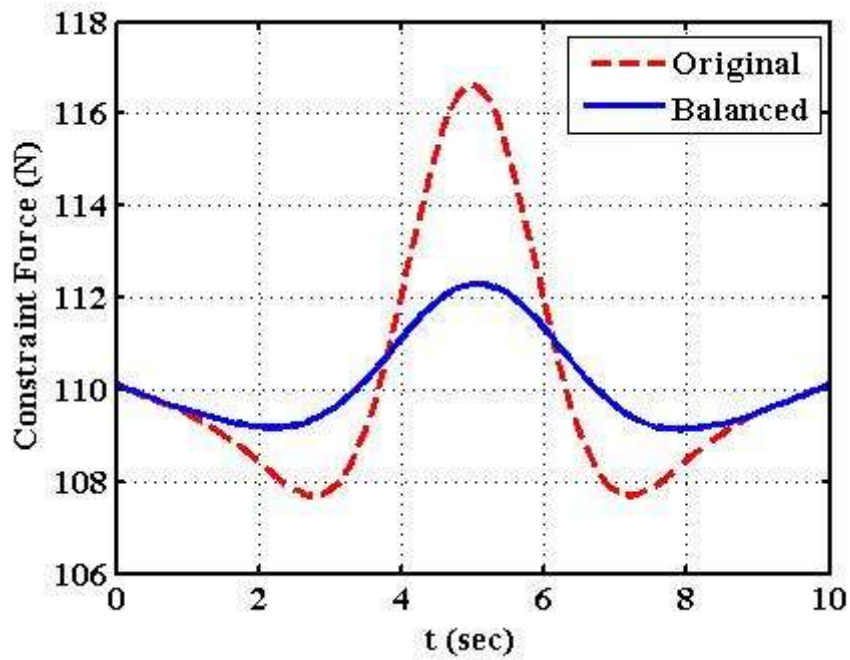
Fig.7.45: Constraint forces of original and optimally balanced PUMA at joint 3 with 4 point-mass model
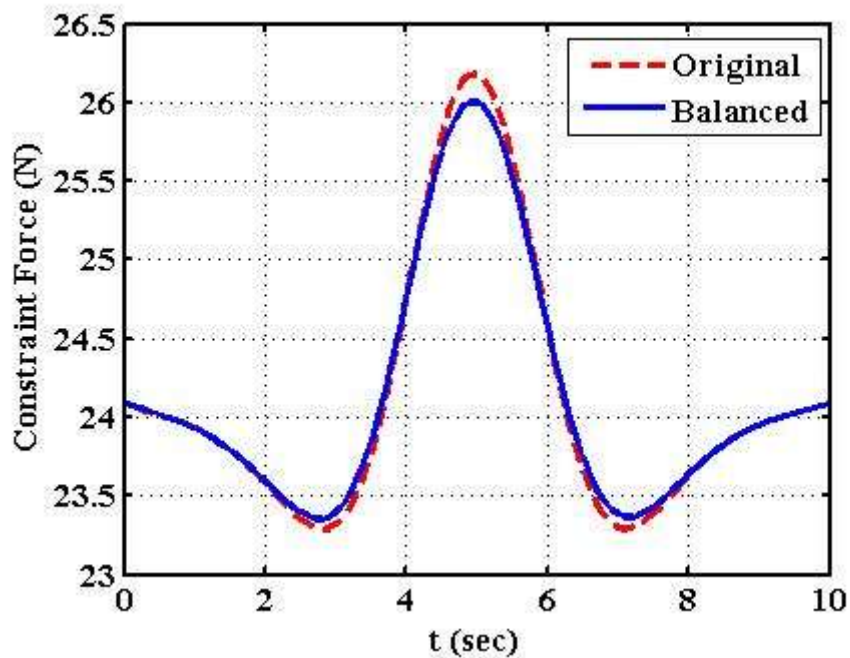
Fig.7.46: Constraint forces of original and optimally balanced PUMA at joint 4 with 4 point-mass model
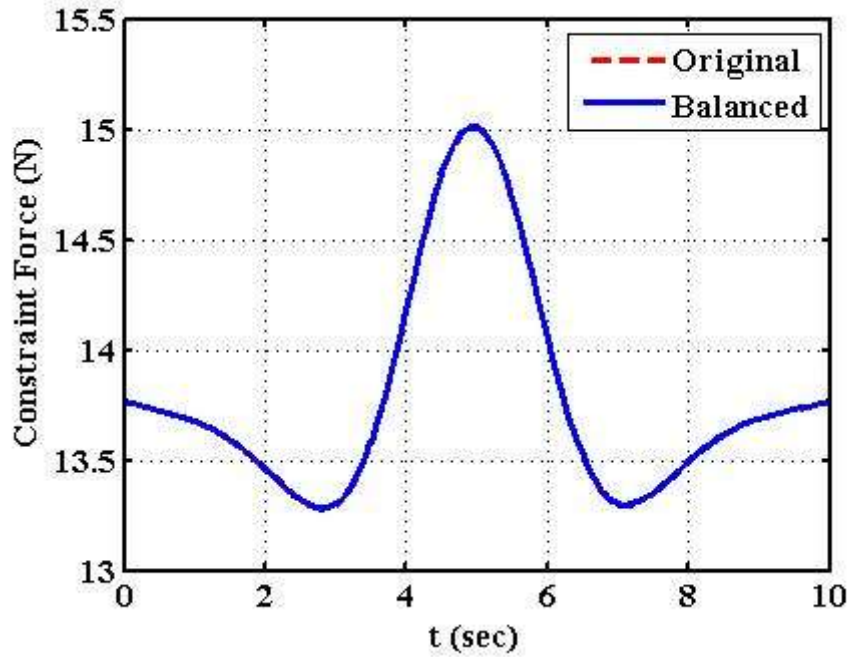
Fig.7.47: Constraint forces of original and optimally balanced PUMA at joint 5 with 4 point-mass model
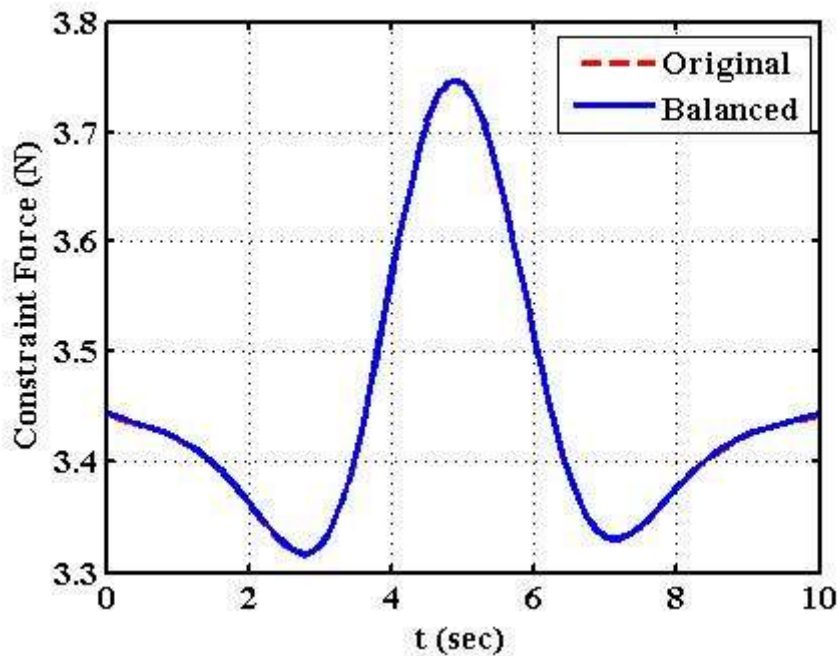
Fig.7.48: Constraint forces of original and optimally balanced PUMA at joint 6 with 4 point-mass model

7.2 Summary

In this chapter, the optimization problem of industrial manipulators is solved using GA for various equimomental point mass model configurations i.e. seven point-mass octahedron model, six point-mass hexahedron model, five point-mass hexahedron model, and four point-mass model. The optimized value of constraint moments and constraint forces at different joint of the manipulator is obtained and presented in tabular form for each of the four models. The variation of constraint moment and constraint force at each joint of manipulator over one cycle of operation is represented graphically for each of the four models. The results with different point-mass models and optimization techniques will be compared in chapter 9.

Optimization Using TLBO

This chapter gives the results in the form of optimized mass distribution for each link of the manipulator. PUMA robot is being considered as the problem for illustration of the proposed methodology on the dynamic balancing of industrial manipulators using different point-masses model developed in chapter 3 and equation of motion given in chapter 4. The optimization problem is formulated in chapter 5 while optimization technique TLBO discussed in chapter 6 and the flow chart of TLBO is developed in this chapter. The coding for TLBO has been developed for the problem using the flow chart of TLBO. Using TLBO the values of optimization function, i.e., the sum of RMS values of shaking moments and shaking forces at each joint of the manipulator is computed by varying the decision variables, i.e., point- masses. The use of "teaching-learning–based-optimization" technique for optimization of the manipulator has not been reported in the literature so far and it has been used by the author for the first time.

Optimized function values for 30 cases are obtained using TLBO. Their mean, standard deviation, optimized point-mass values of each link for minimum function value, constraint moment and constraint force at each joint of the manipulator for minimum function value is presented in tabular form. The variation of constraint moment and constraint force at each joint of manipulator over one cycle of operation is then graphically represented.

8.1 Shaking moments and forces using TLBO

The basic philosophy of TLBO has been discussed in chapter 6. The flow chart of TLBO for optimization problem formulated is discussed here. In the TLBO a group of

learners is considered as population and design variables are different subjects offered to the learner, and the result of the learner is analogous to the objective function. For our problem, population P is a set of design vectors $\mathbf{X}_k$, $k = 1,2, \dots p$ and can be expressed in matrix form as follows:

Population, $\mathbf{P} = [\mathbf{X_1}, ..., \mathbf{X_p}]^T$

The design variables m_{ij} are subjects and the value of the objective function $f(\mathbf{X})$ is the result of the learner. The design vector $\mathbf{X_k}$ for which $f(\mathbf{X_k})$ is minimum becomes $\mathbf{X}^*$ and it acts as the teacher for that iteration.

The TLBO algorithm is divided in to two parts, "Teacher's Phase" and "Learner's Phase". In the "Teacher's Phase", learner, i.e. $7n$ dimensional design vector $\mathbf{X}$(for 7 point-masses model), learns through teacher $\mathbf{X}^*$. The teacher tries to increase the mean of the population $\overline{\mathbf{X}}$ to his/her level $\mathbf{X}^*$. Therefore, design vectors are modified as

$\mathbf{X_{k,new}} = \mathbf{X_k} + \rho(\mathbf{X}^* - \overline{\mathbf{X}})$ where ρ is the $7n \times 7n$ diagonal matrix of random numbers to be generated in the range [0 1]. If the objective function value for the new solution is better than that of old, $f(\mathbf{X_{k,\text{new}}}) < f(\mathbf{X_k})$, the new solution is accepted otherwise the old one is retained. It completes the "Teacher's Phase" as shown in Fig. 8.1.

In "Learner's Phase", learners increase their knowledge by interaction among themselves. A learner learns new things if the other learner has more knowledge than him/her. Any learner, $\mathbf{X_k}$, improves his/her knowledge through interaction with any other two learners, say $\mathbf{X}_q$ & $\mathbf{X}_r$, from the population. The improvement is based on comparison of their objective function values as follows:

$\mathbf{X}_{kq} = \mathbf{X}_k + \rho_{lp}(\mathbf{X}_k - \mathbf{X}_q)$,   if $f(\mathbf{X_k}) < f(\mathbf{X}_q)$

$\mathbf{X}_{kq} = \mathbf{X}_k + \rho_{lp}(\mathbf{X}_q - \mathbf{X}_k)$,   if $f(\mathbf{X_k}) > f(\mathbf{X}_q)$

$\mathbf{X}_{kr} = \mathbf{X}_k + \rho_{lp} (\mathbf{X}_k - \mathbf{X}_r), \quad \text{if} \quad f(\mathbf{X}_k) < f(\mathbf{X}_r)$

$\mathbf{X}_{kr} = \mathbf{X}_k + \rho_{lp} (\mathbf{X}_r - \mathbf{X}_k), \quad \text{if} \, f(\mathbf{X}_k) > f(\mathbf{X}_r)$

Where ρ_{lp} is the $7n \times 7n$ diagonal matrix of random numbers in the learners phase to be generated in the range [0 1]. The objective function values $f(\mathbf{X}_{kq})$, $f(\mathbf{X}_{kr})$ and $f(\mathbf{X}_k)$ are compared to find the minimum function value. The solution $\mathbf{X}_{kq}$ is accepted, if $f(\mathbf{X}_{kq})$ is minimum. The solution $\mathbf{X}_{kr}$ is accepted, if $f(\mathbf{X}_{kr})$ is minimum, otherwise the solution $\mathbf{X}_k$ is retained. This process completes one cycle of iteration. The process from the computation of variable mean $\overline{\mathbf{X}}$ onwards is repeated if the termination criterion is not satisfied. The final solution values for $\mathbf{X}_k$'s are achieved if the termination criterion is satisfied. The design vector for which $f(\mathbf{X}_k)$ is minimum represents the optimal solution.

A MATLAB program is developed based on the flowchart of TLBO algorithm given in Fig. 8.1. The constraint on non-negativity of point masses is handled through penalty function in the objective function. Constraint on the sum of point masses (Eq. 5.4(b)) is implemented by re-defining any one point mass m_{ij} for each link $i = 1, 2, \ldots$ n. This is implemented at the end of initialization of population and whenever the design variable values are changed during teacher phase and learner phase. As the number of the design variables is large, the number of population sets in the solution for 7 and 6 point-masses models is taken as 200. However, with such large number of population sets the solution converges in less number of generations i.e. 20. For 5 and 4 point-masses models 50 numbers of population sets are taken, and the number of generations is increased to 50 for better convergence of the solution.
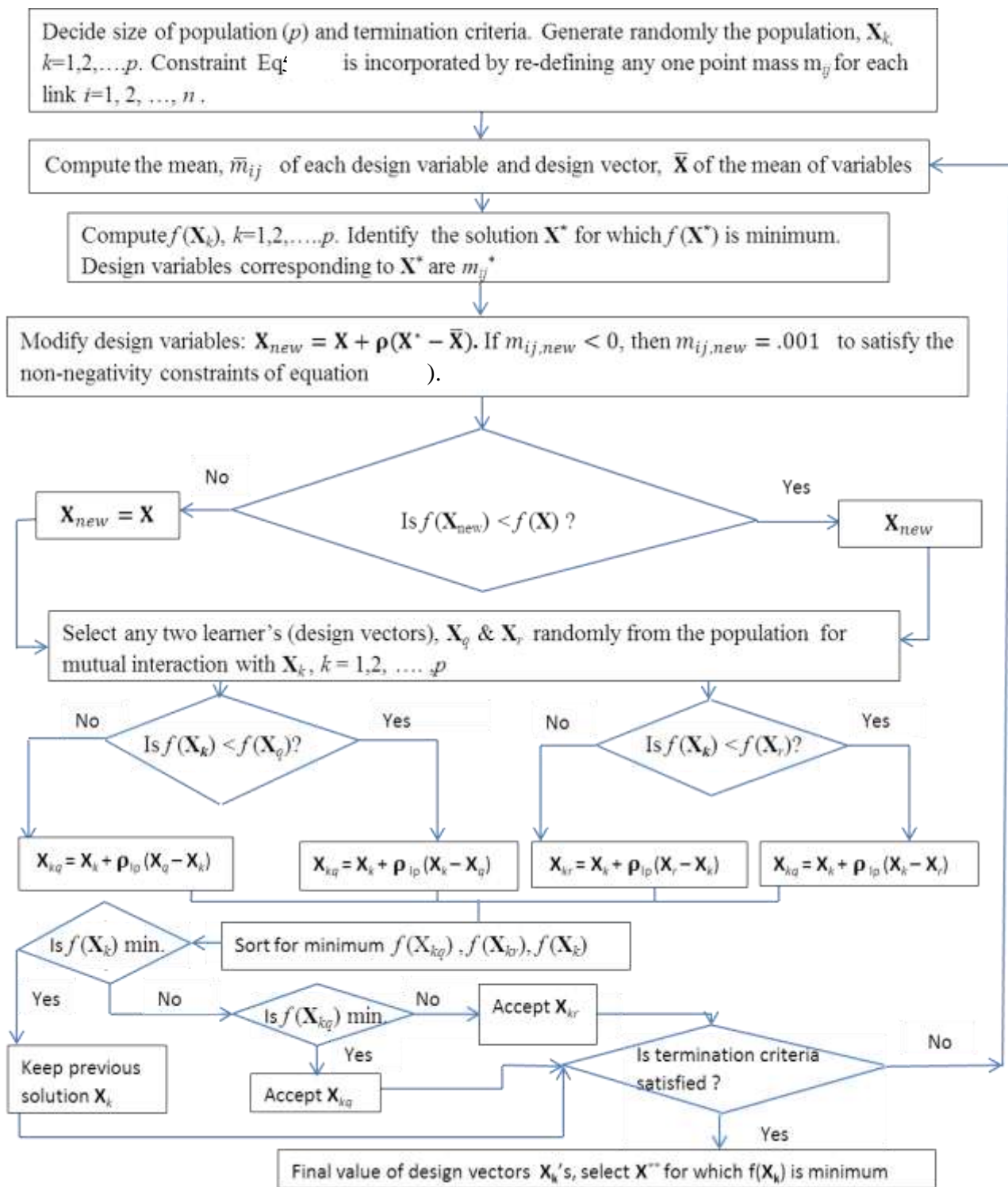
Fig. 8.1: Flow chart of TLBO algorithm

8.1.1 Seven point-mass octahedron model

TLBO solutions were obtained for this point-mass model with population sets of 200, termination criterion (20 number of generation). The initial population sets are generated randomly. Since the number of design variables (42) is large, the increase in population sets improves the value of the objective function. The value of objective function for 30 trials is tabulated in Table 8.1. The average value of objective function obtained, for the number of sets = 200 and the number of generations/iterations = 20, is 814.526 with the standard deviation of 1.1496. The details of improvement in the function value at trial number 29 of table 8.1 during different generations with population set = 200 are given in Table 8.2.

Table 8.1: Objective function value (FV) for different trials

Trial	1	2	3	4	5	6	7
FV	815.404	815.252	813.790	814.599	812.915	812.915	815.499
Trial	8	9	10	11	12	13	14
FV	814.627	815.657	815.048	814.292	816.319	813.215	815.680
Trial	15	16	17	18	19	20	21
FV	812.142	814.228	812.937	815.349	814.802	814.895	814.493
Trial	22	23	24	25	26	27	28
FV	815.698	814.394	813.745	816.230	814.795	813.482	816.417
Trial	29	30					
FV	**812.056**	814.505					

Table 8.2: Improvement in function value (FV) during generations for the
minimum FV = 812.056

generation	min. FV in sets	max. FV in sets	generation	min. FV in sets	max. FV in sets	generation	min. FV in sets	max. FV in sets
0	895.9	1025.6	7	825.289	839.113	14	815.692	818.171
1	882.740	976.913	8	821.863	835.553	15	815.301	817.346
2	845.530	930.799	9	820.381	829.720	16	813.373	817.148
3	841.012	884.280	10	818.662	824.726	17	813.083	815.897
4	827.289	867.315	11	818.553	823.270	18	812.211	815.023
5	827.289	850.922	12	818.072	822.570	19	812.102	814.061
6	827.289	844.331	13	816.600	820.174	20	**812.056**	813.852

Table 8.3: Point mass values for optimized FV of 812.056

Link, i	m_{i1}	m_{i2}	m_{i3}	m_{i4}	m_{i5}	m_{i6}	m_{i7}
1	0.4967	1.8868	0.0010	1.0969	0.0335	0.0195	0.1473
2	2.8189	0.0626	10.714	0.0750	0.0010	0.0021	0.0639
3	2.5182	0.0255	0.2396	2.0293	0.0008	0.0780	0.0672
4	0.6498	0.0010	4.3059	0.2489	0.0087	0.1582	0.0470
5	1.5906	4.9040	0.5221	0.4763	0.1058	0.1666	0.0204
6	0.5600	0.0530	0.4982	0.2828	0.5218	0.0192	0.0082

The Point mass values obtained for Objective function value of 812.056 for all links 1 to 6 are tabulated in Table 8.3. The optimized values of constraint moments and constraint forces at different joints of original and optimized Puma robot obtained using seven point-masses model are given in Table 8.4. The optimized constraint moment values at different joints are reduced significantly. The shaking moment is reduced from 168.817 to 28.091 due to the proper mass distribution of links that affects its inertia and thus shaking moment. The constraint forces that depends on the total mass of the link remains nearly the same because the total mass of the links is retained same. However, the peak value of constraint forces at different joints is reduced somewhat as demonstrated by various graphs of constraint forces, Figs. 8.8-8.13.

Table 8.4: Constraint moments and constraint forces for original and optimized PUMA with FV of 812.056

Constraint moment	$\tilde{n}_1$	$\tilde{n}_2$	$\tilde{n}_3$	$\tilde{n}_4$	$\tilde{n}_5$	$\tilde{n}_6$	Total
Original PUMA	73.120	75.610	14.470	5.430	0.111	0.076	168.82
Optimized PUMA	4.424	16.110	2.376	4.542	0.471	0.168	28.09
Constraint force	$\tilde{f}_1$	$\tilde{f}_2$	$\tilde{f}_3$	$\tilde{f}_4$	$\tilde{f}_5$	$\tilde{f}_6$	
Original PUMA	367.970	264.790	110.220	24.138	13.797	3.452	784.37
Optimized PUMA	367.913	264.703	110.121	24.121	13.794	3.452	784.10

Fig.8.2: Constraint moments of original and optimally balanced PUMA at joint 1 with 7 Point-mass model

Fig.8.3: Constraint moments of original and optimally balanced PUMA at joint 2 with 7 Point-mass model
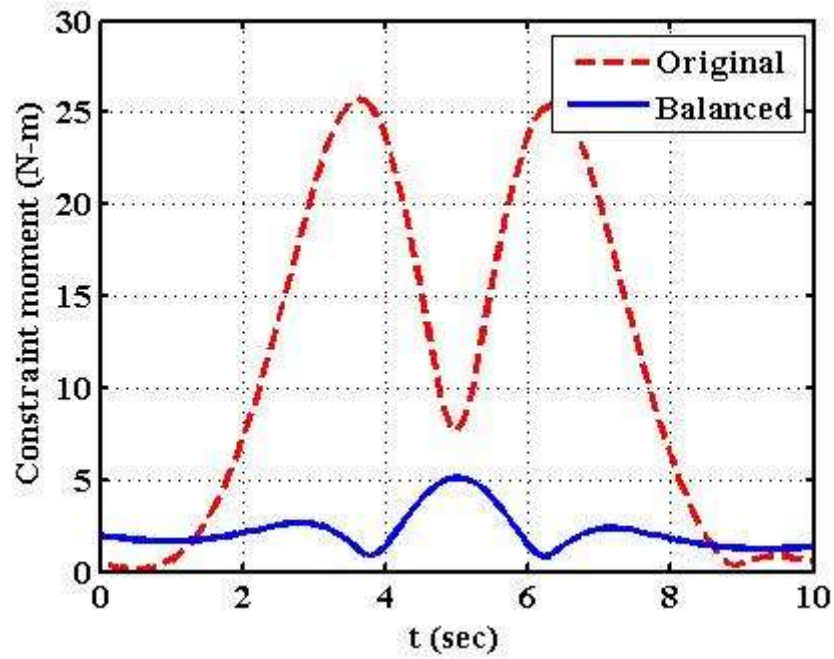
Fig.8.4: Constraint moments of original and optimally balanced PUMA at joint 3 with 7 Point-mass model

Fig.8.5: Constraint moments of original and optimally balanced PUMA at joint 4 with 7 Point-mass model

Fig.8.6: Constraint moments of original and optimally balanced PUMA at joint 5 with 7 Point-mass model

Fig.8.7: Constraint moments of original and optimally balanced PUMA at joint 6 with 7 Point-mass model

Fig.8.8: Constraint forces of original and optimally balanced PUMA at joint 1 with 7 Point-mass model

Fig.8.9: Constraint forces of original and optimally balanced PUMA at joint 2 with 7 Point-mass model

Fig.8.10: Constraint forces of original and optimally balanced PUMA at joint 3 with 7 Point-mass model

Fig.8.11: Constraint forces of original and optimally balanced PUMA at joint 4 with 7 Point-mass model
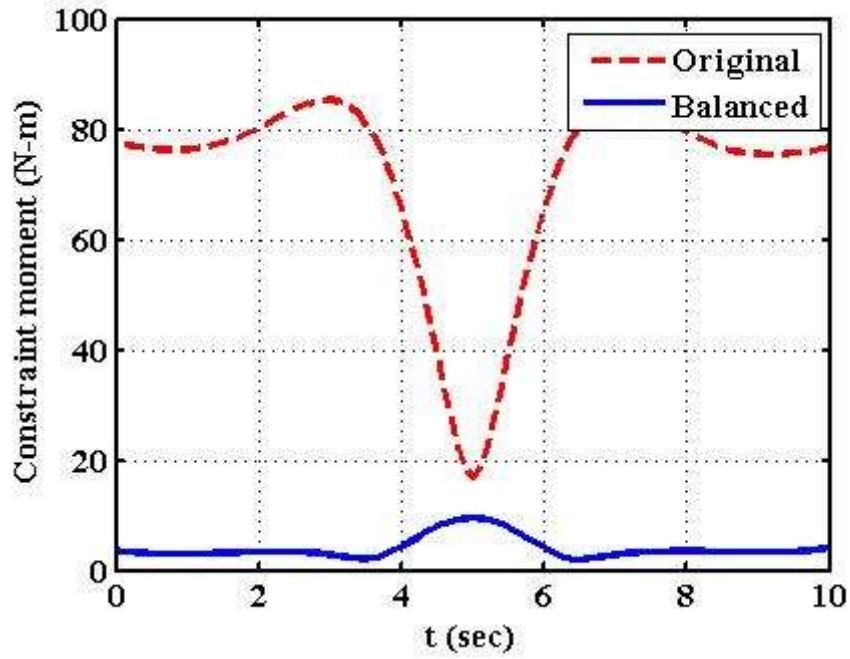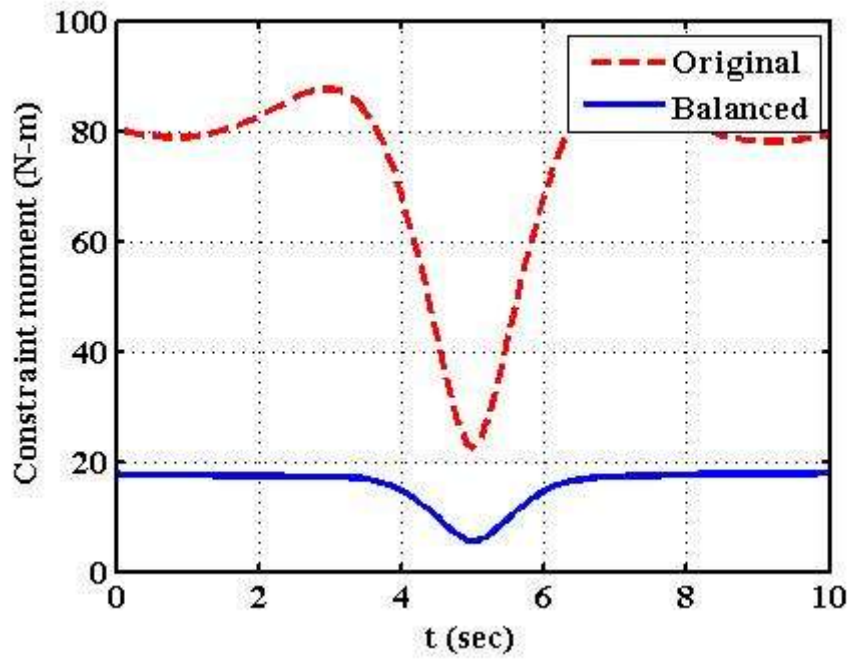
Fig.8.12: Constraint forces of original and optimally balanced PUMA at joint 5 with 7 Point-mass model

Fig.8.13: Constraint forces of original and optimally balanced PUMA at joint 6 with 7 Point-mass model

8.1.2 Six point-mass hexahedron model

TLBO solutions were obtained for six point-mass model with population sets of 100, termination criteria (20 number of generation). The initial population sets are generated randomly. Since the number of design variables (36) is large, the increase in population sets improves the value of objective function. The value of objective function obtained is presented in Table 8.5. It is observed that the average function value (FV) obtained, for the number of sets of 100 and the number of generations/iterations of 20, is 816.878 with the standard deviation of 1.730.The Point mass values obtained for Objective function value of 813.649 for all links 1 to 6 are tabulated in Table 8.6. The details of improvement in function value for the solution at trial number 13 of Table 8.5, during different generations with population set of 100, is given in Table 8.7.

Table 8.5: Objective function value for different trials

Trial	1	2	3	4	5	6	7
FV	815.764	817.358	819.837	814.532	815.782	815.875	815.220
Trial	8	9	10	11	12	13	14
FV	817.083	814.742	815.780	819.288	818.525	**813.649**	815.596
Trial	15	16	17	18	19	20	21
FV	816.350	817.369	817.702	816.551	817.043	814.466	815.234
Trial	22	23	24	25	26	27	28
FV	821.529	816.180	817.709	817.000	818.033	817.548	817.472
Trial	29	30					
FV	817.510	819.608					

Table 8.6: Point mass values for Optimized FV of 813.649

Link, i	m_{i1}	m_{i2}	m_{i3}	m_{i4}	m_{i5}	m_{i6}
1	0.0010	4.5880	2.8029	0.4932	0.5097	2.1263
2	0.0131	0.0399	0.2320	4.6599	0.0010	10.815
3	0.0010	6.2246	0.1015	0.0307	0.1763	2.2330
4	0.0104	0.1717	0.6892	0.0082	0.0393	0.1332
5	0.0052	0.5653	0.1703	0.0458	0.0981	0.1673
6	0.0010	0.0010	0.0010	0.0565	0.2345	0.0570

Table 8.7: Improvement in function value (FV) during generations for min. FV = 813.649

Generation	min. FV in sets	max. FV in sets	generation	min. FV in sets	max. FV in sets	generation	min. FV in sets	max. FV in sets
0	867.6	1059.6	7	818.899	825.999	14	815.566	816.844
1	847.026	905.437	8	817.443	823.625	15	815.468	816.134
2	823.918	893.395	9	816.900	821.354	16	814.600	815.997
3	821.229	864.716	10	816.827	821.354	17	814.500	815.767
4	821.229	850.871	11	815.913	819.000	18	814.306	815.392
5	821.015	839.343	12	815.574	819.000	19	814.287	814.886
6	820.699	829.662	13	815.574	817.245	20	**813.649**	814.607

The optimized values of constraint moments and constraint forces at different joints of original and optimized PUMA robot obtained using six point-mass model are given in Table 8.8. The optimized constraint moment values at different joints are reduced significantly. The shaking moment is reduced from 168.817 to 29.817 due to the proper mass distribution of links that affects its inertia and thus shaking moment. The constraint forces that depends on the total of the link remains nearly the same because the total mass of the links is retained same. However, the peak value of constraint forces at different joints is reduced somewhat as demonstrated by various graphs of constraint forces, Figs. 8.20 to 8.25.

Table 8.8: Constraint moments and constraint forces for original and optimized PUMA with FV of 813.649

| Constraint moment	$\tilde{n}_1$	$\tilde{n}_2$	$\tilde{n}_3$	$\tilde{n}_4$	$\tilde{n}_5$	$\tilde{n}_6$	Total
Original PUMA	73.120	75.610	14.470	5.430	0.111	0.076	168.82
Optimized PUMA	6.144	17.023	2.411	3.768	0.270	0.201	29.82
Constraint force	$\tilde{f}_1$	$\tilde{f}_2$	$\tilde{f}_3$	$\tilde{f}_4$	$\tilde{f}_5$	$\tilde{f}_6$	
Original PUMA	367.970	264.790	110.220	24.138	13.797	3.452	784.37
Optimized PUMA	367.917	264.706	110.118	24.118	13.798	3.452	784.11

Fig.8.14: Constraint moments of original and optimally balanced PUMA at joint 1 with 6 Point-mass model
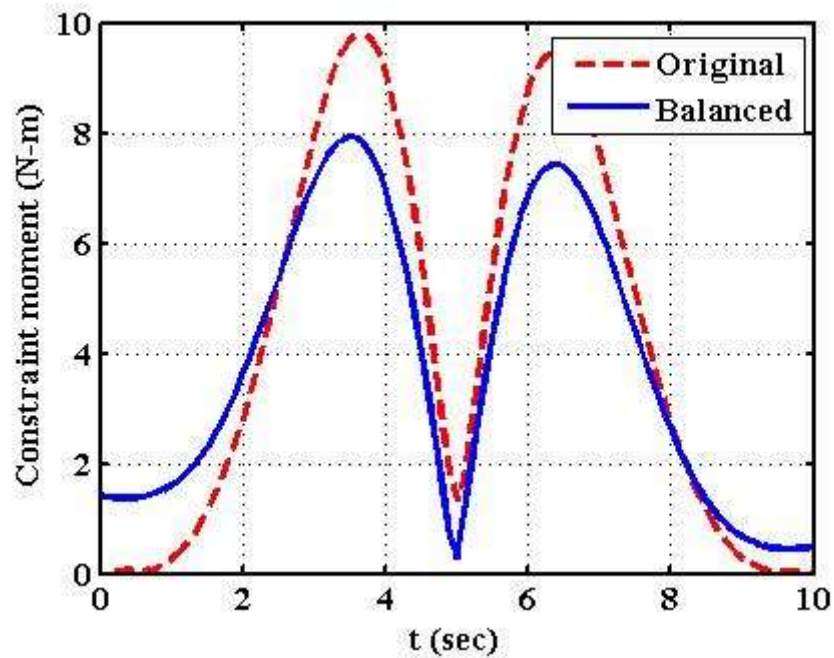

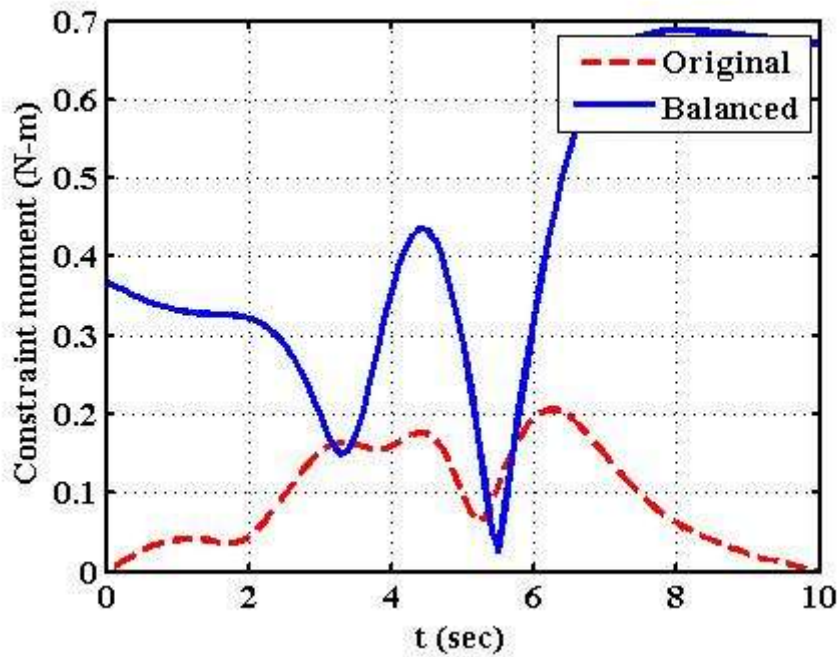**Fig.8.15: Constraint moments of original and optimally balanced PUMA at joint 2 with 6 Point-mass model**

Fig.8.16: Constraint moments of original and optimally balanced PUMA at joint 3 with 6 Point-mass model
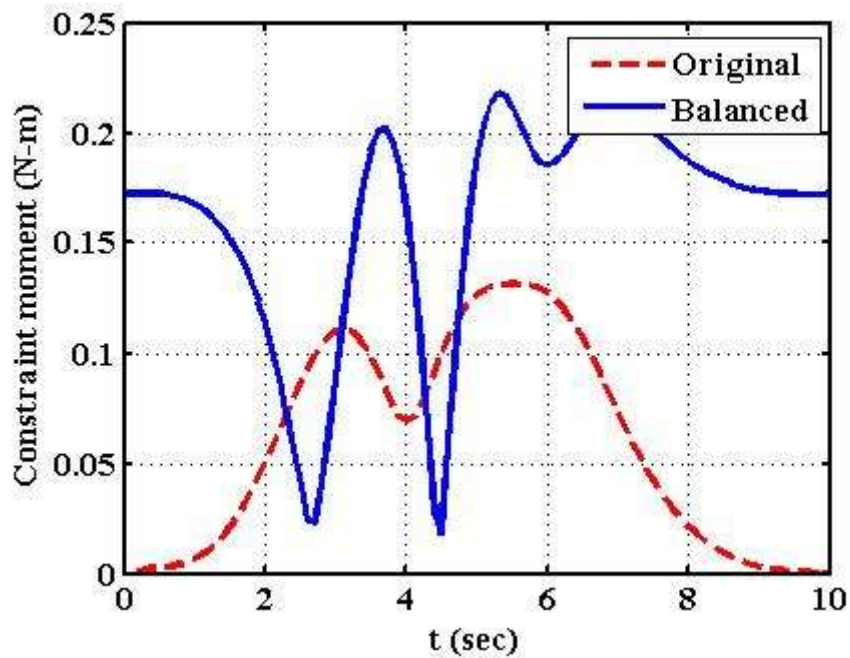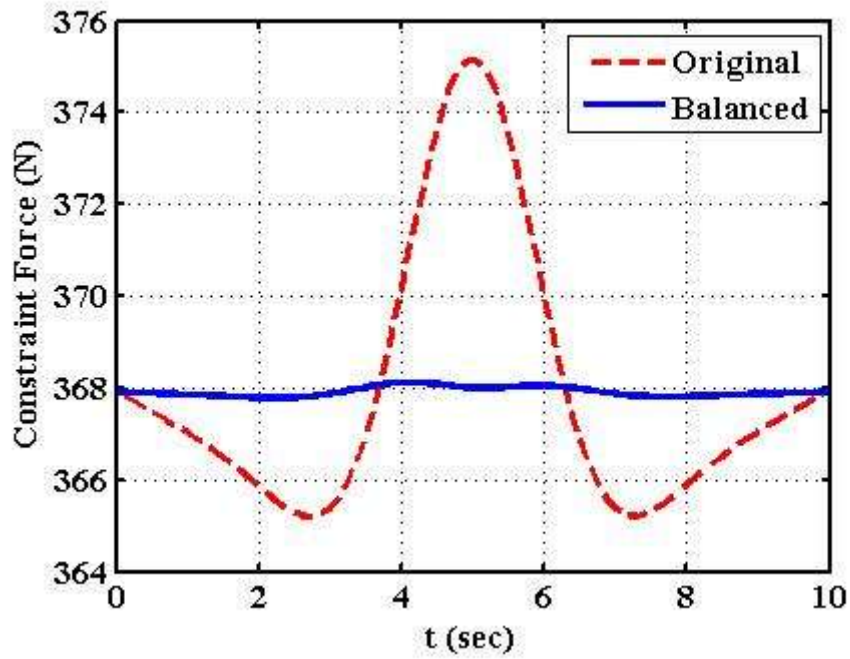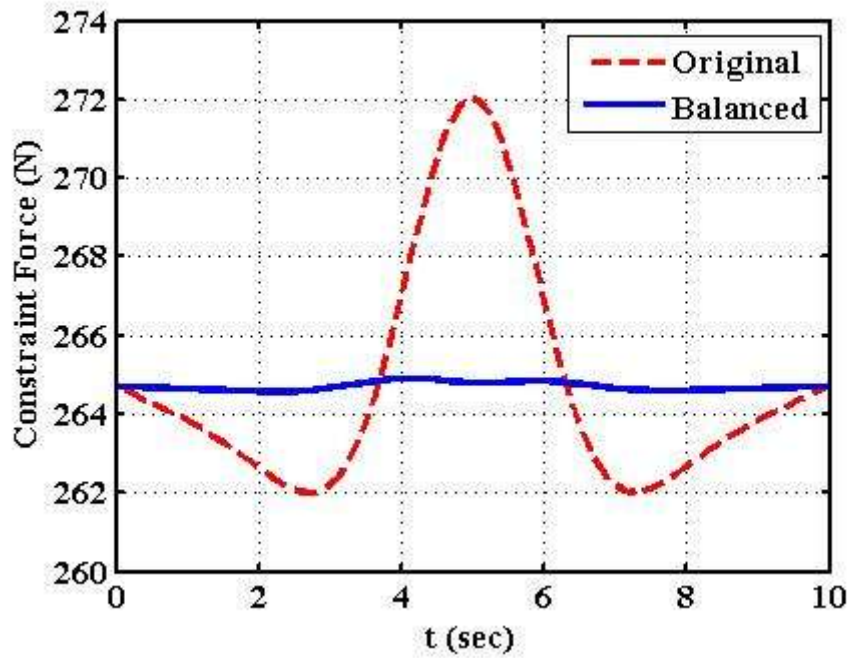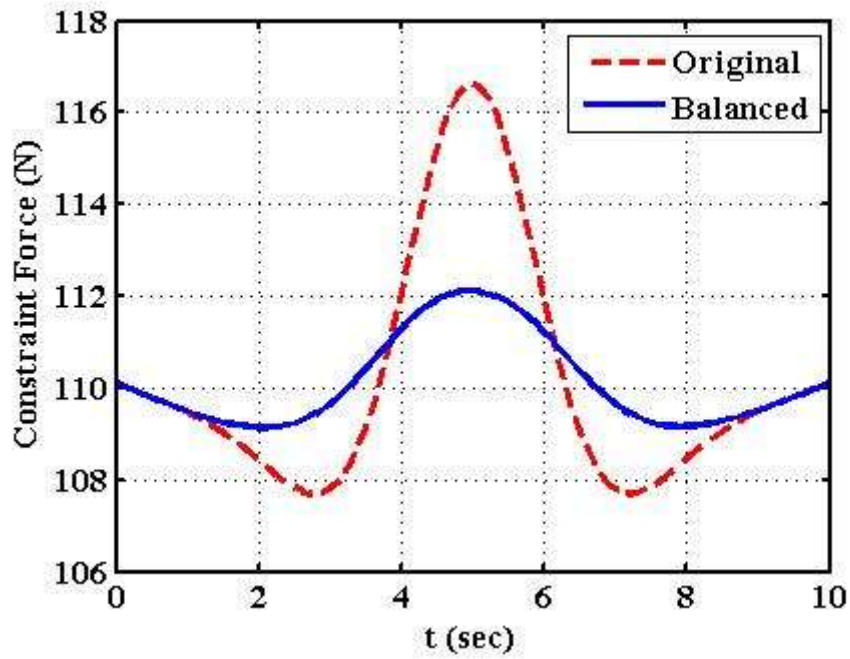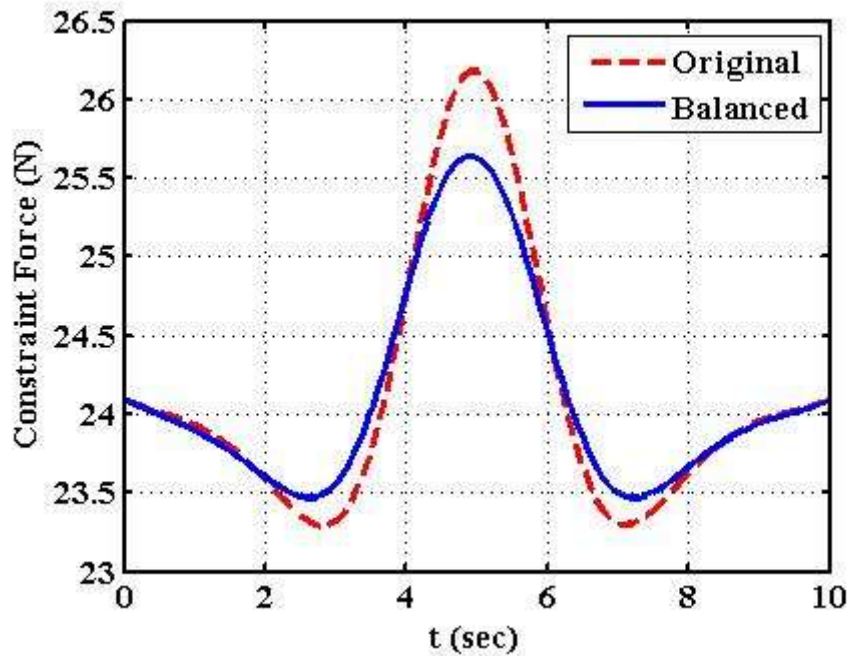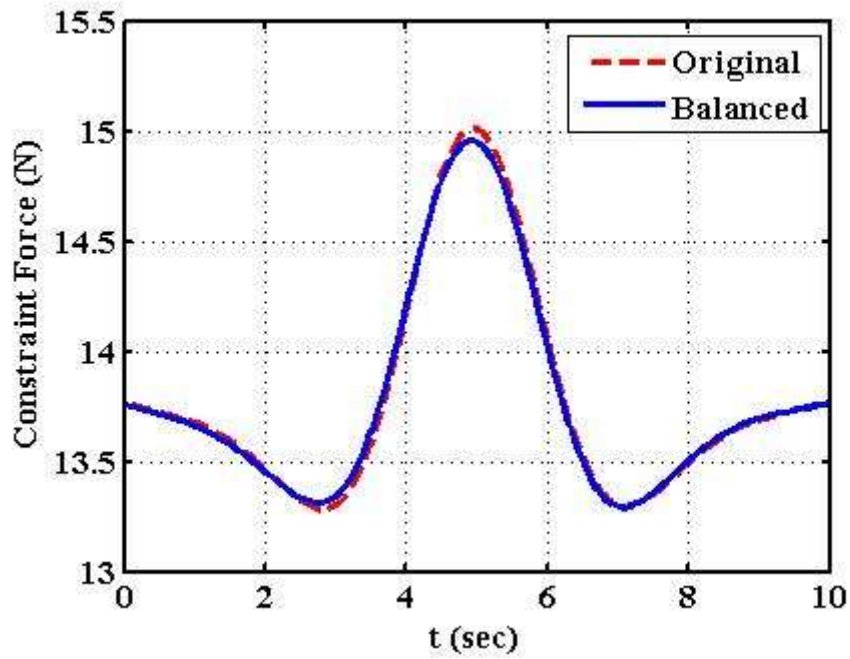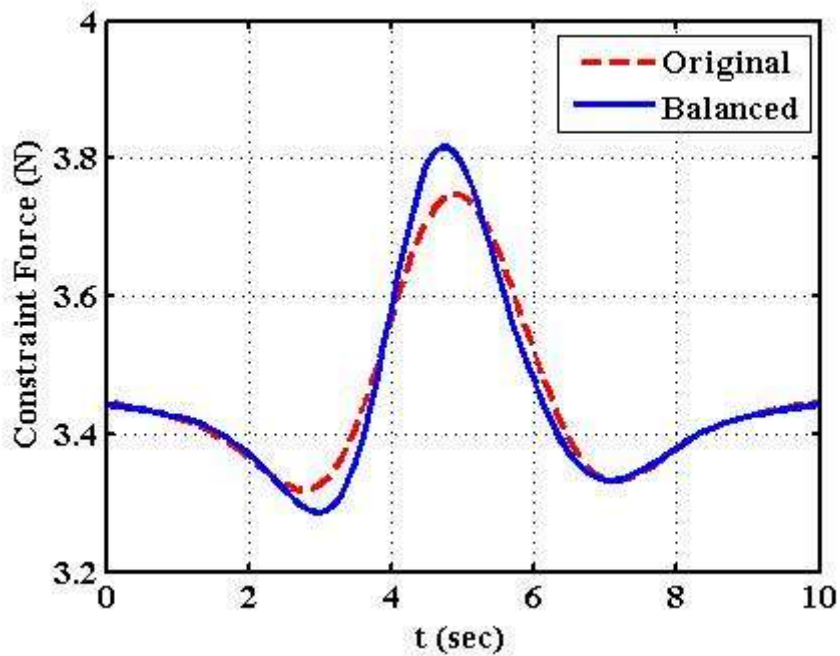

Fig.8.17: Constraint moments of original and optimally balanced PUMA at joint 4 with 6 Point-mass model

Fig.8.18: Constraint moments of original and optimally balanced PUMA at joint 5 with 6 Point-mass model

Fig.8.19: Constraint moments of original and optimally balanced PUMA at joint 6 with 6 Point-mass model

Fig.8.20: Constraint forces of original and optimally balanced PUMA at joint 1 with 6 Point-mass model

Fig.8.21: Constraint forces of original and optimally balanced PUMA at joint 2 with 6 Point-mass model

Fig.8.22: Constraint forces of original and optimally balanced PUMA at joint 3 with 6 Point-mass model

Fig.8.23: Constraint forces of original and optimally balanced PUMA at joint 4 with 6 Point-mass model
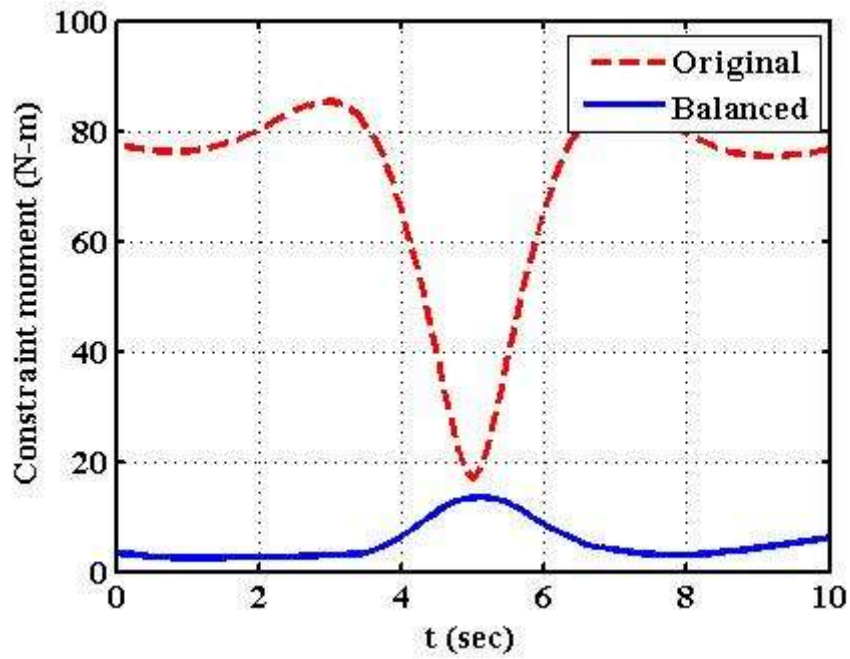
Fig.8.24: Constraint forces of original and optimally balanced PUMA at joint 5 with 6 Point-mass model

Fig.8.25: Constraint forces of original and optimally balanced PUMA at joint 6 with 6 Point-mass model

8.1.3 Five point-mass hexahedron model

TLBO solutions were obtained for this point-mass model with population sets of 50, termination criterion (20 number of generation). The initial population sets are generated randomly. Since the number of design variables (30) is relatively less, population set of 50 with increasing the number of generations to 50 is observed to be satisfactory. The value of objective function obtained is presented in Table 8.9. It is observed that the average function value (FV) obtained, for the number of sets of 50 and the number of generations/iterations of 50, is 820.458 with the standard deviation of 1.390.

Table 8.9: Objective function value for different trials

Trial	1	2	3	4	5	6	7
FV	820.012	819.860	820.529	818.341	823.068	820.328	**817.581**
Trial	8	9	10	11	12	13	14
FV	819.049	818.109	821.164	820.716	821.507	820.349	822.082
Trial	15	16	17	18	19	20	21
FV	821.607	819.802	821.164	820.716	819.459	818.864	821.282
Trial	22	23	24	25	26	27	28
FV	819.450	819.518	819.647	821.441	821.886	822.830	819.759
Trial	29	30					
FV	822.958	820.672					

Table 8.10: Improvement in function value (FV) during generations for min. FV = 817.581

generation	min. FV in sets	max. FV in sets	generation	min. FV in sets	max. FV in sets	generation	min. FV in sets	max. FV in sets
0	1.0e+18	3.688 e+18	10	828.073	845.348	30	818.812	819.346
3	1.0e+17	2.018 e+17	12	826.031	839.701	35	818.470	818.605
5	842.600	1015.6	14	825.937	833.475	40	818.198	818.378
6	840.936	908.399	16	823.518	829.854	45	817.764	817.857
7	832.290	861.944	18	821.693	826.557	48	817.676	817.821
8	832.290	850.189	20	820.586	824.335	49	817.582	817.579
9	830.719	847.417	25	819.018	820.472	50	**817.581**	817.720

The details of improvement in function value at trial number 7 of table 8.9, during different generations, with population set of 50 is given in Table 8.10. The Point mass values obtained for objective function value of 817.581 for all links 1 to 6 are tabulated in Table 8.11.

Table 8.11: Point mass values for FV of 817.581

Link, i	m_{i1}	m_{i2}	m_{i3}	m_{i4}	m_{i5}
1	1.6588	1.0025	3.1234	1.3436	3.3927
2	0.0087	0.0386	5.3825	0.0132	10.318
3	2.1530	2.5746	1.7070	0.0302	2.3020
4	0.0631	0.6606	0.2284	0.0840	0.0519
5	0.3353	0.1818	0.1240	0.1227	0.2883
6	0.0272	0.0896	0.0458	0.0166	0.1719

The optimized values of Constraint moments and Constraint forces at different joints of original and optimized Puma robot obtained using five point-masses model are given in Table 8.12. The optimized constraint moment values at different joints are reduced significantly. The shaking moment is reduced from 168.817 to 33.503 due to the proper mass distribution of links that affects its inertia and thus shaking moment.

Table 8.12:- Constraint moments and constraint forces for original and optimized PUMA with FV of 817.581

Constraint moment	$\tilde{n}_1$	$\tilde{n}_2$	$\tilde{n}_3$	$\tilde{n}_4$	$\tilde{n}_5$	$\tilde{n}_6$	Total
Original PUMA	73.120	75.610	14.47	5.430	0.111	0.076	168.817
Optimized PUMA	5.052	19.072	4.151	4.356	0.799	0.073	33.503
Constraint force	$\tilde{f}_1$	$\tilde{f}_2$	$\tilde{f}_3$	$\tilde{f}_4$	$\tilde{f}_5$	$\tilde{f}_6$	Total
Original PUMA	367.970	264.790	110.220	24.138	13.797	3.452	784.367
Optimized PUMA	367.915	264.704	110.120	24.125	13.793	3.453	784.110

The constraint forces that depends on the total mass of the link remains nearly the same because the total mass of the links is retained same. However, the peak value of

constraint forces at different joints is reduced somewhat as demonstrated by various graphs of constraint forces, Figs. 8.32 to 8.37.
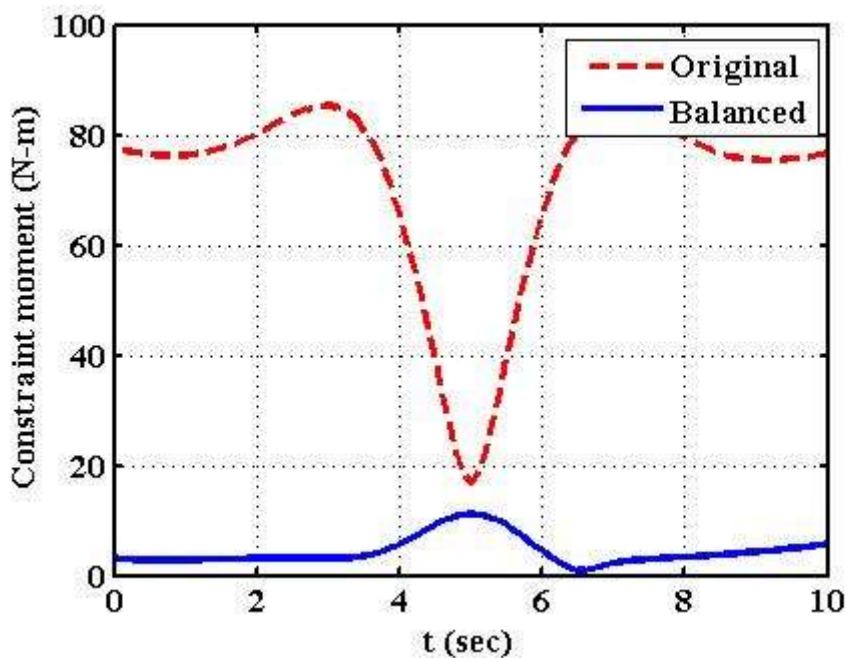
Fig.8.26: Constraint moments of original and optimally balanced PUMA at joint 1 with 5 Point-mass model
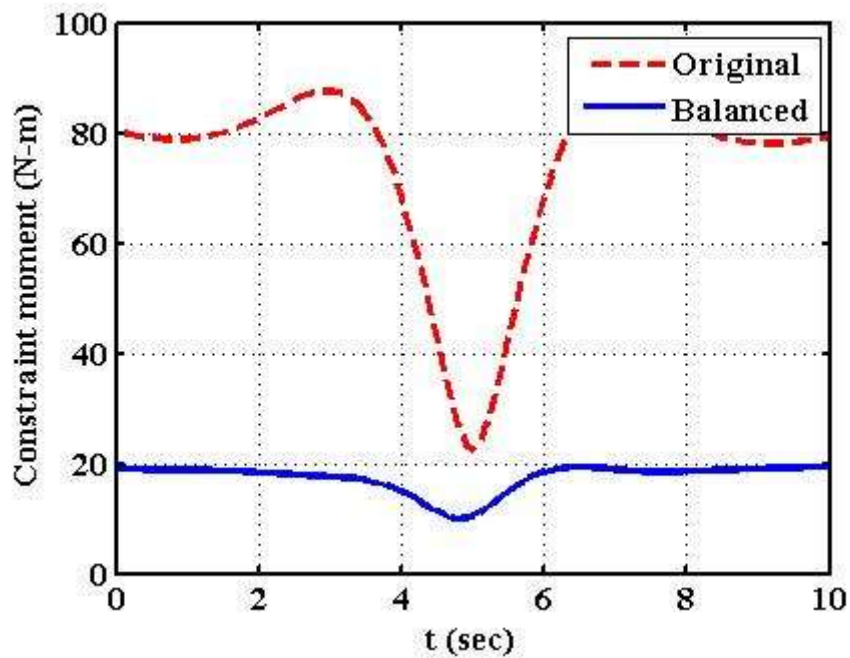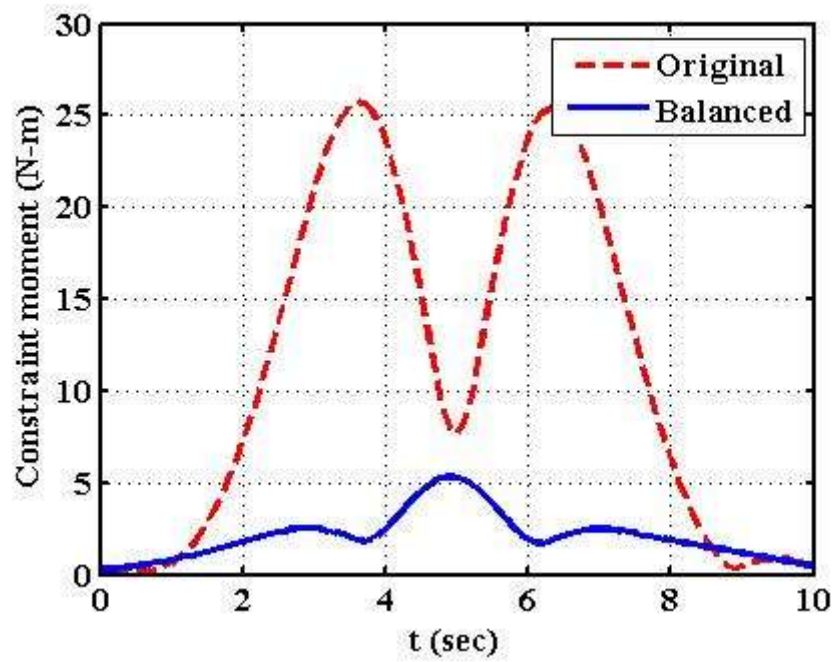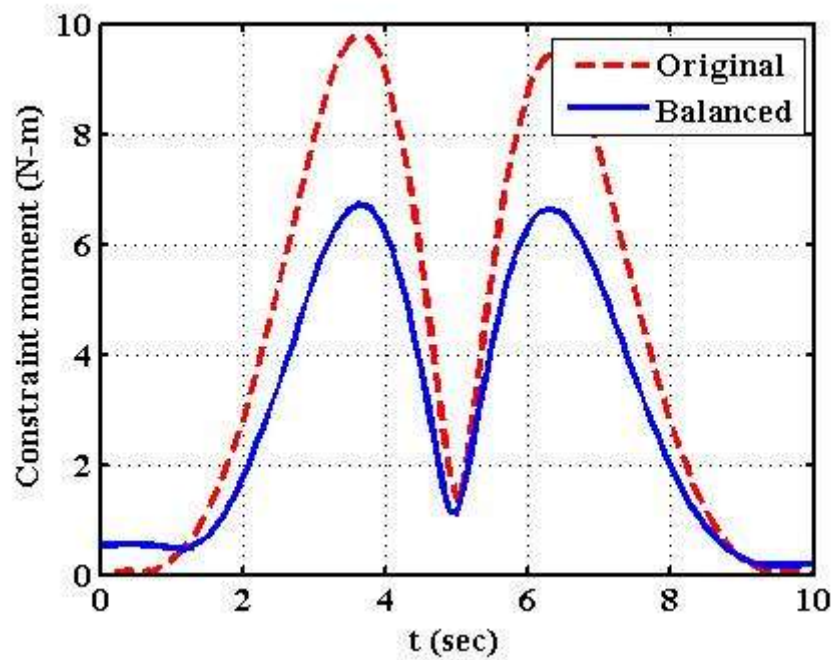

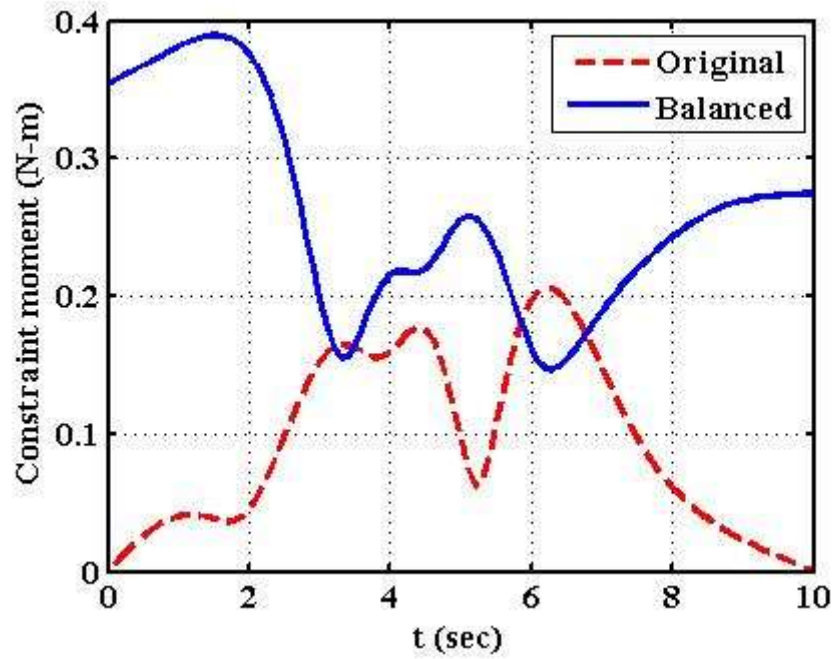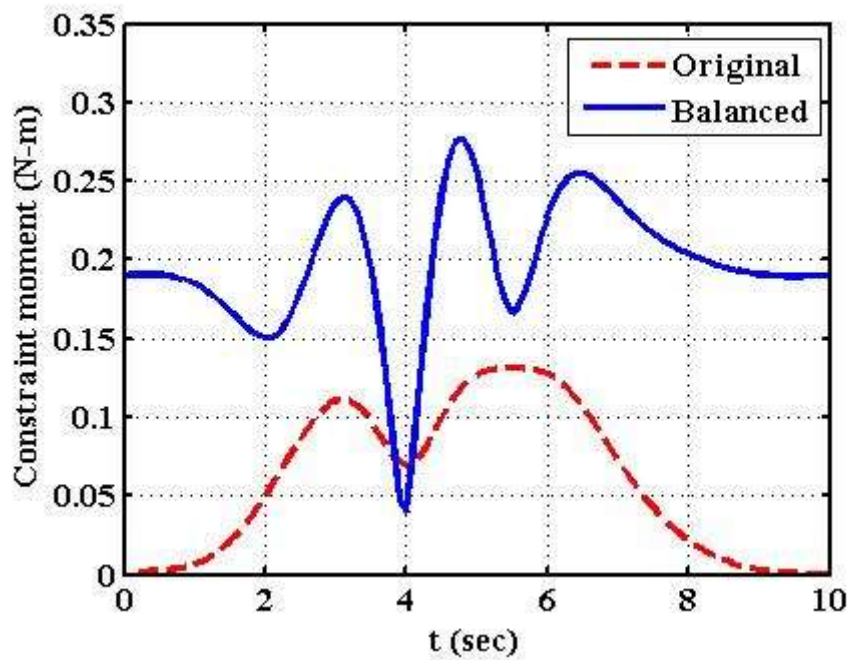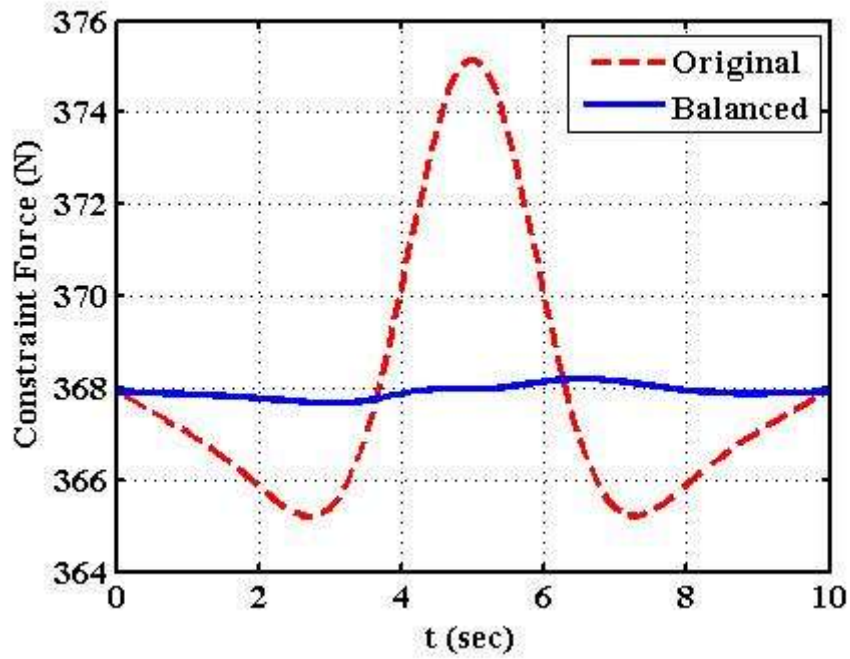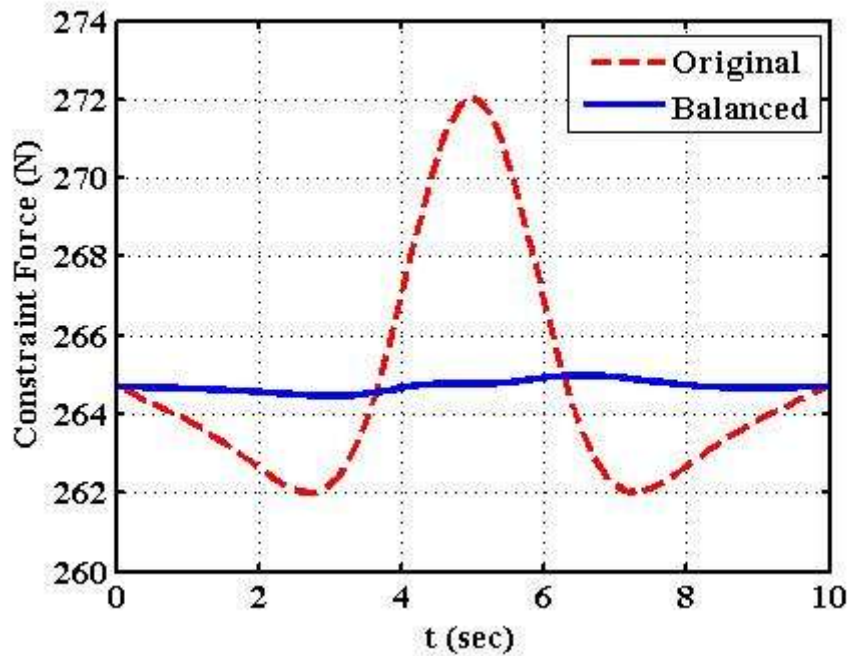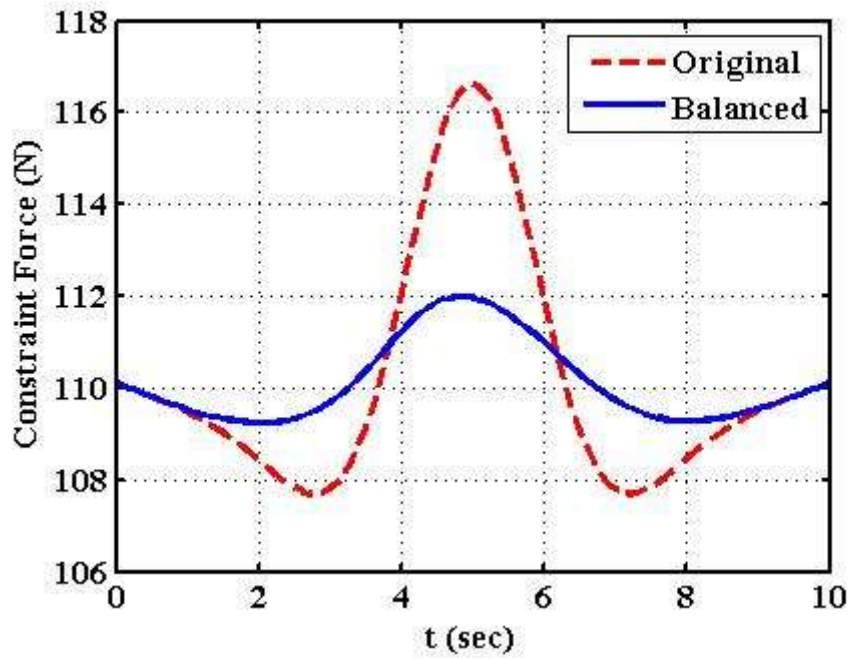**Fig.8.27: Constraint moments of original and optimally balanced PUMA at joint 2 with 5 Point-mass model**

Fig.8.28: Constraint moments of original and optimally balanced PUMA at joint 3 with 5 Point-mass model
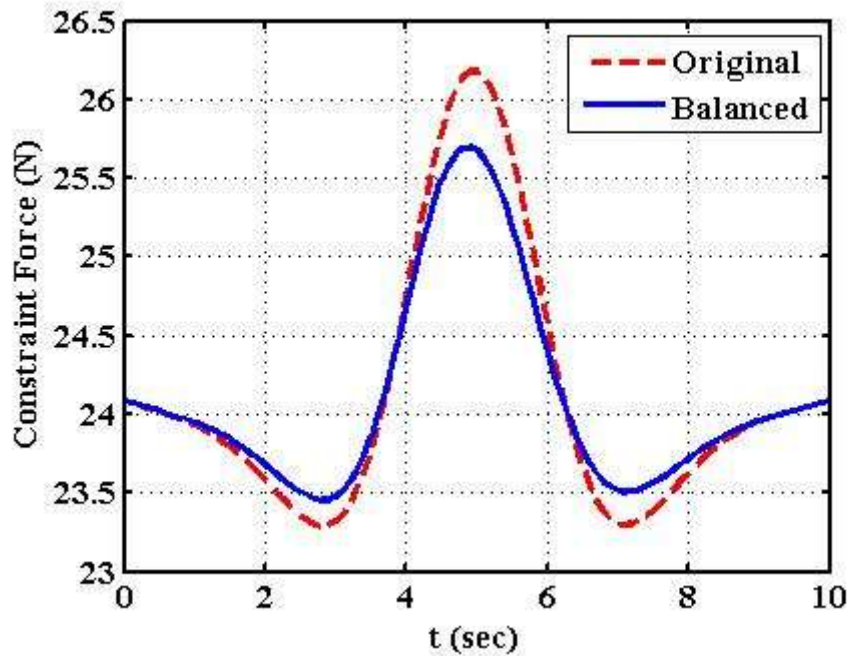

Fig.8.29: Constraint moments of original and optimally balanced PUMA at joint 4 with 5 Point-mass model

Fig.8.30: Constraint moments of original and optimally balanced PUMA at joint 5 with 5 Point-mass model

Fig.8.31: Constraint moments of original and optimally balanced PUMA at joint 6 with 5 Point-mass model
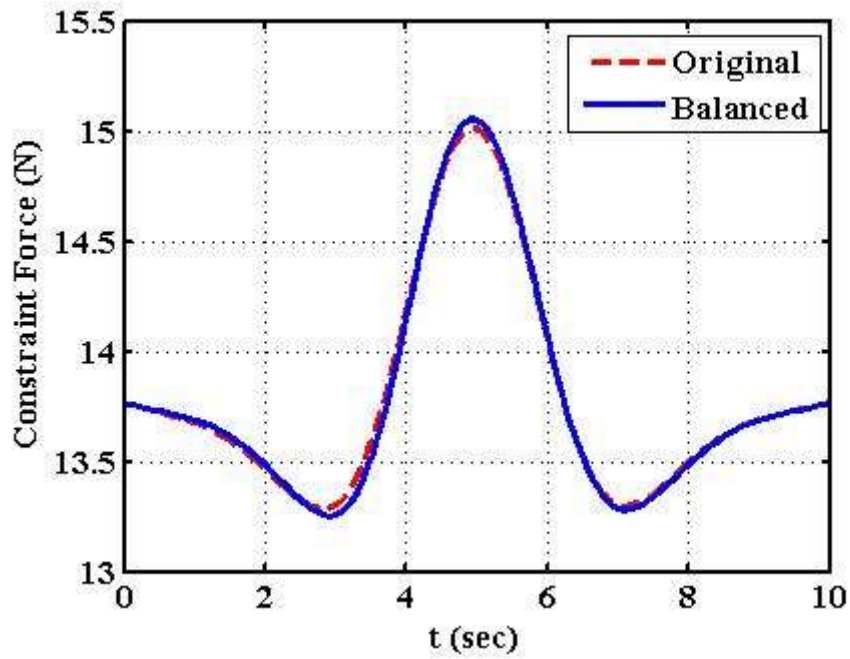
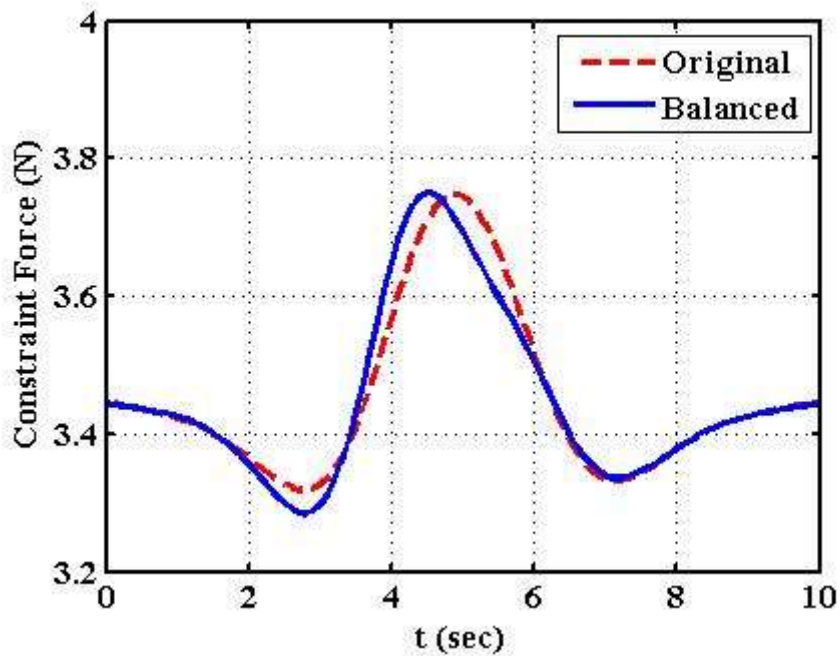**Fig.8.32: Constraint forces of original and optimally balanced PUMA at joint 1 with 5 Point-mass model**

Fig.8.33: Constraint forces of original and optimally balanced PUMA at joint 2 with 5 Point-mass model

Fig.8.34: Constraint forces of original and optimally balanced PUMA at joint 3 with 5 Point-mass model

Fig.8.35: Constraint forces of original and optimally balanced PUMA at joint 4 with 5 Point-mass model

Fig.8.36: Constraint forces of original and optimally balanced PUMA at joint 5 with 5 Point-mass model

Fig.8.37: Constraint forces of original and optimally balanced PUMA at joint 6 with 5 Point-mass model

8.1.4 Four point-mass model

TLBO solutions were obtained for this point-mass model with population sets of 50, termination criteria (50 number of generation). The initial population sets are generated randomly. Since the number of design variables (24) is relatively less, population set of 50 with increasing the number of generations to 50 is observed to be satisfactory. The value of objective function obtained is presented in Table 8.13. It is observed that the average function value (FV) obtained, for the number of sets of 50 and the number of generations/iterations of 50, is 824.242 with the standard deviation of 1.8916.

Table 8.13: Objective function value for different trials

Trial	1	2	3	4	5	6	7
FV	823.311	823.472	826.460	824.387	825.678	827.028	825.162
Trial	8	9	10	11	12	13	14
FV	823.233	821.193	826.624	825.709	827.007	822.991	826.251
Trial	15	16	17	18	19	20	21
FV	823.311	821.550	824.288	821.100	825.456	**820.816**	824.898
Trial	22	23	24	25	26	27	28
FV	827.712	824.796	823.917	825.132	825.634	822.347	823.048
Trial	29	30					
FV	822.480	822.253					

Table 8.14: Improvement in function value (FV) during generations for min. FV = 820.816

generation	min. FV in sets	max. FV in sets	Generation	min. FV in sets	max. FV in sets	generation	min. FV in sets	max. FV in sets
0	1.0e+17	6.0848 e+17	20	825.675	843.989	36	821.550	823.416
2	871.7	1008.0	22	825.430	835.506	39	821.275	821.920
5	869.316	967.687	25	823.532	828.966	41	821.119	821.510
6	855.423	967.687	28	822.627	826.333	44	821.049	821.174
10	846.378	963.522	30	821.995	825.143	46	820.973	821.138
15	832.202	895.573	33	821.747	824.359	48	820.921	821.088
19	827.226	874.885	35	821.653	823.776	50	**820.816**	821.085

Table 8.15: Point mass values for Optimized FV of 820.816

Link, i	m_{i1}	m_{i2}	m_{i3}	m_{i4}
1	2.0874	1.4244	5.2268	1.7823
2	0.0975	0.0200	12.682	2.9610
3	0.3831	2.1654	3.6384	2.5802
4	0.3904	0.1076	0.1441	0.4099
5	0.2581	0.3197	0.1190	0.3522
6	0.0406	0.1639	0.0916	0.0549

The optimized values of shaking moments and constraint forces at different joints of original and optimized Puma robot obtained using four point-masses model are given in Table 8.16. The optimized constraint moment values at different joints are reduced significantly. The total shaking moment is reduced from 168.817 to 36.73 due to the proper mass distribution of links that affects its inertia and thus shaking moment. The constraint forces that depends on the total of the link remains nearly the same because the total mass of the links is retained same. However, the peak value of constraint forces at different joints is reduced somewhat as demonstrated by various graphs of constraint forces, Figs. 8.44 to 8.49.

Table 8.16: Constraint moments and constraint forces for original and optimized

PUMA with FV of 820.816

Constraint moment	$\tilde{n}_1$	$\tilde{n}_2$	$\tilde{n}_3$	$\tilde{n}_4$	$\tilde{n}_5$	$\tilde{n}_6$	Total
Original PUMA	73.120	75.610	14.470	5.430	0.111	0.076	168.817
Optimized PUMA	5.676	20.454	5.283	4.236	0.841	0.240	36.730
Constraint force	$\tilde{f}_1$	$\tilde{f}_2$	$\tilde{f}_3$	$\tilde{f}_4$	$\tilde{f}_5$	$\tilde{f}_6$	Total
Original PUMA	367.970	264.790	110.220	24.138	13.797	3.452	784.367
Optimized PUMA	367.914	264.705	110.124	24.121	13.792	3.451	784.107
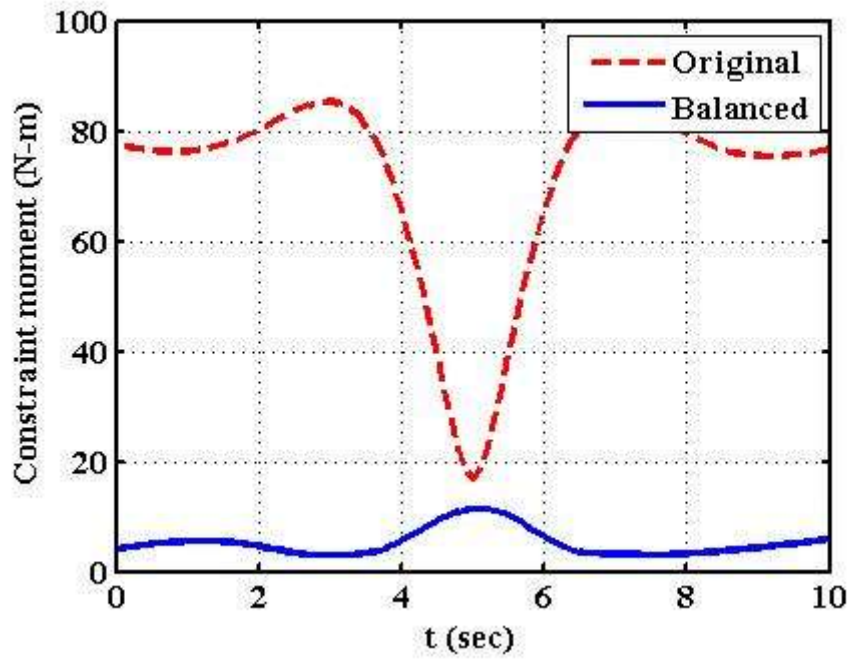
Fig.8.38: Constraint moments of original and optimally balanced PUMA at joint 1 with 4 Point-mass model
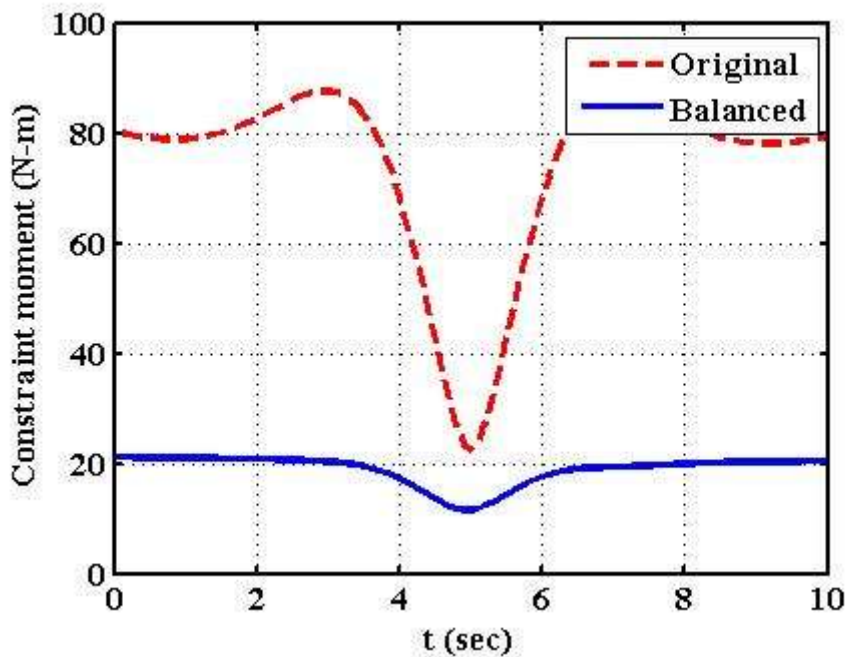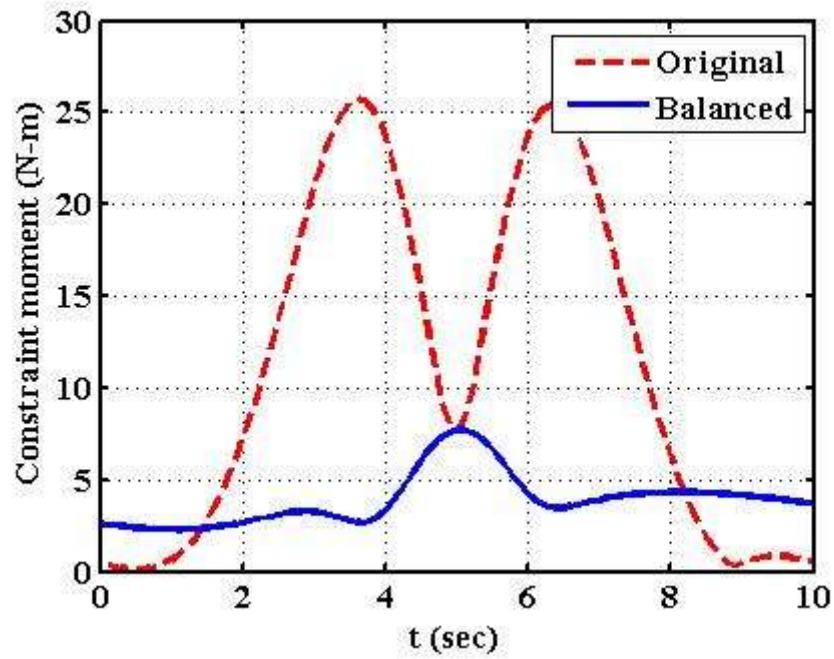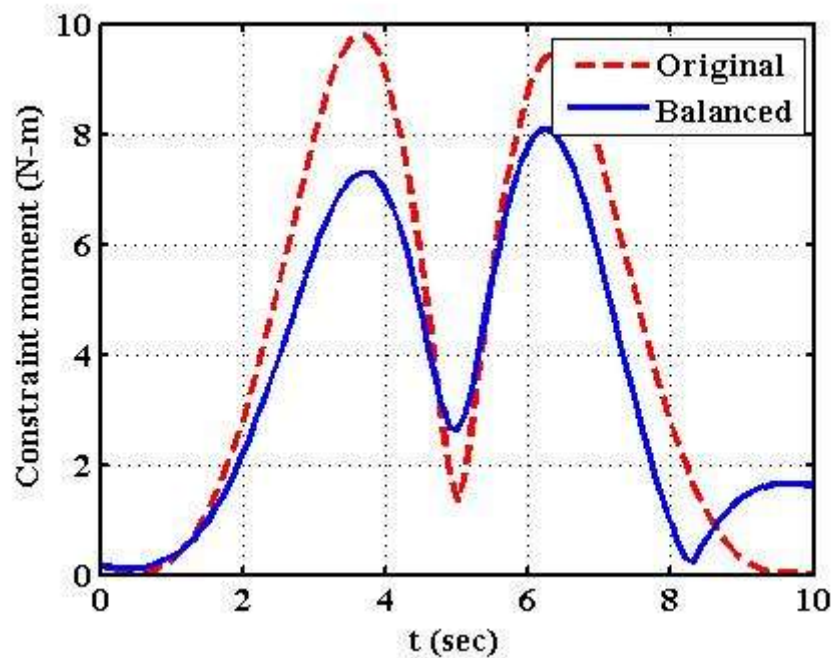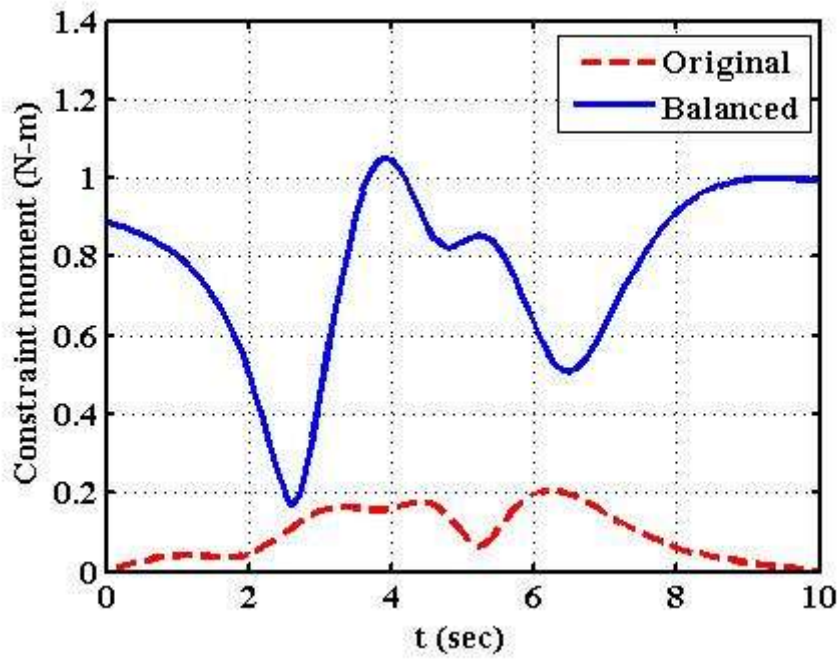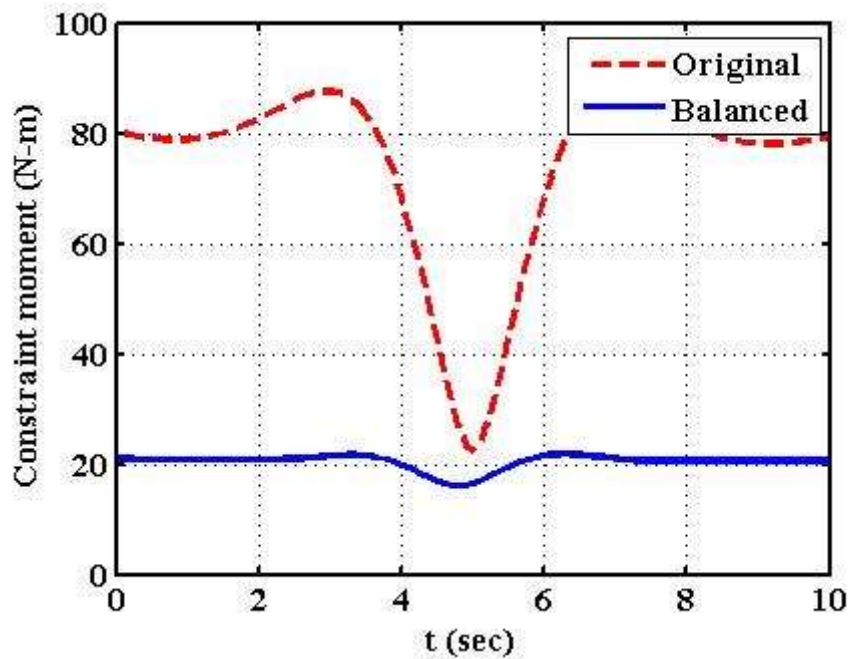

Fig.8.39: Constraint moments of original and optimally balanced PUMA at joint 2 with 4 Point-mass model
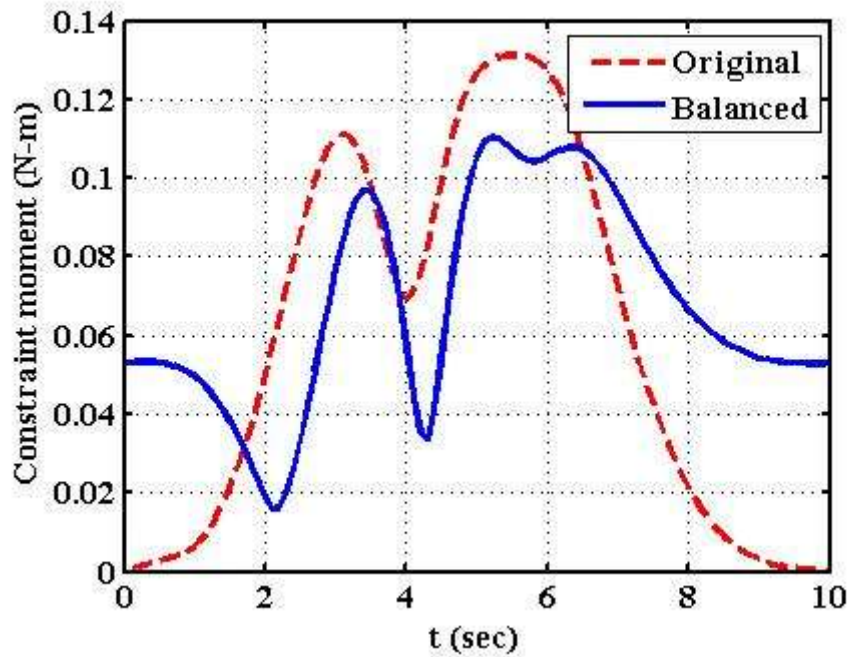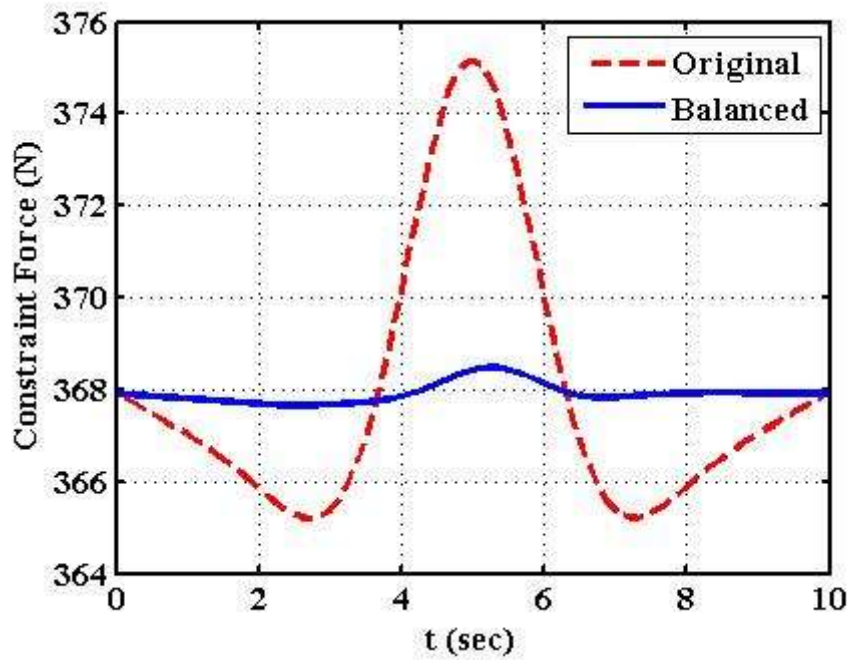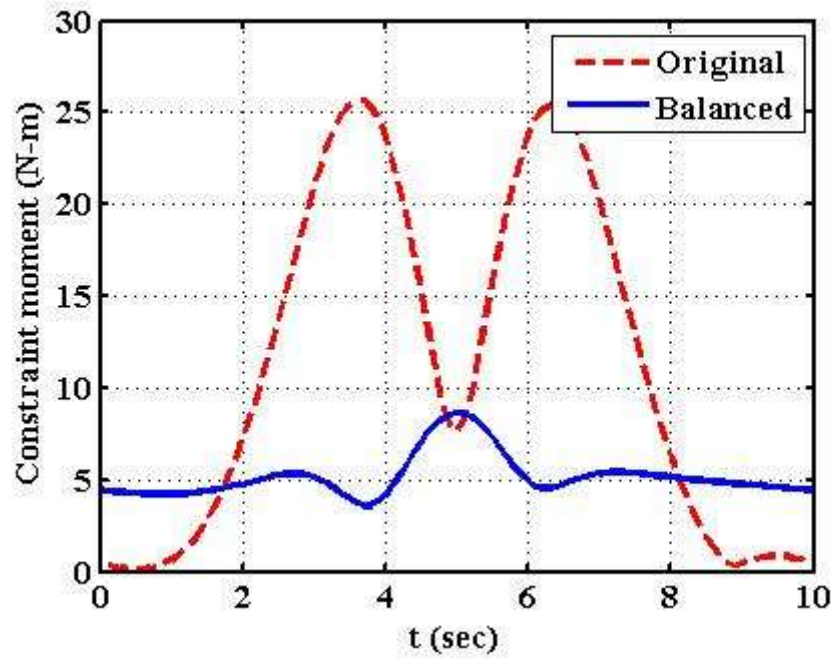
Fig.8.40: Constraint moments of original and optimally balanced PUMA at joint 3 with 4 Point-mass model
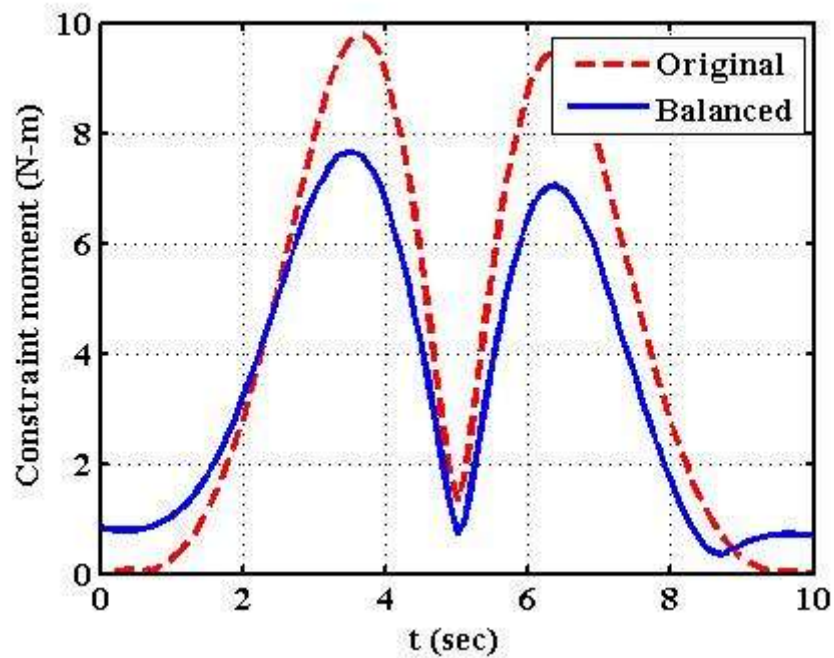
Fig.8.41: Constraint moments of original and optimally balanced PUMA at joint 4 with 4 Point-mass model
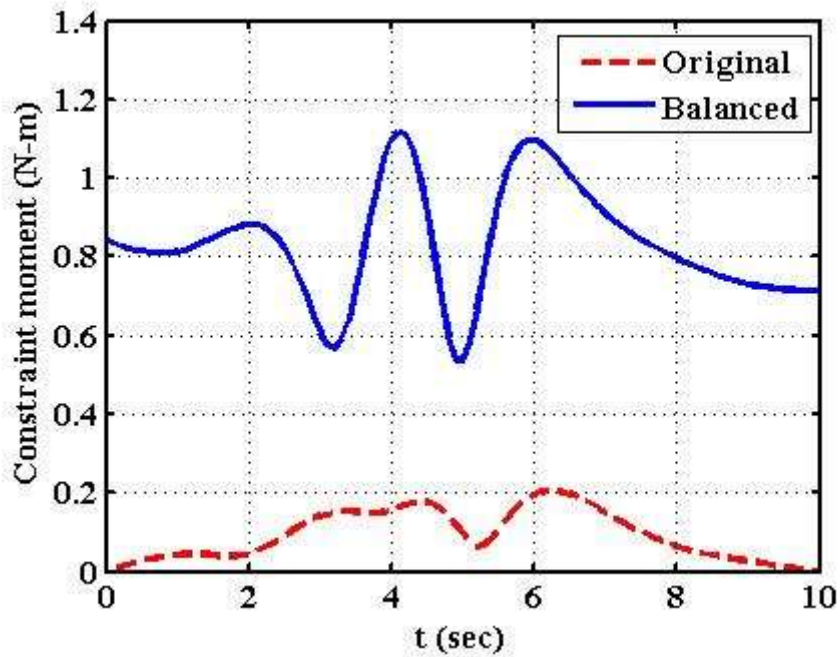
Fig.8.42: Constraint moments of original and optimally balanced PUMA at joint 5 with 4 Point-mass model
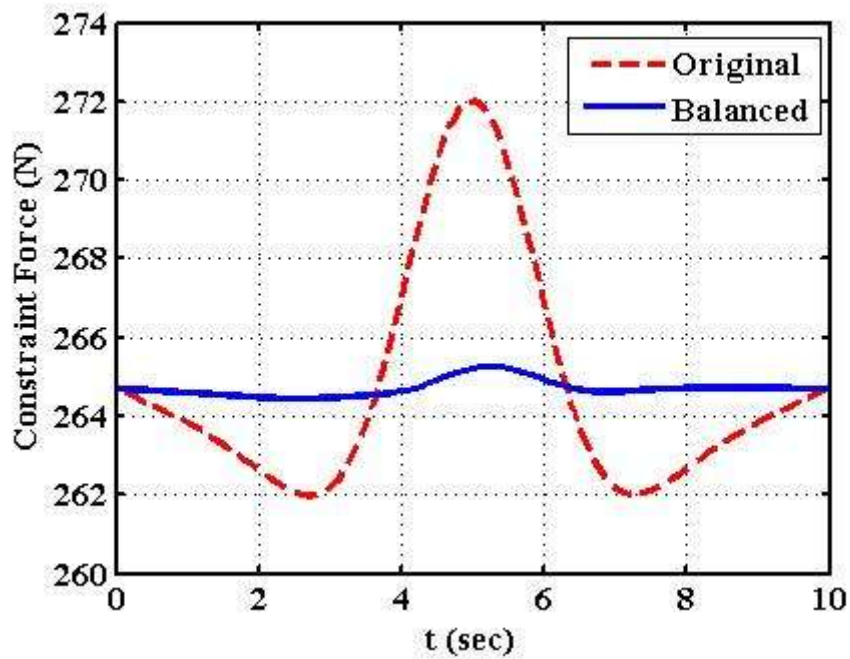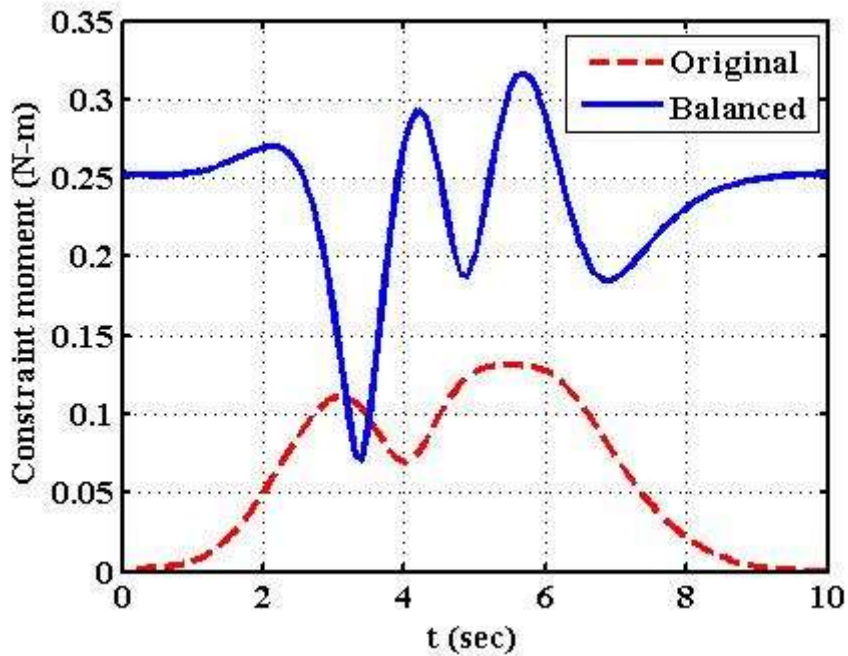

Fig.8.43: Constraint moments of original and optimally balanced PUMA at joint 6 with 4 Point-mass model
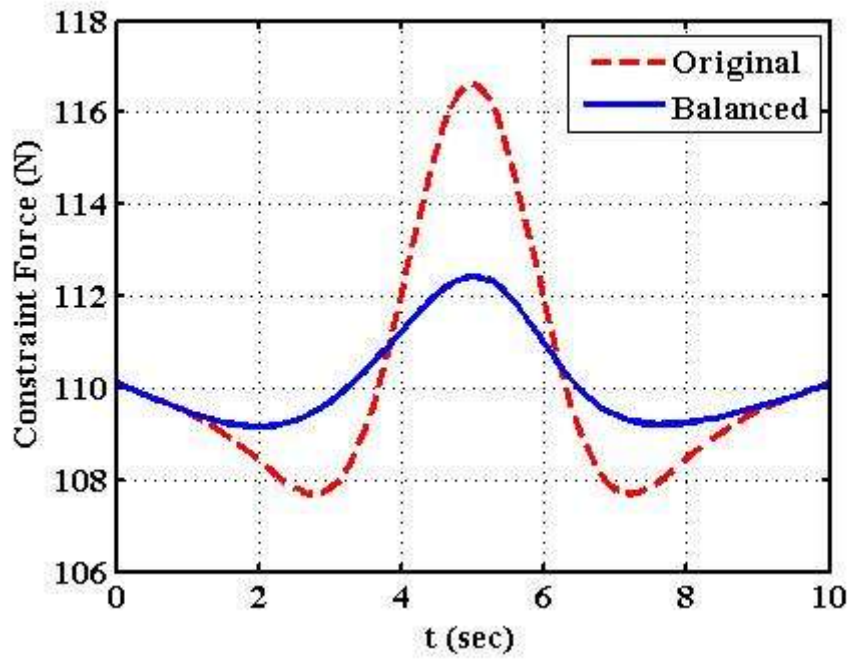
131
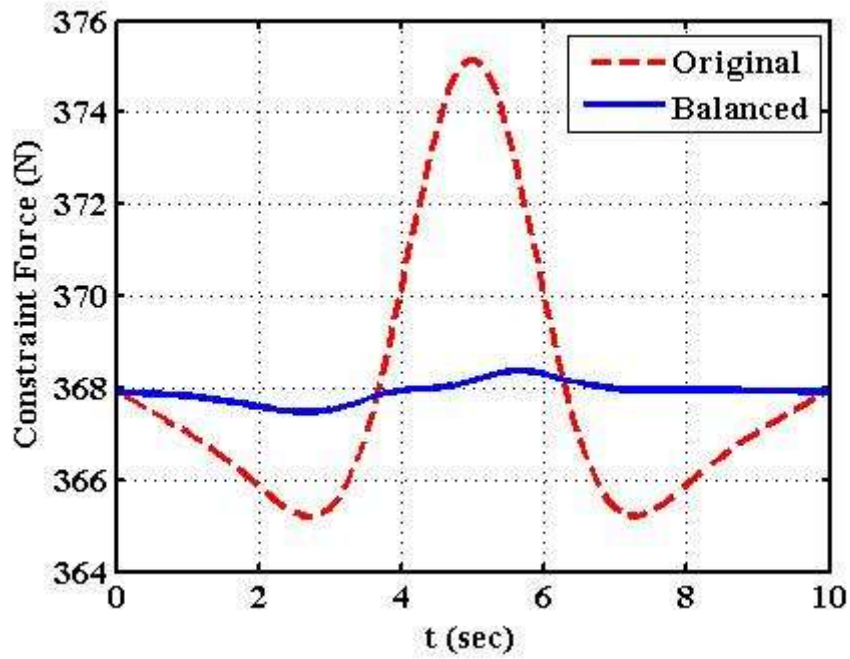
Fig.8.44: Constraint forces of original and optimally balanced PUMA at joint 1 with 4 Point-mass model
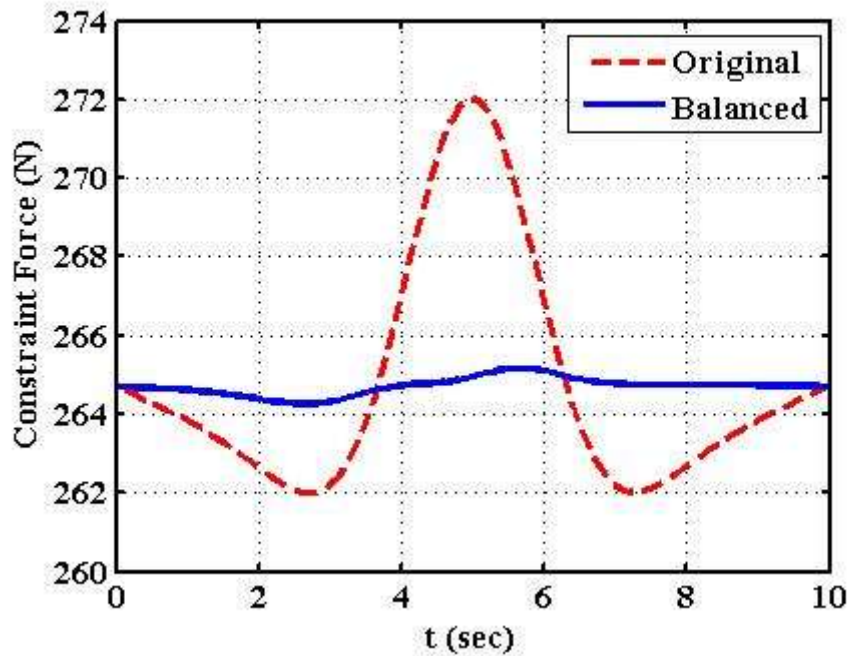
Fig.8.45: Constraint forces of original and optimally balanced PUMA at joint 2 with 4 Point-mass model
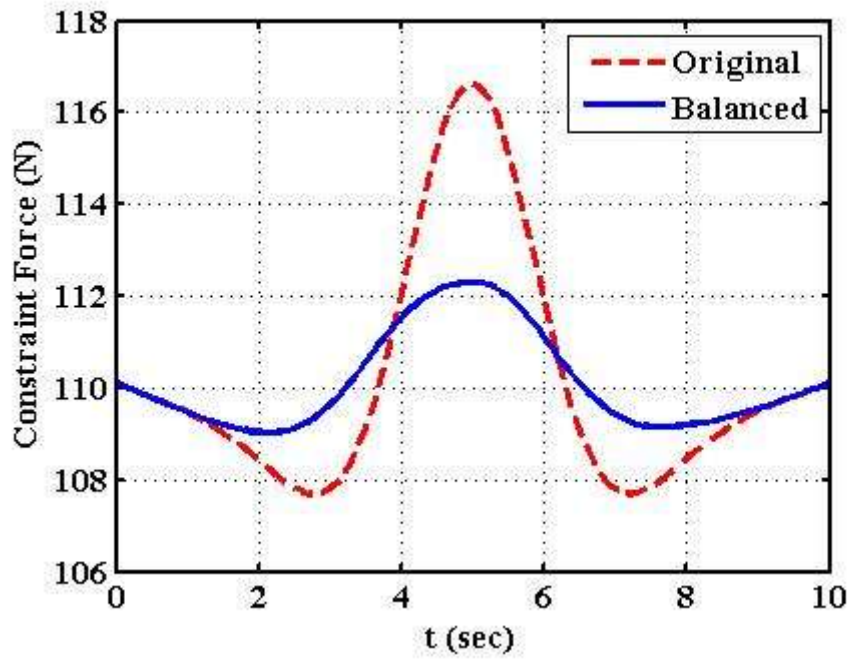
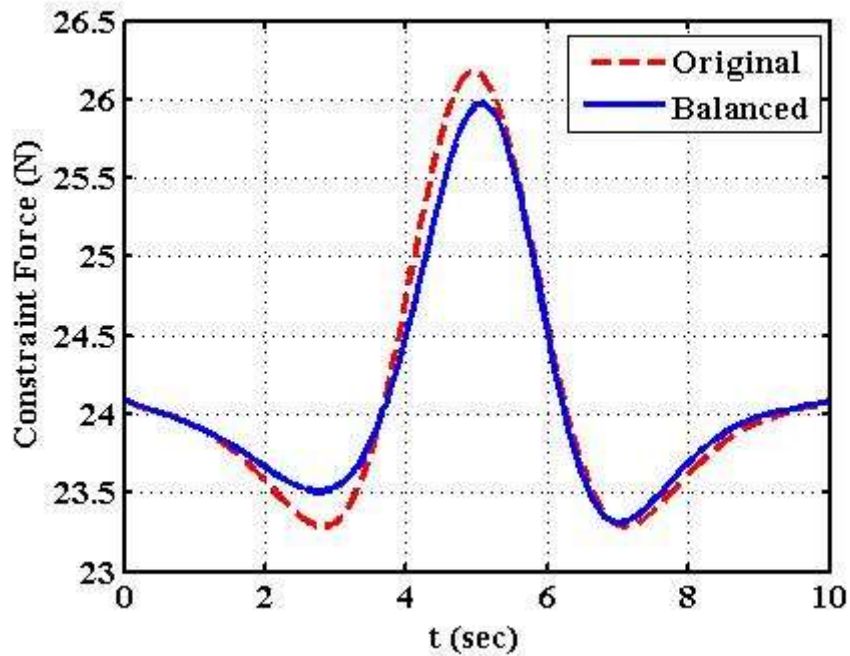**Fig.8.46: Constraint forces of original and optimally balanced PUMA at joint 3 with 4 Point-mass model**
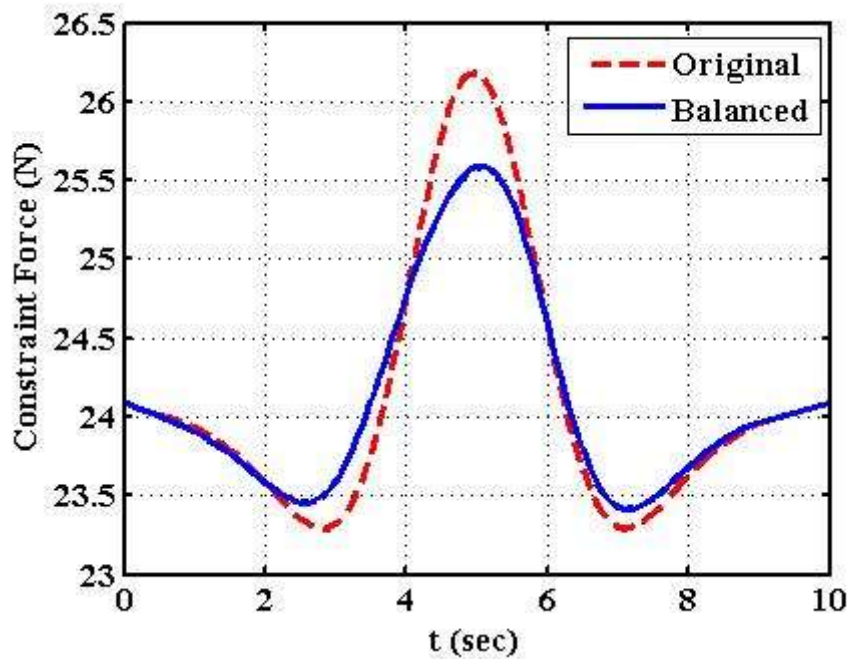
Fig.8.47: Constraint forces of original and optimally balanced PUMA at joint 4 with 4 Point-mass model
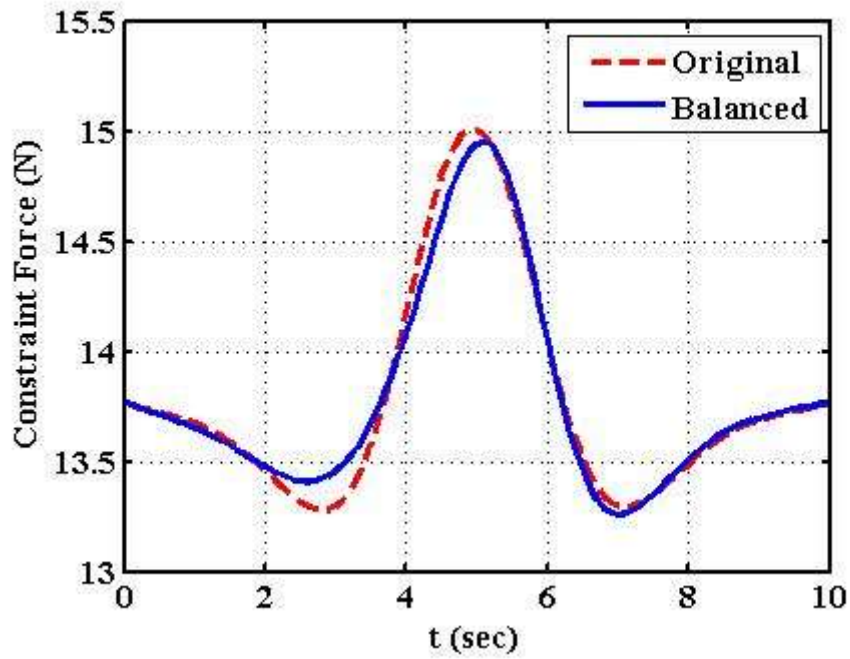
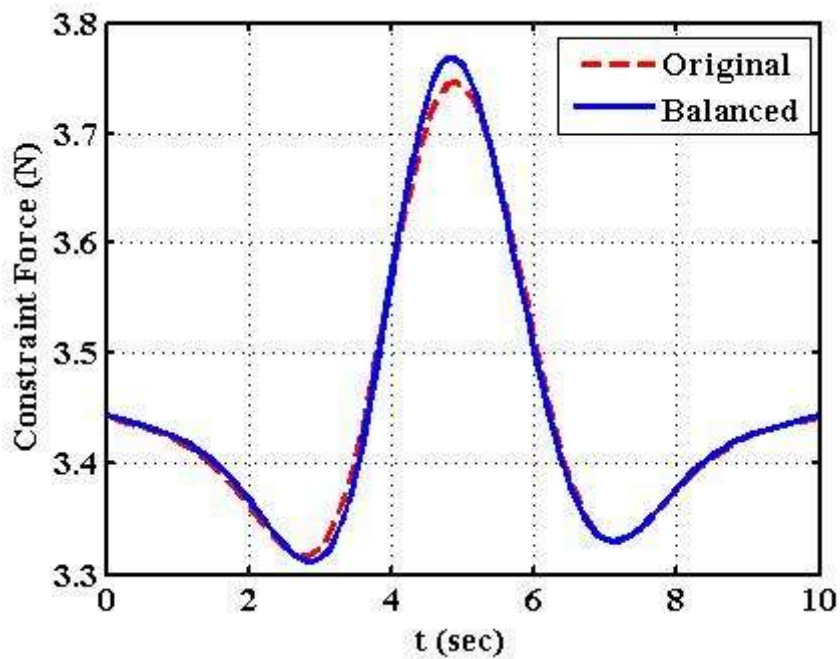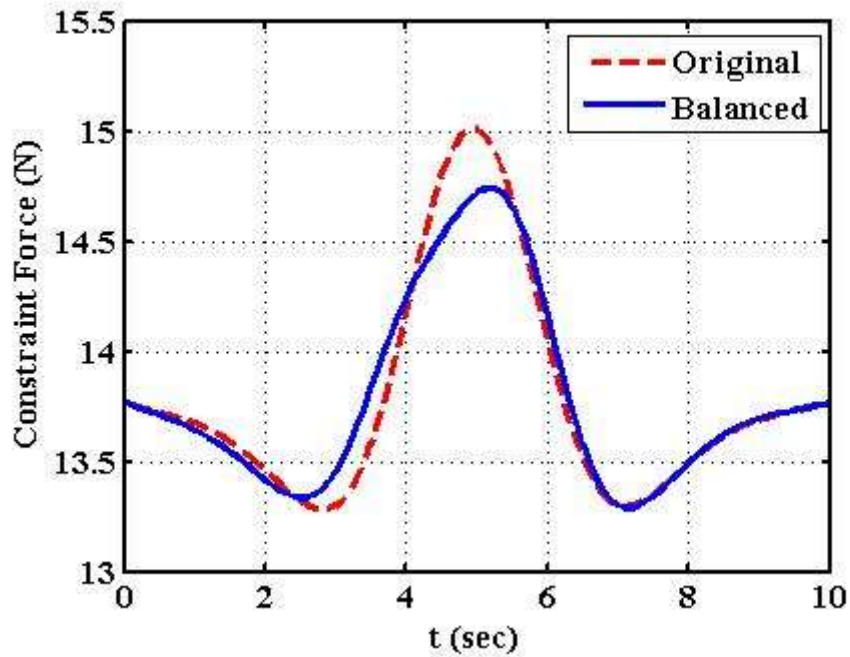**Fig.8.48: Constraint forces of original and optimally balanced PUMA at joint 5 with 4 Point-mass model**
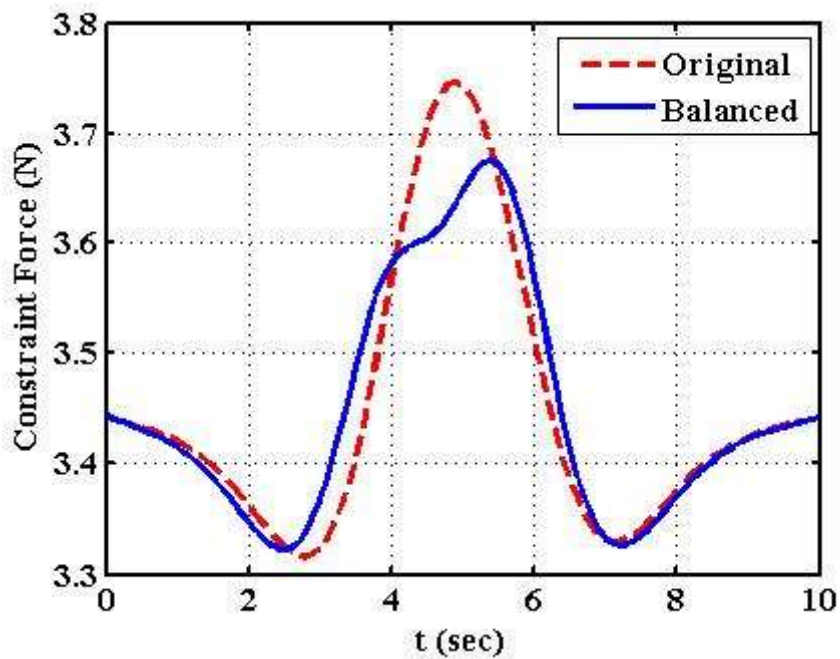
Fig.8.49: Constraint forces of original and optimally balanced PUMA at joint 6 with 4 Point-mass model

8.1.5 Three point mass model (The two-DOF planar RR robotic arm)

Consider a two degree of freedom robotic arm having two rigid links, each of mass 1 Kg and length 1 meter. The links are cylindrical and have very small dimension in Z direction with motion of the arm in XY plane only. We shall analyze the driving torque required at joint 1 and 2 under motion profile of $\theta_1 = \pi$, $\theta_2 = \pi/2$ in 10 secs with initial value of both θ_1 and θ_2 as zero under gravity (g=9.81 m/sec^2) using three point-mass system for the rigid link. This planar robotic arm has been considered as numerical illustration because its results are available in published book "Introduction to robotics" by S.K. Saha (2014). The trajectory of the planar robotic arm can be specified by the following relation.

$$\theta_i = \theta_i(0) + \frac{\theta_i(T) - \theta_i(0)}{T}\left[t - \frac{T}{2\pi}\sin\left(\frac{2\pi}{T}t\right)\right] \quad \text{where T=10 Secs}, \theta_i(0) = 0,$$

We have used the concept of equimomental point mass system and TLBO optimization technique to find constraint force and constraint moment at different joints of 6 dof PUMA robot using different point-mass systems in the thesis. Since the planar robotic arm is having motion in XY plane only, we shall use equimomental three point-mass system to represent the rigid links of the planar robot and find the driving torque required at each joint of the robotic arm. The equations for the driving torque for two dof planar robotic arm are derived in book on "Introduction to robotics" by S.K. Saha (2014). These equations are used after making suitable changes for point-masses in place of rigid mass to compute the inertias of the link and then computing the driving torque at different joints under the action of gravity for the three point-mass model.

Three point-mass system for planar robotic arm

Considering the ith rigid link of length a_i and mass m_i with its mass center C at distance a_i / 2 from point O. It can be represented by three point masses m_{i1}, m_{i2} and m_{i3} respectively retaining its center of mass at C, if point masses m_{i1} and $mi3$ are equal and if r_{i1} equals $r_{i3.}$
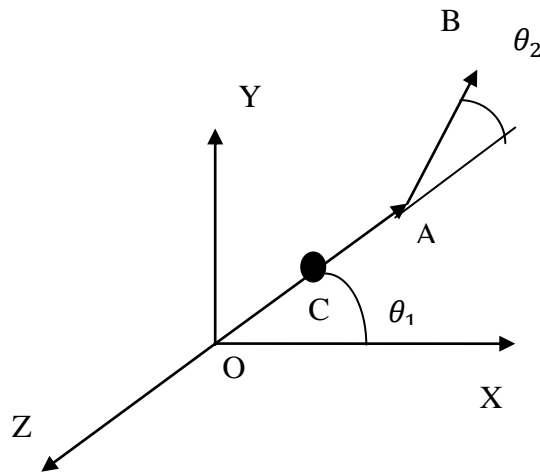
Fig. 8.50 Two degree of freedom Robotic Arm
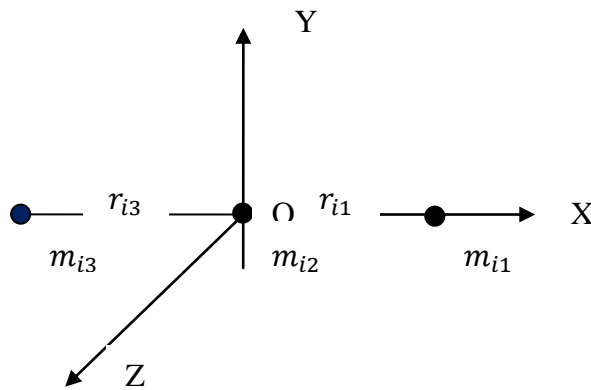
Fig. 8.51 Three Point-mass model for i^{th} link

the ith link at O_i and m_{i2} situated at it automatically satisfies the seven equimomental conditions pertaining to location of center of mass, product of inertias and inertia about X axis. Assuming $m_{i1} = m_{i2} = m_{i3} = m_i$ / 3, to satisfy the total mass condition, the

remaining two conditions of inertia about Y and Z axes give the value of r_{i1} for the known mass moment of inertia of the link about its center of mass .

$I_{iyy} = I_{izz} = 2 \ m_i * r_{i1}^2 \ / \ 3$, Since $I_{iyy} = I_{zz} = m_i * a_i^2 \ / \ 12$, we get $r_{i1} = a_i \ / $ Sqrt (8) = 0.3535 a_i

Driving Torque at joints of the planar robotic arm

The driving torques at joint 1 and 2 of the robotic arm are computed using expressions given in book on "Introduction to Robotics" by S.K. Saha (2014). The inertia values of the links are computed using point mass values. The TLBO optimization technique is used for optimizing the sum of rms values of driving torques at joint 1 and 2 over one cycle of operation of the planar robotic arm.

The minimum value of objective function (i.e. the sum of driving torque at joints 1 and 2) so obtained is 1.6654 N-m as against 2.7462 N-m for original robotic arm. The optimization results in 39.36% reduction in total driving torque of the joints. The value of three point masses for the minimum value of objective function is $m_{11} = m_{12}$ = 0.001 Kg , m_{13} = 0.998 Kg and $m_{21} = m_{22}$ = 0.001 Kg , m_{23} = 0.998 Kg . The mean value of optimized objective function for 10 trials is 1.7372 N-m.

The graph of the driving torque at joints 1 and 2 of the original robotic arm and optimized robotic arm for the minimum objective function value is shown in figures 8.52 and 8.53 given below. The maximum value of driving torque at joint 1 and 2 for the original robotic arm is ~20 N-m and ~ 5 N-m respectively for the original robotic arm which gets reduced to ~13 N-m and ~1.8 N-m for the optimized robotic arm as seen from the Figs. 8.52 and 8.53.
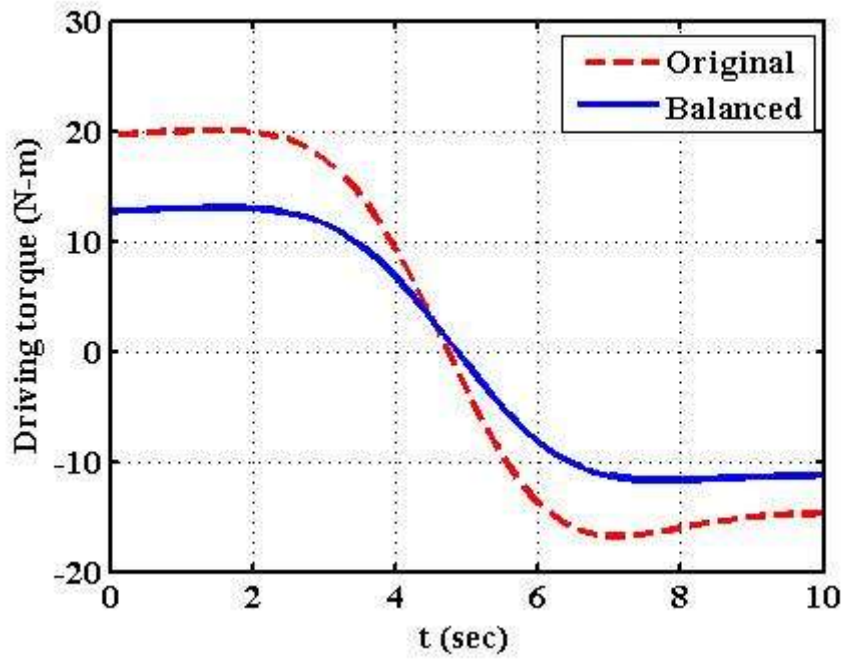
Fig. 8.52 Driving Torque at Joint 1of Planar Robotic Arm with 3 Point mass model
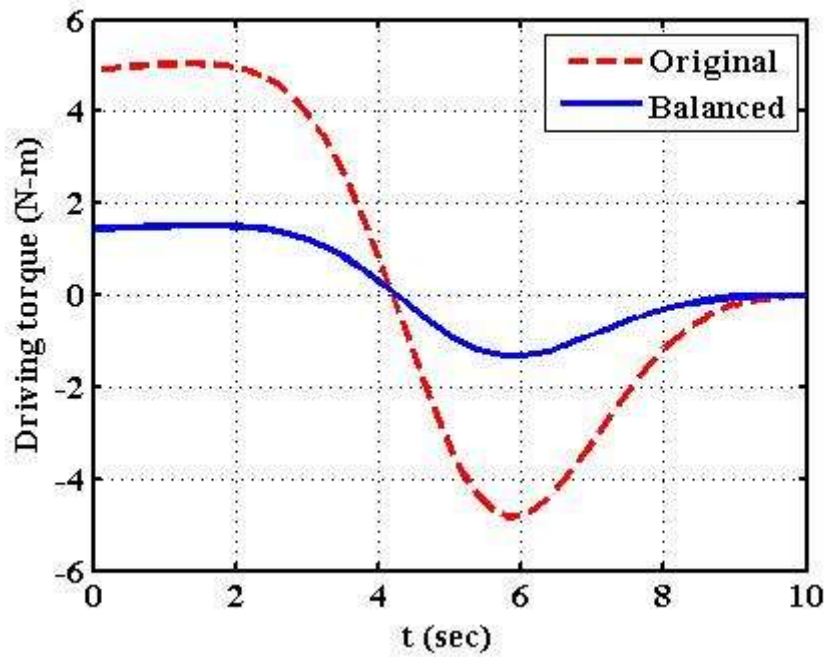
Fig. 8.53 Driving Torque at Joint 2of Planar Robotic Arm with 3 Point mass

model

8.2 Summary

In this chapter, the optimization problem of industrial manipulators is solved using TLBO for various equimomental point mass model configurations. Seven point-mass octahedron model, six point-mass hexahedron model, five point-mass hexahedron model and four point-mass models are considered. The optimized value of constraint moments and constraint forces at different joint of the manipulator is obtained and presented in tabular form for each of the four models. The variation of constraint moment and constraint force at each joint of manipulator over one cycle of operation is presented graphically for each of the four models.

Comparative Results

In this chapter comparison of results obtained using different point-masses models and three different techniques, namely GA, TLBO and "fmincon" is made.   The gist of results for different models and techniques are presented in tabular form. The results are presented through the minimum function value, minimum total values of shaking moment and force, mean function value and standard deviation for TLBO case. Apart from presenting minimum values obtained for constraint moments at various joints using different models and optimization techniques and then inferences are drawn. The inference is also drawn from the graphs, of constraint forces and moments at different joints for various models and optimization techniques, presented in chapters 7 and 8.

Links 5 and 6 posses very low mass and very small size due to which the constraint moment / force of optimal and original link is same (Figs. 7.5,7.6:7.11,7.12;7.17,7.18;7.23,7.24;   7.29,7.30;7.35,7.36;7.41,7.42;7.47,7.48   and 8.24). Further, Figs.8.6,8.7,8.13,8.18 ,8.19,8.30,8.42 and 8.43 representing constraint moment/force for Links 5 & 6,have very low numerical values and thus constraint moment for balanced case is more than the unbalanced case because the overall constraint moment/force is optimized.

Table 9.1: Mean function value (FV), Minimum (Min.) FV, Min. shaking moment(SM) for different point mass models with various optimization techniques

Point mass model	Optimization technique								
	GA			TLBO				Fmincon	
	Mean FV	Min. FV	Min. SM	Mean FV	Std. dev.	Min. FV	Min. SM	Min. FV	Min. SM
seven point	824.50	824.02	39.84	814.53	1.15	812.06	28.09	810.64	26.55
six point	827.30	823.02	38.90	816.88	1.73	813.65	29.82	810.81	26.71
five point	828.08	825.47	41.33	820.46	1.39	817.58	33.50	816.17	32.03
four point	826.54	825.70	41.52	824.24	1.89	820.82	36.73	818.88	34.77

Table 9.1 demonstrates that the minimum optimized objective function value for various point mass model varies from 812.06 to 820.82 and 824.02 to 825.70 for TLBO and GA optimization techniques, respectively. The objective function value obtained using TLBO is better than that of GA. The objective function value converges to 812.056 between 3000 and 4000 function evaluations with the TLBO algorithm as shown in Fig.9.1(a). Moreover, the Fig.9.1(b) shows that it converges to 824.02 after 3×10^6 function evaluations in the case of GA. It shows that the TLBO is computationally more efficient. Fig. 9.1(a) shows the minimum and maximum function value (FV) of population v/s number of the function evaluated. It shows that the difference between minimum (marked in black) and maximum (marked in red) function value of population decreases steeply with the increase in the number of function evaluations. It represents a better convergence of the solution.
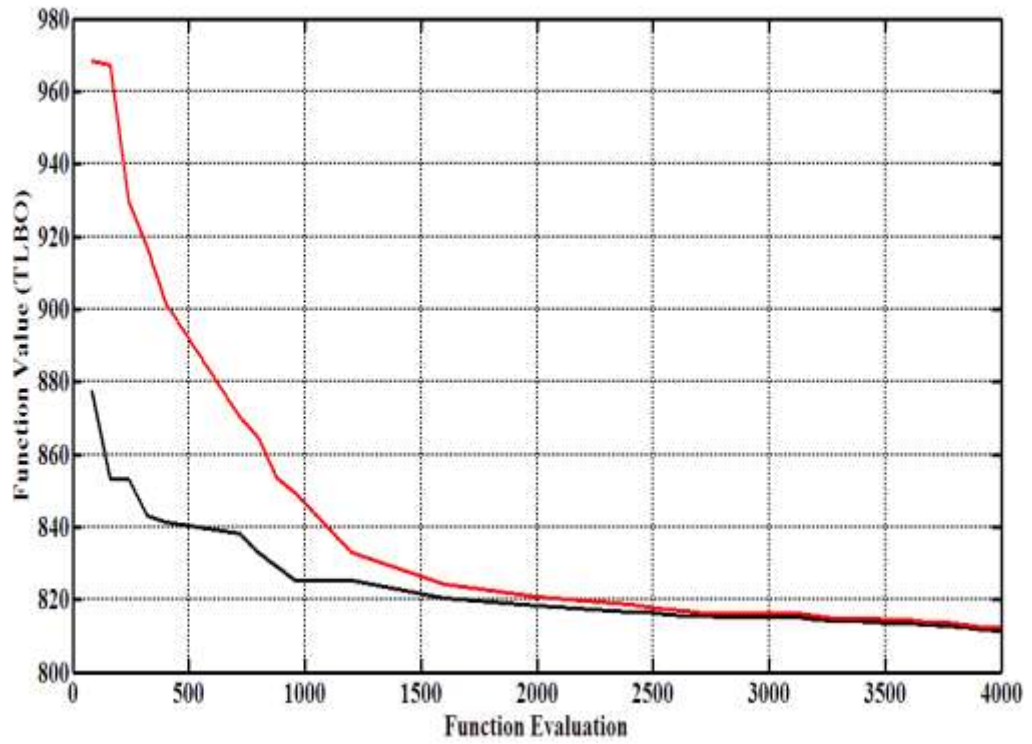
Fig. 9.1 (a) Convergence of Function value in TLBO
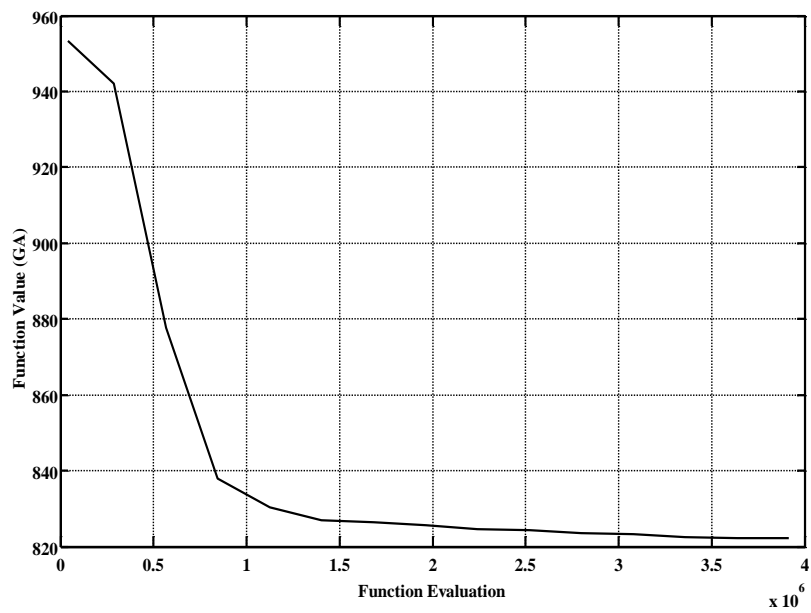
Fig. 9.1 (b) Function evaluations in GA

Table 9.2 shows that the sum of constraint moments at different joint of the robot is reduced by 70.67% to 71.66%, 78.24% to 83.36% and 79.41% to 84.27% through optimization using GA, TLBO and fmincon, respectively due to optimal mass distribution. GA and TLBO optimization offers a number of solutions close to the best optimal solution resulting in choosing the point-mass values that suits best for the link configuration/shape. Therefore, TLBO offers, higher reduction in the sum of constraint moment at the different joint of the manipulator, multiple solutions and requires fewer function evaluations as represented by graphs 9.1(a) and 9.1(b).

Table 9.2:- Constraint moments for original and optimized PUMA for various point-masses models obtained using different optimization techniques

Pt. mass model	Constraint moment	$\widetilde{n}_1$	$\widetilde{n}_2$	$\widetilde{n}_3$	$\widetilde{n}_4$	$\widetilde{n}_5$	$\widetilde{n}_6$	Total
------	Original PUMA	73.12	75.61	14.47	5.43	0.11	0.08	168.82
Seven point octahedron model	GA optimized	6.086	22.244	6.694	4.627	0.111	0.076	39.838
	TLBO optimized	4.424	16.110	2.376	4.542	0.471	0.168	28.091
	"fmincon" optimized	4.492	16.192	3.906	1.898	0.027	0.034	26.549
Six point hexahedron model	GA optimized	5.102	26.812	2.663	4.132	0.112	0.076	38.897
	TLBO Optimized	6.144	17.023	2.411	3.768	0.270	0.201	29.817
	"fmincon" Optimized	4.983	15.094	3.823	2.777	0.007	0.030	26.714
Five Point Hexahedron model	GA Optimized	4.508	26.186	5.573	4.873	0.112	0.076	41.328
	TLBO Optimized	5.052	19.072	4.151	4.356	0.799	0.073	33.503
	"fmincon" Optimized	4.679	18.727	5.317	3.239	0.072	0.039	32.073
Four Point model	GA Optimized	4.158	28.495	3.516	5.169	0.111	0.076	41.524
	TLBO Optimized	5.676	20.454	5.283	4.236	0.841	0.240	36.730
	"fmincon" Optimized	5.365	19.878	5.758	3.633	0.085	0.055	34.774

On comparing minimum constraint moment values for various point-masses model given in Table 9.1, it is observed that the minimum constraint moment value increases as the number of point masses decreases to represent the mass of the link. It is so because the overall mass of the link can be distributed better with the increase in the number of point masses for the link.

Table 9.3 shows that the constraint force at different joint remains nearly same numerically for various point mass models and optimization techniques, i.e., there is no reduction in its value even after optimization because it depends on the total mass of the link. The total mass of various link of the manipulator is kept same as the change in it would affect the load capacity of the manipulator. However, the variation in the constraint force is reduced over the complete one cycle of operation mainly for links 1, 2 and 3 as can be seen from various constraint force graphs for various models presented in chapters 7 and 8.

On comparing the constraint moments at joint 2 and the optimized overall constraint moment based on the results obtained using TLBO and given in Table 9.2, it is observed that overall constraint moment varies from 28.091, 29.817, 33.503 and 36.730 for 7. 6, 5 and 4 point-mass model respectively, whereas constraint moment at joint 2 varies from 16.110, 17.023, 19.072 and 20.454 for 7, 6, 5 and 4 point-mass models respectively. This shows that 7 and 6 point mass model reduces constraint moment at joint 2 as well as sum of constraint moment due to better mass distribution among more number of point-masses for complex shape link. For non-complex shape i.e. linkages simpler in shape 5 and 4 point-mass model shall be used. Further, model with lesser number of point- masses would make link shape optimization easier. Therefore, Four point-mass model shall be preferred for simpler

shape linkages and 6/7 point-mass model should be preferred for complex shape linkages.

Table 9.3:- Constraint forces for Original Puma and Optimized PUMA for various point-masses models obtained using different optimization techniques

Pt. mass model	Constraint force	$\tilde{f}_1$	$\tilde{f}_2$	$\tilde{f}_3$	$\tilde{f}_4$	$\tilde{f}_5$	$\tilde{f}_6$	Total
------	original PUMA	367.97	264.79	110.22	24.14	13.80	3.452	784.37
seven point octahedron model	GA optimized	367.95	264.72	110.13	24.14	13.80	3.452	784.19
	TLBO optimized	367.91	264.70	110.12	24.12	13.80	3.452	784.10
	"fmincon" optimized	367.91	264.70	110.12	24.10	13.80	3.451	784.08
six point hexahedronmodel	GA optimized	367.92	264.71	110.13	24.12	13.80	3.453	784.13
	TLBO optimized	367.92	264.71	110.12	24.12	13.80	3.452	784.12
	"fmincon" optimized	367.92	264.71	110.12	24.11	13.80	3.454	784.11
five point hexahedron model	GA optimized	367.92	264.71	110.11	24.13	13.80	3.452	784.12
	TLBO optimized	367.92	264.70	110.12	24.13	13.79	3.453	784.11
	"fmincon" optimized	367.91	264.70	110.12	24.11	13.80	3.452	784.09
four point model	GA optimized	367.94	264.71	110.13	24.14	13.80	3.453	784.17
	TLBO optimized	367.91	264.71	110.12	24.12	13.79	3.451	784.10
	"fmincon" optimized	367.91	264.71	110.12	24.11	13.80	3.452	784.10

Conclusions and Future Work

In this chapter, the thesis work is summarized and the recommendations / suggestions based on the findings in the thesis are also made. Further, the recommendations for future work are also presented.

It is important to consider the effect of shaking forces and moments in the design of an industrial manipulator. Therefore, their minimization is posed as an optimization problem. To formulate the problem, the dynamic modeling of the manipulators is presented in terms of the equimomental system of point-mass using the different point-mass model that ensures positive values for all point masses and eliminates non-linear constraints on link inertias. The optimization problem is solved using recently introduced algorithm TLBO. The results are compared and validated using the GA algorithm and fmincon optimization tool. It has been shown that the TLBO algorithm converges very fast with better optimization results as shown in Fig. 9.1. The various point mass models (7/6/5/4 point masses model) provides the redistribution of the link masses such that the constraint moments and forces at joints are reduced to the minimum. Simultaneously, it provides positive values for all point masses and thus offering feasible solutions for minimizing constraint forces, constraint moments and reducing the driving torques of the manipulator. The TLBO solution converges faster, it takes lesser computational time in comparison to GA. Furthermore, the various point mass models given solves the   problem of negative inertia faced with parallelepiped model.

The different point-masses model (7/6/5/4) configurations presented for spatial linkages of industrial manipulator gives positive value for all point masses that

eliminates non-linear constraints on link inertias and should offer easier link shape formulation.

The comparative results presented in chapter 9 shows that 7 or 6 point mass model should be used for complex shape links. For non-complex shape links (simpler in shape), 5 or 4 point-mass model shall be used.

Further, model with lesser number of point- masses would make link shape optimization easier. Therefore, Four point-mass model shall be preferred for simpler shape linkages and 6/7 point-mass model should be preferred for complex shape linkages.

Since, the optimization results are trajectory dependent, we need to make computations for all possible trajectory combinations and select the solutions best suited for all possible trajectories for which the manipulator/robot is likely to be used.

The TLBO solution converges faster, it takes lesser computational time than GA and thus should be preferred vis-à-vis GA for optimization of industrial manipulators.

Future Scope of the Work

The balancing methodology gives the mass and inertia of each link such that the shaking force and shaking moment are made simultaneously minimum. Link shape realization can be taken up as future work using the appropriate point mass model and optimized point masses values obtained that reduces the inertia induced shaking forces and shaking moments.

REFERENCES

1. Lowen, G.G., and Berkof, R.S., 1968, "Survey of Investigations Into The Balancing of Linkages", Mechanism and Machine Theory, 3(4), pp. 221-231.
2. Kamenskii, V.A., 1968a, "On The Questions of The Balancing of Plane Linkages", Journal of Mechanisms, 3 (4), pp. 303-322.
3. Kamenskii, V.A., 1968b, "On The Problem of The Number of Counterweights In The Balancing of Plane Linkages", Journal of Mechanisms, 3(4), pp. 323–333.
4. Shchepetilnikov, V.A., 1968, "The Determination of the Mass Centres of Mechanisms In Connection With the Problem of Mechanism Balancing", Mechanism and Machine Theory, 3(4), pp. 367-389.
5. Berkof, R.S., and Lowen, G.G., 1969, "A New Method For Completely Force Balancing Simple Linkages", ASME Journal of Engineering for Industry, 91(1), pp. 21-26.
6. Kaufman, R.E., and Sander, G.N., 1971, "Complete Force Balancing of Spatial Linkages", ASME, Journal of Engineering for Industry, pp. 620-626.
7. Tepper, F.R., and Lowen, G.G., 1972, "General Theorems Concerning Full Force Balancing of Planar Linkages By Internal Mass Redistribution", ASME Journal of Engineering for Industry, 94 (3), pp. 789-796.
8. Lowen, G.G., Tepper, F.R., and Berkof, R.S., 1974, "The Quantitative Influence of Complete Force Balancing on The Forces and Moments of Certain Families of Four-bar Linkages", Mechanism and Machine Theory, 9, pp. 299-323.
9. Smith, M., 1975, "Dynamic Analysis And Balancing of Linkages With Interactive Computer Graphics", Computer Aided Design, 7(1), pp. 15–19.
10. Walker, M.J., and Oldham, K., 1978, "A General Theory of Force Balancing Using Counterweights", Mechanism and Machine Theory, 13, pp. 175-185.
11. Walker, M.J., and Oldham, K., 1979, "Extensions To The Theory of Balancing Frame Forces In Planar Linkages", Mechanism and Machine Theory, 14, pp. 201-207.
12. Bagci, C., 1979, "Shaking Force Balancing of Planar Linkages With Force Transmission Irregularities Using Balancing Idler Loops", Mechanism and Machine Theory, 14(4), pp. 267-284.
13. Bagci, C., 1983, "Complete balancing of Space mechanisms – Shaking force only", ASME Journal of Mechanisms, Transmissions, and Automation in Design, 105, pp. 609 – 616.
14. Chen, Ning-Xin, 1984, "Partial Balancing of the Shaking Force of a Spatial 4 bar RCCC Linkage by the Optimization Method", Mechanism and Machine Theory, 19(2), pp. 257-265.
15. Kochev, I.S., 1987, "General Method for Full Force Balancing of Spatial and Planar Linkages by Internal Mass Redistribution", Mechanism and Machine Theory, 22(4), pp. 331-341.
16. Park, C., and Kwak, B., 1987, "Counterweight Optimization For Reducing Dynamic Effects of Clearance At A Revolute Joint", Mechanism and Machine Theory, 22(6), pp. 549-556.

17. Segla, S., Kalker-Kalkman, C. M., and Schwab, A.L., 1998, "Statical Balancing of a Robot Mechanism with the Aid of a Genetic Algorithm", Mechanism and Machine Theory, 33(1/2), pp. 163–174.
18. Lowen, G.G., Tepper, F.R., and Berkof, R.S., 1983, "Balancing of Linkages – An Update", Mechanism and Machine Theory, 18 (3), pp. 213-220.
19. Lee, T.W., and Cheng C., 1984, "Optimum Balancing of Combined Shaking Force, Shaking Moment, and Torque Fluctuations In High Speed Linkages", ASME Journal of Mechanisms, Transmissions, and Automation in Design, 106(2), pp. 242-251.
20. Yu, Y.Q., 1987a, "Research On Complete Shaking Force and Shaking Moment Balancing of Spatial Linkages. Mechanism and Machine Theory, 22(1), pp. 27-37.
21. Yu, Y.Q., 1987b, "Optimum Shaking Force and Shaking Moment Balancing of Spatial Linkages. Mechanism and Machine Theory, 22(1), pp. 39-45.
22. Kochev, I.S., 1992, "Active Balancing of The Frame Shaking Moment In High Speed Planar Machines", Mechanism and Machine Theory, 27(1), 53–58.
23. Sherwood, A.A., and Hockey, B.A., 1968, "The Optimization of Mass Distribution in Mechanisms Using Dynamically Similar Systems", Journal of Mechanisms, 4, pp. 243-260.
24. Rahman, S., 1996, "Reduction of Inertia-Induced Forces In A Generalized Spatial Mechanism", Ph.D. Thesis, Department of Mechanical Engineering, The New Jersey Institute of Technology.
25. Chiou, S.-T., Shieh, M.-G, and Tsai, R.-J. 1997, "The Two Rotating Mass Balancers for Partial Balancing of Spatial Mechanisms", Mechanism and Machine Theory, 32(5), pp. 617–628.
26. Wawrzecki, J., 1998, "A method of balancing of spatial mechanisms", Mechanism and Machine Theory, 33(1998), pp. 1195–1209.
27. Papakostas, K.D., Mouroutsos, S.G., Porter, B., 1998, Genetic design of dynamically optimal robotic manipulators, Proceedings of Institute of mechanical engineers Part-I, Journal of systems & control engineering, 212(6), pp. 423-436.
28. Kochev, I.S., 2000, "General Theory of Complete Shaking Moment Balancing of Planar Linkages: A Critical Review", Mechanism and Machine Theory, 35, pp. 1501-1514.
29. Feng, B., Morita, N., Torii,T., Yoshida, S.,2000, "Optimum Balancing of Shaking Force and Shaking Moment for Spatial RSSR Mechanisms using Genetic Algorithm", JSME International Journal Series C, 43(3), pp. 691-696.
30. Guo, G., Morita, N., and Torii, T., 2000, "Optimum Dynamic Design of Planar Linkage Using Genetic Algorithms", JSME International Journal Series C, 43 (2), pp. 372-377.
31. Arakelian, V., and Dahan, M., 2001, "Partial Shaking Moment Balancing of Fully Force Balanced Linkages," Mechanism and Machine Theory, 36, pp. 1241-1252.
32. Attia, H.A., 2001, "A simplified recursive formulation for the dynamic analysis of planar mechanisms", Acta Mechanica, 149, pp. 11-21.

33. Attia, H.A., and Quasseem, Al., 2003, "A matrix formulation for the dynamic analysis of spatial mechanisms using point coordinates and velocity transformation", Acta Mechanica, 165, pp. 207-222.
34. Ouyang, P.R., Li, Q., and Zhang, W.J., 2003, "Integrated Design of Robotic Mechanisms for Force Balancing and Trajectory Tracking", Mechatronics, 13, pp. 887-905.
35. Alici, G., and Shirinzadeh, B., 2004, "Optimum Dynamic balancing of Planar Parallel Manipulators", Proceedings of 2004 IEEE, International Conference on Robotics and Automation, New Orleans, LA, pp. 4527-4532.
36. Korayem, M.H., and Ghariblu, H., 2004, "The effect of base replacement on the dynamic load capacity of robotic manipulators", International J Adv. Manufacturing Technology, 23, pp. 28-38.
37. Arakelian, V.H., and Smith, M.R., 2005, "Shaking Force and Shaking Moment Balancing of Mechanisms: A Historical Review With New Examples", ASME Journal of Mechanical Design, 127, pp. 334-339.
38. Marcelin, J.-L., 2005, "Using genetic algorithms for the optimization of mechanisms", International J Adv. Manufacturing Technology, 27, pp. 2-6.
39. Kucuk, S., and Bingul, Z., 2008, *Robot Manipulators,* Chapter 15 on Link mass optimization using genetic algorithms for industrial robot manipulators, pp. 275-290.
40. Kim, J.Y., 2006, "Task based kinematic design of a two DOF manipulator with a parallelogram five bar mechanism", Mechatronics, 16, pp. 323-329.
41. Verschuure, M., Demeulenaere, B., Swevers, J., and Schutter, J.D., 2006, "Counterweight balancing for machine frame vibration reduction: Design and robustness analysis", ISMA Proceedings of ISMA 2006, pp. 3699-3714.
42. Nguyen, V.K., and Nguyen, P.D., 2007, "Balancing conditions of spatial mechanisms", Mechanism and Machine Theory, 42, pp. 1141-1152
43. Chaudhary, H. and Saha, S.K., 2007, "Minimization of Constraint forces in Industrial Manipulators," IEEE International Conference on Robotics and Automation, Roma, Italy, pp. 10-14.
44. Chaudhary, H., Saha, S.K., 2007, "Balancing of Four-bar linkages using Maximum Recursive Dynamic Algorithm", Mechanism and Machine Theory, 42(2), pp. 216-232.
45. Verschuure, M., Demeulenaere, B., Aertbelien, E., Swevers, J., and Schutter, J.D., 2008, "Optimal counterweight balancing of spatial mechanisms using voxel-based discretizations", ISMA Proceedings of ISMA 2008, pp. 2159-2174.
46. Chaudhary, H., Saha, S.K., 2008, "Balancing of Shaking forces and Shaking moments for Planer Mechanisms using the Equimomental Systems", Mechanism and Machine Theory, 43, pp. 310-334.
47. Arakelian, V.H., and Smith, M.R., 2008, "Design of a Planar 3-DOF 3-RRR Reactionless Parallel Manipulators", Mechatronics, pp. 601-606.
48. Chaudhary, H., Saha, S.K., 2008, "An optimization technique for the balancing of spatial mechanisms", Mechanism and Machine Theory, 43, pp. 506-522.
49. Volkert van der Wijk, Just L. Herder and Bram Demeulenaere, 2009, "Comparison of Various Dynamic Balancing Principles Regarding Additional

Mass and Additional Inertia", Journal of Mechanisms and Robotics, ASME, Vol 1/041006, pp. 1-9.

50. Briot, S., and Arakelian, V., 2009, "Complete Shaking force and Shaking moment balancing of the Position-Orientation De-Coupled PAMINSA Manipulator", IEEE/ASME International Conference on Advanced Intelligent Mechatronics, Singapore, pp. 1521-1526.

51. Farmani, M.R., Jaamialahmadi, A., and Babaie, M., 2011, "Multiobjective Optimization for Force and Moment Balance of A Four-bar Linkage Using Evolutionary Algorithms", Journal of Mechanical Science and Technology, 25 (12), pp. 2971-2977.

52. Nehemiah, P., Sundara Shiv Rao, B.S.K., and Ramji, K., 2012, "Shaking Force and Shaking Moment Balancing of Planar Mechanisms with High Degree of Complexity", Jordan Journal of Mechanical and Industrial Engineering, 6, pp. 17-24.

53. Wijk, V.V., Demeulenaere, B., Gosselin, C., and Herder, J.L., 2012, "Comparative Analysis of Low- Mass, Low- Inertia Dynamic Balancing of Mechanisms", ASME Journal of Mechanisms and Robotics, 4, pp. 031008-1 to 8.

54. Earkaya, S., 2013, "Investigation of balancing problem for a planar mechanism using genetic algorithm", Journal of Mechanical Science and Technology, 27(7), pp. 2153-2160.

55. Salinic, S., and, Bulatovic, R, 2015, "Minimization of Joint Reaction Forces of the 2-DOF Planar Serial Manipulators", Conference Paper, 5th Intl. Congress of Serbian Society of Mechanics, Serbia, 15-17 June, pp 1-10. http://www.research.net/publication/278410032,

56. Chaudhary, H., and Saha, S.K., 2009, *Dynamics and Balancing of Multibody Systems*, Springer-Verlag, Berlin.

57. Saha, S.K., 2010, *Introduction to Robotics*, Tata McGraw Hill publishing company Limited, New Delhi.

58. MATLAB Optimization Toolbox, version 7.7.0.471 (R2008b).

59. Rao, R.V., Savsani V.J., and Vakhariya, D.P., 2011, "Teaching-Learning-based Optimization: A novel method for constrained mechanical design optimization problem", Computer-Aided Design, 43, pp. 303-315.

60. Rao, R.V., and Savsani, V.J., 2012, *Mechanical Design Optimization Using Advanced Optimization Techniques*, Springer-Verlag London, UK.

61. Rao, R.V., and Patel, V., 2012,"An elitist teaching- learning- based optimization algorithm for solving complex constrained optimization problems", International Journal of Industrial Engineering Computations, 3, pp. 535-560.

62. Rao. R.V., and Waghmare, G.G., 2014, "A comparative study of teaching learning based optimization algorithm on multi-objective unconstrained and constrained functions," Journal of King Saud University – Computer and Information Sciences, 26(3), pp. 332-346.

63. Waghmare, G., 2013, "Comments on A note on teaching-learning-based optimization algorithm", Information Sciences 229, pp. 159-169.

64. Tayfun Dede, 2014, "Application of Teaching-Learning-based Optimization Algorithm for the Discrete Optimization of Truss Structures", KSCE Journal of Civil Engg., 18(6), pp1759-1767.

65. Tayfun Dede, 2013, "Optimal design of grillage structures to LRFD-AISC with teaching-learning based optimization", Struct Multidisc Optim 48, pp.955-964.

66. Satpathy, S.C., Naik, Anima, and Parvathi, K., 2013,"A teaching learning based optimization based orthogonal design for solving global optimization problem," 130 (2), pp. 1-12.

67. Kunjir Yu, Xin Wang, and Zhenlei Wang, 2014,"An improved teaching-learning-based optimization algorithm for solving numerical and engineering optimization problems," J of Intll Manf, 27(4), pp. 831-843.

68. Rao, R.V. and Kalyankar, 2014, "Optimization of modern machining processes using advanced optimization techniques: a review," Int J Adv Manuf Technol, 73(5-8), pp. 1159-1188.

69. Debai Chen, Fung Zou, Jiangtao Wang and Wujie Yuan, 2014," A teaching-learning-based optimization algorithm with Producer-Scrounger model for global optimization,"Soft Comput, 19(3), pp. 745-762.

70. Keesari, H.S. and Rao, R.V., 2013, "Optimization of job shop scheduling problems using teaching-learning-based optimization algorithm", OPSEARCH, 51(4), pp. 545-561.

71. Yildiz, Ali R., 2013, "Optimization of multi-pass turning operations using hybrid teaching-learning- based approach," Int J Adv Manf Technolo vol. 66, pp. 1319-1326.

72. Panwar, P.J. and Rao, R.V., 2013, "Parameter optimization of machining processes using teaching-learning-based optimization algorithm," The Intl Journal of Advanced Manufacturing, vol. 67, pp. 995-1006.

73. Ye Xu, Ling Wang, Sheng-yao and Min Liu, 2015, "An effective teaching-learning-based algorithm for the job-shop scheduling problem with fuzzy processing time," Neurocomputing, 148, pp. 260-268.

74. Adil Baykasoglu, Alper Hamzadayi and Simge Yelkenci Kose, 2014, "Testing the performance of teaching-learning based optimization (TLBO) algorithm on combinatorial problems: Flow shop and job shop scheduling cases," Information Sciences 276, pp. 204-218.

75. Michael Skinner, 2011, "*Genetic Algorithms Overview _ GA Warehouse*", geneticalgorithm.ai-dopot.com/Tutorial/overview.html., pp. 1-3.

76. Co-Director, Genetic Algorithms Research and Application Group (GARAGe),   "*Introduction to Genetic Algorithms*" _ *Michigan State University*", www.egr.msu.edu/.../GECSummitintroToGA_Tutorial_goodman.pdf. pp. 1-..

77. Bhattacharya, R.K., 2013, "*Introduction to Genetic Algorithm _ IIT Guwahati*", www.iitg.ernet.in/rkbc/CE602/CE602/Genetic% 20 Algorithm.pdf.

78. Kalyanmoy, Deb, 2004, *Optimization for Engineering Design*, PHI Learning Pvt. Ltd.

Appendix A

Genetic Algorithm (GA)

Genetic Algorithms (GA) mimics the biological evolution process for solving problems in the wide domain and is an attractive class of computational models. GA was proposed by Professor John Holland in 1975. GA's mechanism was later analyzed and explained by Goldberg, De Jong, Davis, Muehlenbein, Chakraborti, Fogel, Vose and many others. GA has three major applications, namely, intelligent search, optimization and machine learning. Currently, GA is used along with neural networks and fuzzy logic for solving complex problems.

GA uses principles of natural genetics and natural selection to constitute a search (i.e. Survival of the fittest principle of nature is used for search process) and solve the optimization problem. The cycle of Genetic Algorithm is presented below

Fig. A.1: Flow chart of Genetic Algorithm (GA) cycle [76]

It operates through a simple cycle of following stages:

(i)   Creation of a "population" of strings,

(ii)   Evaluation of each string,

(iii)   Selection of best strings and

(iv)   Genetic manipulation to create a new population of strings.

Each cycle in Genetic Algorithm produces a new generation of possible solutions for a given problem. In the first phase, an initial population describing representatives of the potential solution is created to initiate the search process. The elements of the population are encoded into bit-strings, called chromosomes. The performance of the strings called fitness is then evaluated using some functions, representing the objective function and constraints of the problem. Depending on the fitness of the chromosomes they are selected for a subsequent genetic manipulation process. The selection process is mainly responsible for assuring the survival of the best-fit individuals. After selection of the population strings is over, the genetic manipulation process consisting of two steps, crossover, and mutation, is carried out.

In the crossover operation, new strings are created by exchanging information among strings of mating pool. Generally, two strings are picked from the mating pool at random and some portions of the strings are exchanged between the strings. Either single point or two point crossover operation is performed. A single point crossover operation is performed by randomly choosing a crossing site along the string and then exchanging all bits on the right side of the crossing site as shown in Fig. 6.2 given below.
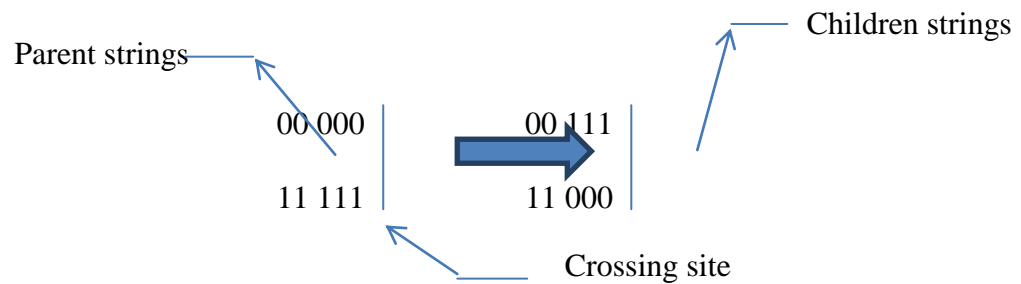
Fig. A.2: Representation of crossover operation in binary strings of mating pool [76]

The two strings participating in the crossover operation are known as parent strings and resulting strings as children strings. Even though the random site for crossover may or may not create good strings by crossover but it does not matter because, if good strings are not created by crossover they will not survive too long, reproduction will not select these strings in subsequent generations. Since the effect of crossover may be detrimental or beneficial, thus to preserve some of good strings that are already present in the mating pool, all strings in the mating pool are not used in the crossover. When a crossover probability of p_c is used, only 100 p_c % strings in the population are used in crossover population and 100 (1- p_c) % of the population remains as they are in the current population. A crossover operation is mainly responsible for the search of new strings. Crossover probability is kept high between 0.7 and 0.8.

In the second step, mutation operator changes 1 to 0 and vice versa with a small probability p_m. The mutation operation is performed bitwise by choosing a number between 0 and 1 randomly. If the number chosen is smaller than p_m than the bit is altered otherwise bit is kept unchanged. The need for mutation is to create a point in the neighborhood of the current point, thereby achieving a local search around the current solution. Mutation is also used to maintain diversity in the population. For

example, if the population has four eight-bit strings such as 0110 1101,   0011 1110, 0001 0101,   0101 0110. Here, all four strings have a 0 in leftmost bit position. If the true optimum solution requires 1 in that position, then neither reproduction nor crossover operations will be able to create 1 in that position. The mutation operation introduces some probability (Np_m), for a population size of N, of turning 0 to 1 in that position. Mutation probability is kept low i.e. from 0.05 to 0.08.

The different steps involved in solving a given optimization problem can be summarized as follows:

Step 1:- Choose a coding (Binary/Real number) to represent problem parameters (variables), a selection operator (Objective/Fitness function), a crossover operator, and a mutation operator.

Decide on population size N, crossover probability p_c, mutation probability p_m. Initialize a random population of strings of decided size and maximum allowable generation number $t_{max,}$ set t = 0.

Step 2: Evaluate each string in the population.

Step3:If the number of iteration t > t_{max} or other termination criteria is satisfied, Terminate.

Step 4: Perform reproduction in the population.

Step 5: Perform crossover on random pairs of strings.

Step 6: Perform mutation on every string.

Step 7: Evaluate strings in the new population, set t = t + 1 and go to step 3.

Consider the following example to understand the GA

Maximize: $Z = 30(Y_1)^2 - Y_2$ where Y_1 & Y_2 lies between 0 and 1.

Step 1:- Choosing binary coding to represent decision variables Y_1 and Y_2 and 4 bit for each variable.It makes total string length equal to $2*4 = 8$ and gives solution accuracy of $(1-0)/(2^4-1) = 0.0667$.Choose roulette – wheel (random number generator) for selection, Z as selection operator, a single point crossover, and a bit-wise mutation operator. Choose crossover and mutation probabilities as 0.8 and 0.05 respectively. Set maximum number of iteration $t_{max} = 10$ and initialize generation counter $t = 0$.

Step 2:- Random population is initialized based on Knuth's random number generator for the population size of $2*4 = 8$ (for 2 decision variables each with 4 bit). Four bit binary number 0000 represents 0 that corresponds to the variable value of 0.0 and binary number 1111 represents 15 that correspond to variables real number value of 1.0. Sixteen binary numbers, between 0 and 15 integer numbers with increment in real value of variable by $(1-0) / (16-1) = 0.0667$ are given in following Table 6.1 along with real number value of the variable represented by each of them. Same random numbers are generated for both variables. However, we select strings combination for variables Y_1 and Y_2 at random.

Table A.1: Four bit binary numbers and the corresponding real number value of variables

Random Number	0	1	2	3	4	5	6	7
Binary number	0000	0001	0010	0011	0100	0101	0110	0111
Variable value (Real number)	0.0	0.0667	0.1334	0.2001	0.2668	0.3335	0.4002	0.4669
Random Number	8	9	10	11	12	13	14	15
Binary number	1000	1001	1010	1011	1100	1101	1110	1111
Variable value (Real number)	0.5336	0.6003	0.6670	0.7337	0.8004	0.8671	0.9338	1.0005

Table A.2: Initial Population (Pop.), Mating Pool, Intermediate Pop., Population after Mutation and Function Value after one generation/cycle of Genetic Algorithm

| S.No. | R. No. | | Initial Population (Binary) | Function value | Reproduction Phase | | | | Intermediate Population (Binary) | Population after Mutation (Binary) | Real Number value of variables | Function Value |
	Y_1	Y_2			Exp.count(Fval/Avg.	Probability=Exp. Count/8	Random Number	Mating Pool				
1	11	09	1010 1000	12.800	1.1497	0.1437	0.27767	1011 110**0**	1011 **1**100	1011 0100	0.733 0.267	15.867
2	04	01	0011 0000	1.200	0.1078	0.0135	0.13025	1010 100**0**	1010 1000	1010 1000	0.667 0.533	12.800
3	05	03	0100 0010	2.000	0.1796	0.0225	0.80217	1111 0**011**	1111 0000	1111 0000	1.000 0.000	30.000
4	12	13	1011 1100	15.333	1.3772	0.1721	0.10875	1010 1**000**	1010 1011	1010 1011	0.667 0.733	12.600
5	14	11	1101 1010	21.867	1.9641	0.2455	0.54127	1**101 1010**	1111 0011	1111 0011	1.000 0.200	29.800
6	16	04	1111 0011	29.800	2.6767	0.3346	0.60311	1**111 0011**	1101 1010	1101 1010	0.867 0.667	21.867
7	03	02	0010 0001	0.4662	0.0419	0.0052	0.49739	1101 101**0**	1101 1011	1101 1011	0.867 0.733	21.800
8	08	15	0111 1110	5.6000	0.5030	0.0629	0.78626	1111 001**1**	1111 0010	1111 0010	1.000 0.133	29.867
Sum				89.066		1.0000						174.60
Avg.				11.133								21.825

We have taken last two digits between 01 and 16 of five digits random number table as random numbers for generating the initial population of variables in the binary form. The random numbers are obtained for variables Y_1 and Y_2 (Col. 2 and 3 of Table A.2). The initial population is generated based on these numbers. It is in eight-bit form, using a four-bit number for each variable (Col. 4 of Table A.2).

The value of variables Y1 and Y2 in real numbers for the initial population of randomly generated variables in binary form is obtained from Table A.1 while the function value / fitness value using objective function is computed (Col. 5 of Table A.2).The average fitness value of the initial population (i.e. 11.1333) is computed by dividing the sum of mod of function value with the size of population i.e. 8 in this case (Last row of Table A.2).

Step 4: Next step is to compute the expected count of each string which is obtained by dividing the function value with average function value (Col. 6 of Table A.2). The Probability of each string (from 1 to 8) being considered in the mating pool is computed by dividing expected count (Column 6 of Table A.2) by population size that is 8 (Col 7 of Table A.2). Then the cumulative probability is computed.

Random number between 0 and 1 is created to form mating pool. Taking random numbers from five-digit random number table (Col. 8 of Table A.2). Strings which are specified by each of the above random numbers are entered in column 9 of the table. These strings make the mating pool (for example the cumulative probability of the 3rd string is 0.1797, and that of 4th string is 0.3518 thus 4th string best represents the probability 0.2777). Thus strings (4, 1, 6, 1, 5, 6, 5 and 6) best represents the random numbers given in col. 8 of Table A.2. It completes the Evaluation and Reproduction phase.

Step 5:The strings in the mating pool are used in crossover operation. In a single point crossover, two strings are selected at random and crossed at the random site. Since the mating pool contains strings at random, we pick pairs from the top of the list (i.e. 1 and 4 participate in the first crossover). As crossover probability p_c is 0.80, we observe first two digits of 5-digit random number table, and if it lies between 01 and 80, the crossover operation is performed on selected pair otherwise the strings are placed as is in an intermediate population. The next step is to find a crossover site at random by creatinga random number between (0,8).Selecting the last column of 5-digit random number table with first two digits for p_c and last digit for crossover site, we get (48, 74, 59, 41) and (7, 5, 1, 7) numbers. Therefore, we perform crossover operation on all four pairs at the site of 7, 5, 1 and 7 respectively. The intermediate population after crossover operation is given in column 10 of Table A.2.

Step 6: Next we have to perform mutation on strings bitwise with probability p_m = 0.05 in intermediate population as above, we can expect to alter $0.05*8*2 = 0.8$, say 1 bit.

Since only two strings at serial number 1 and 2 in the above intermediate population remains unchanged after crossover, i.e., these strings are identical to single parent strings selected in reproduction process and therefore mutation operation is performed on the string at serial number 1only. One random number between 1 and 8 selected from random number table is 5.The bit to be muted is marked bold.The population after mutation operation is as given in column 11 of Table A.2.The resulting population is new population (obtained after reproduction, crossover, and mutation).

Next, we compute the real number value of decision variables corresponding to the binary number of above-resulting population (Col. 12 of Table A.2).

The Function Value (FV) represented by objective function Z of resulting population is computed (Last column of Table A.2). The average FV after the first iteration n is 21.8250, i.e., there is a significant improvement over initial population average of 11.1333. Subsequent generations/iterations improve the new population average further. Even after first iteration one of the strings pertains to exact solution value of 30.0000 and two strings have FV of ~ 29.8 close to exact solution value.

Papers presented/accepted based on this work

Referred Journal

[1] "Minimizing Constraint Forces and Moments of Serial Industrial Manipulator using Teaching Learning Based Optimization and point-mass Model", is published as DOI: 10.1177/0954406217736341, Proc IMechE Part C by Journal of Mechanical Engineering Science, 0(0) pp 1-12 in Sept'17.

[2] "Point-mass models for Dynamic balancing of Industrial Manipulators using Genetic Algorithm", presented in CARS FoF 2016 International Conference held at Kolaghat in Jan16 and published by Springer as Lecture Notes in Mechanical Engineering.

Referred Conference Proceedings

[1] "Hexahedron Point – mass model and Teaching Learning Based Optimization for Balancing of Industrial Manipulators", Proc. of International Conference on Machines and Mechanisms, iNaCoMM 2015-96, IIT Kanpur, pp. 28.

[2] "Dynamic balancing of Industrial Manipulators using Octahedron Point–mass model", Proc. of International Conference on Advances in Materials and Product Design, AMPD, SVNIT Surat, pp. 1-7, 2015.

BIO-DATA

NAME: DEVI SINGH KUMANI

FATHER'S NAME: Late Shri Anand Singh Kumani

DATE OF BIRTH :   7 th January 1948   Age - 70 Yrs

ADDRESS   **:**   D. S. Kumani ,

                  E – 172 , Shiv Kutir , Ramesh Marg ,

                  C – Scheme , **JAIPUR – 302001**

                  (Email : profdevs@gmail.com and

                  Mobile No. 9461203337)

QUALIFICATIONS

- Passed B.E.(Mech.) in 1969 , with first class with distinction and consistent 1st Rank in the University, from S.V.Regional Engineering College, Surat (Now SVNIT, Surat).
- Passed M.Tech(Mech.) in 1971, with a good CPI of 8.54/10.0, from Indian Institute of Technology, Kanpur (IIT Kanpur).
- Passed Post-Graduate Diploma in Marketing Management(PGDMM) in 2003 from IGNOU.
- **Ph D, MNIT, Jaipur (Thesis viva-voce held on 23rd Feb'18).**

EXPERIENCE

- Total experience of nearly ~45 years (Research & Development 16 ½ years; Teaching 17 years and Industrial 11years).Worked at different organizations in multidisciplinary functions/capacities.

- Associated with teaching for 17 years (2000 onwards). Worked as HOD & Professor in teaching. I have taught variety of courses to mechanical engineering students. Presently working as professor.
- Associated with Research and development for 16 ½ years at VSSC, HAL and CVRDE.
- Associated with Industries for 11years and worked as Plant Head, Quality Head, Management representative for ISO 9002 Quality Systems, Maintenance & Engineering Head, Planning & Engineering Chief.

- Worked as Professor (Mech. Engg.) at Poornima College of Engg.,Jaipur (Sept'06 to Dec'17).
- Worked as Head and Professor, Mechanical Engg. at Gyan Vihar Engg. College, Jaipur (June'01 to Sept'06).
- Visiting faculty at IIIM, MKMIM and AIM, Jaipur for MBA and MCA courses.

- Sr. Manager (Operations) at Highland House Pvt. Ltd, Mandawa (Raj.) for 1 year (Oct'99 to Sept'00).
- Plant Manager at Varun Flair Filtration Pvt. Ltd., Jaipur for 2 years (April'97 to March'99).
- Manager Works Engineering and Quality at Wires & Fabriks Ltd., Jaipur for nearly 2 years & 8 months (Aug'94to March'97).
- Dy. GM(Quality Mgt.) at Autolite (India) Ltd., Jaipur for nearly 1 year & 8 months(Oct'92 to June'94).
- Chief Manager at Rajasthan Communications Ltd., Jaipur for nearly 3 years and 7 months (Aug'88 to March'92).
- Sr. Manager (Design) and Design Engineer at Hindustan Aeronautics Ltd., Lucknow for nearly 9 years and 6 months (March'79 to August'88).
- Engineer SD and Engineer SC at Vikram Sarabhai Space Centre, Trivandrum for nearly 6 years and 2 months (Jan'73 to Feb'79).
- SSO–II at Combat Vehicle and Research & Development Establishment, Avadi, Madras for nearly 9 months (Apr'72 to Jan'73).